Alma Mater Studiorum - Università di Bologna

DEI - Dipartimento di Ingegneria dell'Energia Elettrica e dell'Informazione

Dottorato di Ricerca in Ingegneria Elettronica, delle Telecomunicazioni e Tecnologie dell'Informazione

XXVIII Ciclo

Settore Concorsuale: 09/F2 - Telecomunicazioni

Settore Scientifico Disciplinare: ING-INF/03

Heterogeneous Networks for the IoT and Machine Type Communications

Tesi di:

Melchiorre Danilo Abrignani

Coordinatore:

Chiar.mo Prof. Ing. **Alessandro Vanelli-Coralli**

Relatori:

Chiar.mo Prof. Ing. **Roberto Verdone**

Esame anno finale 2016

"The important thing is to not stop questioning.
Curiosity has its own reason for existing." (A. Einstein)

Table of Contents

Contents

Abstract

The *Internet of Things* promises to be a key-factor in the forthcoming industrial and social revolution. The *Internet of Things* concept rely on pervasive communications where 'things' are 'always connected'. The focus of the thesis is on *Heterogeneous Networks* for *Internet of Things* and *Machine Type Communications*. *Heterogeneous Networks* are an enabling factor of paramount important in order to achieve the 'always connected' paradigm. On the other hand, *Machine Type Communications* are deeply different from Human-to-Human communications both in terms of traffic patterns and requirements. This thesis investigate both concepts. In particular, here are studied short and long range solutions for Machine-to-machine applications. For this work a dual approach has been followed: for the short-range solutions analysis an experimental approach has been privileged; meanwhile for the long-range solutions analysis a theoretical and simulation approach has been preferred. In both case, a particular attention has been given to the feasibility of the solutions proposed, hence solutions based on products that already exist in the market have been privileged.

List of Acronyms

3GPP 3rd Generation Partnership Project

6LoWPAN IPv6 over Low power Wireless Personal Area Networks

ABC Access Barring Check

ACK acknowledgment

AGGR Aggregation Layer

AODV Ad-hoc On-demand Distance Vector

ATBC Aggregated Transmission Bandwidth Configuration

AP Access Point

AS Active Scan

BER Bit Error Rate

BLER Block Error Rate

BP Backoff period

List of Acronyms

BPSK Binary Phase Shift Keying

BS Base Station

BSR Buffer Status Report

CA Carrier Aggregation

CAP Contention Access Period

CC Component Carrier

CEN Comité Europen de Normalisation - European Commitee for Standardization

CENELEC Comité Européen de Normalisation Électrotechnique - European Committee for Electrotechnical Standardization

CFP Contention Free Period

CoAP Constrained Application Protocol

COMP Coordinate Multipoint Transmission

CRC Cyclic Redundancy Check

CSMA/CA Carrier Sense Multiple Access with Collision Avoidance

CSI Channel State Information

DAO Destination Advertisement Object

DATASENS Data Sensing and Processing

DIO DODAG Information Object

DIS DODAG Information Solicitation

DL Downlink

DODAG Destination-Oriented Directed Acyclic Graph

DRB Data Radio Bearer

DSSS Direct Sequence Spread Spectrum

eNB evolved Node B

EB Exabyte

eCDF empirical Cumulative Distribution Function

ED Energy Detection

EPC Evolved Packet Core

EPS Evolved Packet System

ESSID Extended Service Set Identification

ETSI European Telecommunications Standards Institute

EuWIn European Lab on Wireless Communications for the Future Internet

E-UTRAN Evolved UMTS Terrestrial Radio Access Network

FDD Frequency Division Duplex

FDPS Frequency Domain Packet Scheduling

FIFO First In First Out

FLEXTOP Flexible Topology

FWD Forwarding Layer

GBR Guaranteed Bit-Rate

GTS Guaranteed Time Slot

H2H Human to Human

HARQ Hybrid Automatic Repeat reQuest

HeNB Home evolved Node B

HII High Interference Indicator

HQ High Quality

ICI Intercell Interference

ICIC Inter-Cell Interference Coordination

ICS Independent Carrier Scheduling

IETF Internet Engineering Task Force

IEEE Institute of Electrical and Electronics Engineers

IMT-A International Mobile Telecommunications Advance

IoT Internet of Things

IPv6 Internet Protocol v6

ISM Industrial Scientific Medical

IT Information Technology

ITU International Telecommunication Union

ITU-T International Telecommunication Union Telecommunication Standardization Bureau

JCS Joint Carrier Scheduling

KPI Key Performance Indicator

KPIs Key Performance Indicators

L1 Layer 1

L2 Layer 2

LBT Listen-before-talk

LE Low Energy

LENA LTE-EPC Network Simulator

LL Link Layer

LLC Link Layer Controller

LNA Low-Noise Amplifier

LOS Line-of-Sight

LQ Low Quality

LTE Long Term Evolution

LTE-A LTE-Advanced

M2M Machine to Machine

MAC Medium Access Control layer

MCS Modulation and Coding Scheme

MF Maximum Fairness

MFR MAC Footer

MHR MAC Header

MILP Mixed Integer Linear Programming

MIP Mixed Integer Programming

MME Mobility Management Entity

MPDU MAC Payload Data Unit

MSK Minimum Shift Keying

MWSN Metropolitan Wireless Sensor Network

MSDU MAC Service Data Unit

MTC Machine Type Communications

MTCD Machine Type Communications Device

MTCG Machine Type Communications Gateway

MTO Many-to-One

MTO-RR Many-to-One Route Request

NLOS Non Line-of-Sight

NoE Network of Excellence

NOS Network Operating System

NS3 Network Simulator v.3

OFDM Orthogonal Frequency Division Modulation

OFDMA Orthogonal Frequency Division Multiple Access

OI Overload Indicator

OPL Optimization Programming Language

OTA Over-the-Air

O-QPSK Offset Quadrature Phase Shift Keying

PA Power Amplifier

PAN Personal Area Network

PCC Primary Carrier Component

PAPR Peak to Average Power Ratio

PDCP Packet Data Converge Protocol

PDF Probability Density Function

PDCCH Physical Downlink Control Channel

PER Packet Error Rate

PF Proportional Fair

PHY Physical layer

PHR Physical Header

PLR Packet Loss Rate

PMF Probability Mass Function

PPDU Physical Protocol Data Unit

PSD Power Spectral Density

PSDU Physical Service Data Unit

P-GW Packet data network Gateway

QCI QoS Class Indicator

QoE Quality of Experience

QoS Quality of Service

RA Random Access

RACH Random Access Channel

RAN Radio Access Network

RB Resource Block

REM Radio Enviromental Map

RF Radio Frequency

RFC Request for Comment

RLC Radio Link Control

RN Relay Node

RNTP Relative Narrowband Transmit Power

RPL Routing Protocol for Low power and Lossy Networks

RQAP Rectangular Quadratic Assignment Problem

RR Round Robin

RRA Radio Resource Assignment

RRC Radio Resource Control

RREC Route Record

RREP Route Replay

RREQ Route Request

RRH Radio Remote Head

RRM Radio Resource Management

RSSI Received Signal Strength Indicator

RTT Round Trip Time

Rx receiver

SAR Specific Absorption Rate

SCC Secondary Carrier Component

SDN Software Defined Network

SDWN Software Defined Wireless Network

SER Symbol Error Rate

SF Superframe

SHR Synchronization Header

SI System Information

SIFS Short Inter Frame Spacing

SINR Signal-to-Interference-and-Noise Ratio

SIR Signal-to-Interference Ratio

SC-FDMA Single Carrier Frequency Division Multiple Access

SC Small Cell

SCF Small Cell Forum

SINR Signal to Interference plus Noise Ratio

SMRF Stateless Multicast RPL Forwarding

SNR Signal-to-Noise Ratio

SON Self-Organized Network

SR Source Routing

SRB Signalling Radio Bearers

SRS Sounding Reference Signal

S-GW Serving Gateway

TB Transport Block

TDMA Time Division Multiple Access

TDPS Time Domain Packet Scheduling

TG Task Group

TTI Transmission Time Interval

TLM Wideband Top Loaded Monopole

Tx transmitter

UDP User Datagram Protocol

UE User Equipment

UL Uplink

UP User Priority

URBA User Resource Block Allocation

UTM Universal Transverse Mercator

VoIP Voice over IP

WG4 Working Group 4

WMTS Wireless Medical Telemetry System

WPAN Wireless Personal Area Network

WSN Wireless Sensor Network

List of Figures

List of Tables

Introduction

This thesis focuses on the paradigm of *Heterogeneous Networks*, whose concept is proposed in next chapter, along with the motivations supporting the study performed and the research approach followed. Since a significant part of the thesis results were obtained within the European FP7 Network of Excellence (NoE) "Newcom♯", its structure and main goals are presented hereafter. Finally, the description of the thesis outline concludes this introduction. The Ph.D. was performed in the the Department of Electrical, Electronic and Information Engineering "Guglielmo Marconi" (DEI) at the University of Bologna (Italy). A large part of the contributions presented in this dissertation have been produced in collaboration with different universities and research centers along with periods of stay as visiting researcher over the three-year Ph.D. period.

Motivation

In the last 3-5 years the Internet of Things (IoT) became a paradigm very well know even outside the telecommunication specialist community. Among the plethora of different definitions of IoT, in this context the more interesting is the one provided by

International Telecommunication Union (ITU) [1], i.e. "A dynamic global network of infrastructure with self-configuring capabilities based on standard and inter-operable communication protocols where physical and virtual 'things' have identities, physical attributes and virtual personalities, use intelligent interfaces and are seamlessly integrated into the information network". In a sense, the latter definition is the *leitmotiv* of this Ph.D., in fact according to this vision it is very important to understand the performance limits, advantages and disadvantages to use a certain approach or another. In this thesis different approaches to IoT concept are analyzed, standard and proprietaries solutions are tested and results highlight when it is more convenient to use one solution against another. One purpose of this thesis is focus on short to medium term research: solution already existing on the market are used and a particular emphasis is given to the implementation issues and to development tools.

Context of the Thesis: Newcom♯

NEWCOM♯ (Network of Excellence in Wireless Communications) was a project funded under the umbrella of the 7th Framework Program of the European Commission. NEWCOM♯ pursued long-term, interdisciplinary research on the most advanced aspects of wireless communications like Finding the Ultimate Limits of Communication Networks, Opportunistic and Cooperative Communications, or Energy- and Bandwidth-Efficient Communications and Networking.

Complementarily, NEWCOM♯ aimed to build the so-called European Lab on Wireless Communications for the Future Internet (EuWIn), a federation of three sites in three European Countries that will host researchers working on a number of topical areas like Advanced Radio Interfaces, the Internet of Things, and Flexible

Communication Terminals.

The NEWCOM♯ project is structure in 4 tracks:

- Track 1 - Theoretical Research Issues (R&I)
- Track 2 EuWIn: The European Lab of Wireless Communications for the Future Internet (R&I)
- Track 3 Training, Dissemination and Human Capital (S&I)
- Track 4 Management (M)

As the tracks' title suggested the research activities have been performed in track 1 and track 2. Track 1 has been mainly devoted to theoretical research activities; meanwhile track 2 has been devoted to experimental activities. The main contribution of this this Ph.D. have been performed in WP1.3 and WP 2.2.

EuWIn

Due to its novelty and the potential impact of EuWIn onto European research and industrial context, in this subsection the main goals and a briefly description are given. EuWin aims to create a European reference lab on wireless communications where an experimental validation and realistic performance assessment of a selected subset of theoretical research activities conducted in Track 1. On one hand, EuWIn is expected to further strengthen the integration of partners research activities and agendas, both at the theoretical and experimental levels; and, on the other, to foster Industry-academia cooperation, dissemination and liaison by making academic research closer to industrial needs and interests. Furthermore, the lab provides a unique training

environment for a new generation of researchers with solid skills and background in experimental research.

Three main sites were selected to host EuWIn: CTTC in Barcelona (Spain), CNRS/EURECOM in Sophia-Antipolis (France), and CNIT/Univerisity of Bologna (Italy).

EuWIn@CNIT/Bologna

Networking technologies for the Internet of Things (IoT) with mobile clouds, where networks characterized by mobile nodes that interact with the fixed infrastructure are investigated. Large scale wireless sensor networks are studied and modelled in the context of Smart City as well as indoor applications. Lab facilities allow the implementation of different routing and cooperative signal processing algorithms and the measurements of different metrics (delays, consumed energy, packet losses, throughput) over the network. The lab targets also the implementation of delay tolerant networking paradigms, through the mobile component of the network made accessible; the mobility patterns of mobile clouds are measured and modeled. Finally, indoor localization algorithms based on UltraWideBand (UWB) nodes are studied, in cooperation with the EuWIn@CTTC site. The HW/SW platforms are remotely accessible.

Structure of the Thesis and Approach

The description of the goals of this thesis, given in previous sections, and of the approach followed highlights the complexity of the investigated topic and the challenges behind it.

During this Ph.D. two different approaches have been used: experimental and theoretical. The experimental approach takes advantages from the use of EuWIn, hence the main achievements obtained in short range solution for IoT have been obtained through experimental results. Meanwhile, due to its complexity a theoretical/simulation approach to cellular network solution for IoT have been used.

Chapter 1 is devoted to the IoT concept: applications, issues and challenges are addressed. A focus on the IoT standardization world is given. Finally, the Machine to Machine (M2M) concept is presented and the traffic model used in this dissertation is shown.

In Chapter 2 IoT short range solutions are addressed. Different standards and proprietary solutions are described. This chapter is mainly devoted to experimental activity, hence most of the results have been obtained through EuWIn.

As it is well known M2M application are of paramount important in the cellular world. Chapter 3 is devoted to present the main issues and research challenges related to M2M applications in cellular network with a special focus on 4G networks.

Chapter 4 presents results obtained mainly in a joint research activity within the track 1 of NewCom♯ project. In particular, a mathematical framework is provided and simulation results are given when M2M application are running on Long Term Evolution (LTE) system. This work is mainly focus on Radio Resource Management (RRM).

Finally, Chapter 5 is devoted to LTE-Advanced (LTE-A) network, and in particular it describe the Carrier Aggregation feature, its implementation on a network simulator and a mathematical model for RRM in LTE-A network.

Chapter 1

IoT and M2M

In [1] ITU, highlight the huge impact of the IoT above the Internet. In fact, Internet and modern communications technologies introduced the possibility to be connected *any time communication*, on the move, night and daytime (first dimension); *any place communication*, indoor with or without the computer and outdoor (second dimension). IoT adds the third dimension: *any thing communication*; between computers, human to human, human to thing, thing to thing. It is clear that Machine Type Communications (MTC) and M2M applications are key components of the IoT concept. MTC are defined as a form of data communications which do not need human interaction. The number of human users of mobile networks is coming to saturation, while the M2M domain is seen as a new revenue opportunity. In general, the esteems agree that the number of M2M connections will grow in the coming years [2]. Market researches such as [3] [4] predict up to 800 million machine to machine (M2M) connections by 2015, while standardization organizations argue for very high densities of M2M devices in broadband bandwidths [5]. Mobile operators like Telnor, Vodafone and Telefonica have created dedicated units or even companies to focus on M2M business opportunities. Similarly, mobile vendors are creating their own visions, such

as the Ericsson's "50 billion connected devices". Large Information Technology (IT) vendors like IBM or HP also have ambitious plans to connect and exploit information generated by trillions of sensors. At the present time, the most interesting applications from the commercial point of view are related to smart grids, automatic water and gas meter readings. However, the M2M application space is vast and includes security, health monitoring, remote management and control, intelligent transport systems, ambient assisted living, etc. In addition, M2M is more than just connected devices sharing data, but it is also about collecting and distributing the data efficiently, often in real time and with desired Quality of Service (QoS) requirements, in terms of e.g. latency. The communication network plays an important part of the ecosystem and its ability to support M2M services and traffic requirements, will be crucial for such a distributed setup.

1.1 IoT Applications

This section provides an overview of major applications of the IoT paradigm. The main application fields considered are:

- Smart Cities: the IoT can help the design of smart cities e.g., monitoring air quality, discovering emergency routes, efficient street lighting, watering gardens etc.
- Prediction of natural disasters: the combination of sensors and their autonomous coordination will help to predict the occurrence of land-slides or other natural disasters and to take appropriate actions in advance.
- Industry applications: the IoT can find applications in industry e.g., managing a

fleet of cars for an organization. The IoT helps to monitor their environmental performance and process the data to determine and pick the one that needs maintenance.

- Water scarcity monitoring: the IoT can help to detect the water scarcity at different places. The networks of sensors, might not only monitor long term water interventions such as catchment area management, but may even be used to alert if an upstream event, such as the accidental release of sewage into the stream, might have dangerous implications.

- Medical applications: the IoT can also find applications in medical sector for saving lives or improving the quality of life e.g., monitoring health parameters, monitoring activities, support for independent living, monitoring medicines intake etc.

- Agriculture application: a network of different sensors can sense data, perform data processing and inform the farmer through communication infrastructure e.g., SMS about the portion of land that needs particular attention. This may include smart packaging of seeds, fertilizer and pest control mechanisms that respond to specific local conditions and indicate actions. Intelligent farming system will help agronomists to have better understanding of the plant growth models and to have efficient farming practice by having the knowledge of land conditions and climate variability. This will significantly increase the agricultural productivity by avoiding the inappropriate farming conditions.

- Smart security: the IoT can also find applications in the field of security and surveillance e.g., area surveillance, tracking of people and assets, infrastructure

and equipment maintenance, alarming etc.

- Smart metering and monitoring: the IoT design for smart metering and monitoring will help to get accurate automated meter reading invoice delivery to the customers. the IoT can also be used to design such scheme for wind turbine maintenance and remote monitoring, as well as gas, water and environmental metering and monitoring.

- Smart Homes: the IoT can facilitate the design of smart homes e.g., energy consumption management, interaction with appliances, detecting emergencies, home safety and security etc.

- Intelligent transport system design: the Intelligent transportation system will provide efficient transportation control and management using advanced technology of sensors, information and network. The intelligent transportation can have many interesting features such as non-stop electronic highway toll, mobile emergency command and scheduling, transportation law enforcement, vehicle rules violation monitoring, reducing environmental pollution, anti-theft system, avoiding traffic jams, reporting traffic incidents, smart beaconing, minimizing arrival delays etc.

1.1.1 Issues and challenges

The IoT can change the shape of the Internet and can offer enormous economic benefits but it also faces many key issues and challenges. Some of them are briefly described below.

- **A Low Power Communication Stack.** The majority of objects are not

able to draw power from the mains, and have batteries at best. This means that finding enough energy to power processing and communication is a major challenge. Whilst we are ready to recharge our mobile phones on a daily basis, changing batteries in millions of objects is impractical. Any stack must therefore exhibit a low average power consumption.

- **A Highly Reliable Communication Stack.** Although the Internet is a best-effort transport medium, protocols incorporate error detection, retransmissions and flow control. These techniques are applied at various protocol layers concurrently, which leads to a reliable end-to-end experience, albeit in a rather inefficient way. For the IoT to merge seamlessly into the Internet, it is necessary to offer the same reliability we are used to on the Internet with the additional requirement that is the highest possible efficiency.

- **An Internet-Enabled Communication Stack.** Enabling another dialect of the Internet has profound implications on the protocol design. The Internet is exhibiting emergent behavior today because communication is bidirectional; it is hence of utmost importance to ensure that communication from objects but also towards objects is facilitated. Furthermore, the explosion of the Internet can arguably be attributed to the ability of any machine around the world to talk to any other machine, all this facilitated by one universal language, IP; it is hence of paramount importance that the IoT is IP enabled.

1.2 IoT scenarios - Heterogeneous networks

In the past years, IoT market players tried to build silos or vertical applications. This means that for each vertical IoT application they maintain the entire communication chain from gathering the data to provide the information in aggregated form through web applications. This behaviour results on a huge amount of both standard and proprietary solutions. In fact, the main challenge for the future of IoT is for sure the needs to interconnect and integrate heterogeneous networks. The standardization bodies are already spending effort to try to contain the phenomenon. The integration of heterogeneous network for IoT face several challenges, including:

- integrate together communication protocols into a IP-based environment
- integrate communication protocols used in different application layer

1.3 Standardization players

This section is given an overview on the main standardization players that are very active on the IoT.

1.3.1 3GPP

As it is well known, 3GPP is a standardization body for cellular network standards. In the last years, it has been growing attention on IoT, according to this several functionality M2M related have been added in LTE and LTE-A releases starting from R10.

1.3.2 ETSI

ETSI is a pan-European standards producers for ICT. In the past it has been provided standard for fixed, mobile, radio and internet technologies. ETSI already spent a huge effort on IoT contest, it published documents in different fields, e.g. smart metering, smart grid, Internet of vehicle and so on. However, the main focus of ETSI is on system level platform and in particular:

- end-to-end security
- abstraction layer and data models
- define procedure and model for M2M networks inter-operability
- define inter-operability with the 3GPP cellular networks.

1.3.3 oneM2M

oneM2M is a worldwide Partnership Project that has as partner ETSI, Association or Radio Industries and Business (ARIB - Japan), China Communications Standard Association (CCSA - China), Telecommunications Technology Association (TTA - Korea), Telecommunication Technology Committee of Japan (TTC - Japan), Alliance for Telecommunications Industry Solutions (ATIS - US). Moreover, several industry organization partners have been joined this project, like **HGI!** (**HGI!**) and Open Mobile Alliance (OMA). The main purpose and goal of oneM2M is to develop technical specifications which address the need for a common M2M Service Layer that ca be readily embedded within various hardware and software, and relied upon to connect the myriad of devices in the field with M2M application servers worldwide.

1.3.4 CEN/CENELEC

CEN/CENELEC play a complementary roles in the development for IoT standards with ETSI. The primary tasks for this two European standardization bodies are:

- integrate sensor data RFID driven system to enhance their performance and effectiveness
- define application system that using ubiquitous sensor networks
- integrate smart object on the Future Internet with particularly focus on object discovery services.

1.3.5 IEEE

Several IEEE associations have been dealing with IoT context. Within the IEEE societies several standards have been published spanning from Cloud Computing, to eHealt, eLearning and Intelligent Transportation Sytems. However, one of the main achievement in the standardization for IoT is for sure the publication of IEEE 802.15.4 which is the 'de facto' standard for several M2M application protocols nowadays.

1.3.6 IETF

IETF is a worldwide association structured in different working group according to the topic they address. Indeed in the IoT context the most valuable product is the adaptation of Internet Protocol v6 (IPv6) for embedded devices, i.e. IPv6 over Low power Wireless Personal Area Networks (6LoWPAN). Moreover, IETF released

different Request for Comment (RFC) on Routing Protocol for Low power and Lossy Networks (RPL).

1.3.7 ITU-T

ITU-T is involved in the IoT standardization activities since 2005 when the report "The Internet of Things" was published. The interest of ITU-T span from IoT applications to terminology, requirement, business models as well as security and testing. Moreover several IoT related study group have been formed within the ITU-T.

1.4 M2M Traffic Models

In this section a briefly description of M2M applications and services is presented, moreover some references on M2M traffic model are given. As for the traffic models, contributions in literature for MTC are still little. Among them, in this section are highlighted the advancements achieved in the context of the FP7 Lola Project, where different M2M applications are analysed to found a model that generally describes the M2M traffic. The adopted model is based on Markov Chains and on a general On-Off model with different distribution for the packet sizes and inter-arrival times of packets (LogNormal, Gaussian, Weibull, Constant size). Also 3GPP has devoted efforts to the classification and modelling of M2M traffic, in 3GPP TSG RAN WG1. Additional work can also be found in this contribution in literature [6].

The peculiarities of M2M devices are addressed in the 3GPP Technical Report TS22.368 [7], where a detailed prediction and classification for the M2M services is

presented. In the following the main characteristics of the M2M services are summarized:

- The number of M2M devices is expected to be 1-2 order of magnitude larger than the number of Human to Human (H2H) devices
- Currently the M2M traffic is almost uplink
- A M2M transmission session is short in time, but the sessions are frequently initiated
- In each session just few packets are sent and, in general, those packets are expected to be very short
- Several M2M applications are insensitive to delay.

Another degree of complexity in modelling the M2M traffic is related to the possibility of aggregate data. The same M2M application running on the same network protocol can produce two different traffic patterns if data aggregation is performed or not.

In [8] and [9] the M2M traffic models are studied more in details. The M2M traffic model generally adopted in this thesis is a typical On-Off model and it is defined in the follow. Figure 1.1 shows the state diagram of the traffic model of a M2M device, which is based on three states:

- OFF State: in this state the devices are in a deep sleep mode and only a very low power clock is running. The devices move to the ON state when a timer expires.

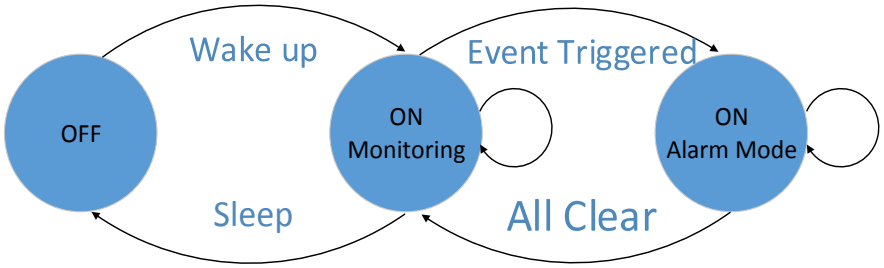

Figure 1.1: M2M state diagram

- ON/Monitoring Mode: the devices in this state generate information on a time-driven fashion. In practice, the device monitors some physical variable and sends periodical information.

- ON/Alarm Mode: this model depends on the application and type of sensor the device is equipped with. In general, the device is triggered by a particular event, when there is the need to send more frequent information than in the monitoring mode. For instance, a temperature sensor in a building provides regular information, e.g., every 5-10 minutes, on the temperature in the building. However, if the temperature exceeds a certain threshold, this may be associated to a fire alarm, so that the device enters the alarm mode and sends information every 1-5 seconds.

1.5 Conclusions

In this chapter the definition of IoT was given. The main trends, applications and challenges have been addressed. Furthermore, a view on the standardization landscape for IoT has been given. Then a focus on M2M world has been presented. In this context, the main advancements have been referenced and the M2M device

communication model used in this thesis has been introduced.

Chapter 2

IoT short range solutions

This chapter aims at presenting three communication protocols stacks for IoT short range applications. More in details, it presents two standard solutions (i.e. Zigbee [10] and 6LowPan [11]) and a Software Defined Network (SDN) approach called Software Defined Wireless Network (SDWN). All those communication protocols stacks rely on IEEE 802.15.4 standard [12] for Physical layer (PHY) and Medium Access Control layer (MAC) layers. For that reason section 2.1.1 is dedicated to the common PHY and MAC layers where the specification of IEEE 802.15.4 standard are briefly summarized. This chapter is not intended to be a comprehensive survey on all the IoT short range solutions. On the opposite, the author choose to focus on these solutions since IEEE 802.15.4 based Wireless Sensor Network (WSN) solutions seem to be the most used in industrial applications. The rest of the chapter is organized as follows: section 2.1 briefly describes the standard of interest; meanwhile in section 2.2 the testing platform is presented. Sections 2.4 and 2.5 presents a performance analysis: i) comparison between the three protocol stacks introduced above; ii) a study of co-existence issue between IEEE 802.11 and Zigbee; iii) tools usage for fast deploying a real WSN.

2.1 Standards

In this section, the WSN protocol stack of interest are presented, a briefly introduction on the common PHY and MAC layers in also given.

2.1.1 IEEE 802.15.4

IEEE 802.15.4 is 'de facto ' standard for WSN applications. It is a wireless technology standardized and optimized for short-range communication, with relaxed throughput and latency requirements, that are also called in WPAN. As anticipated above, the IEEE 802.15.4 Working Group[1] focuses on the standardization of the Layer 1 (L1) and Layer 2 (L2) of the ISO/OSI protocol stack, i.e. PHY and MAC. In the following, are briefly described the main features and characteristics of IEEE 802.15.4 standard. For a exhaustive description refer to the standard [12].

2.1.1.1 IEEE 802.15.4 PHY

The standard specifies 27 half-duplex channels in total. Those channels are define across three frequency bands as follows:

- 868 MHz band, only 0.6 MHz are reserved (it is ranging from 868.0 MHz to 868.6 MHz) and it is used only in Europe. The modulation format is a cosine-shaped Binary Phase Shift Keying (BPSK), with Direct Sequence Spread Spectrum (DSSS) at chip rate 300 kchip/s. Due to the few bandwidth reserved only one channel is defined with a data rate of 20 Kbps.

[1] see the IEEE 802.15.4 web site:http://www.ieee802.org/15/pub/TG4.html

- 915 MHz band, in this case 26 MHz in total are reserved, ranging between 902 and 928 MHz. This band is used only in North America and Pacif area. As modulation format a raised-cosine-shaped BPSK is implemented with DSSS at chip-rate 600 kchip/s. In total 10 channels with 40 Kbps data rate are available.

- 2.4 GHz Industrial Scientific Medical (ISM) band, in total 83.5 MHz are reserved (from 2400 to 2483.5 MHz). This band is worldwide used. The modulation format is half-sine-pulse-shaped Offset Quadrature Phase Shift Keying (O-QPSK) with DSSS at 2 Mchip/s. In total 16 channels are available. The data rate is 250 Kbps.

Regarding the channel bandwidth, in the first two cases is 0.6 MHz where the carriers are separated by 2 MHz; meanwhile in the latter case, the channel bandwidth is 3 MHz (first lobe) and the carriers are separated by 5 MHz. One of the keys of success of IEEE 802.15.4 standard is the low energy consumption. In fact, the standard defines a duty cycle of (up to) 99 % of inactive time. This feature allows networks properly designed to work for months rely on a commercial small size battery supply. The transmission, according to IEEE 802.15.4 standard, is organized in frames. More in details, depending on the purpose, four different frame structures are designated as Physical Protocol Data Unit (PPDU): a beacon frame, a data frame, an acknowledgement frame and a MAC command frame. All those frame structures have in common the following fields: Synchronization Header (SHR), Physical Header (PHR) and a Physical Service Data Unit (PSDU). The latter is composed of a MAC Payload Data Unit (MPDU) which in turn is constructed with a MAC Header (MHR), a MAC Footer (MFR) and a MAC Service Data Unit (MSDU). Only exception is the acknowledgement frame, which does not contain an MSDU. In order to detect the

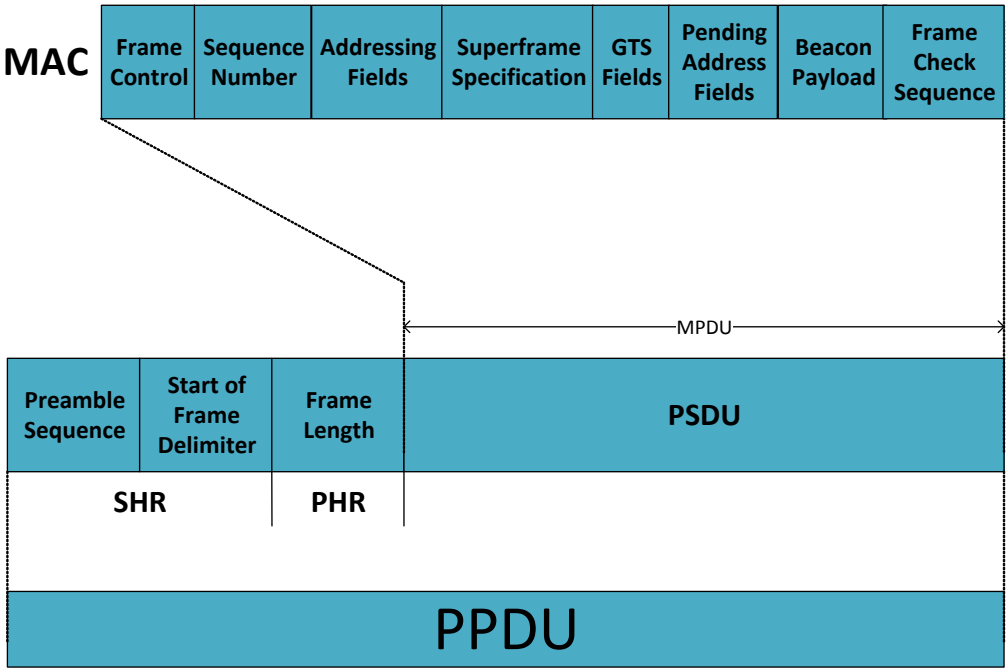

Figure 2.1: IEEE 802.15.4 physical layer frame structure

correctness of received messages, a Cyclic Redundancy Check (CRC) is used. A IEEE 802.15.4 PHY frame example is given in figure 2.1, this in particular is related to the beacon frame.

2.1.1.2 IEEE 802.15.4 MAC

MAC layer provides access control to a shared channel and reliable data delivery. IEEE 802.15.4 MAC layer, together with the Link Layer Controller (LLC), defined the data link layer of ISO/OSI model. The main function of IEEE 802.15.4 MAC layer are: provide support for the possible network topologies described in the standard (i.e. star and peer-to-peer topologies), generate the acknowledgment (ACK) frame, association and disassociation, security control. IEEE 802.15.4 uses a Listen-before-talk (LBT) protocol in order to reduce the probability of collision with other

ongoing transmissions. In fact, it relies on a Carrier Sense Multiple Access with Collision Avoidance (CSMA/CA) algorithm. In the standard two different operational modes are defined, i.e. *beacon-enabled* and *non beacon-enabled*. Unslotted CSMA/CA protocol is used in non beacon-enabled mode. The algorithm is implemented using units of time called backoff periods and it is shown in Fig. 2.2. Each node initializes two variables, NB and NE, for each transmission attempt. NB defines the number of times the CSMA/CA algorithm is required to backoff while attempting the transmission; the initial value is set to zero and cannot be larger than NB_{max}, i.e. equal to 4 by default. Meanwhile, BE ranges between $BE_{min} = 3$ and $BE_{max} = 5$. As it is shown in figure 2.2, BE is used for defining the range of random number of backoff periods, i.e. $range(0, 2^{BE} - 1)$. The node that wants to transmit: i) initializes NB and BE; ii) delays transmission for a random number of backoff periods; iii) performs sensing; iv) checks if the channel is free, in the positive case it transmits; in the negative case it jumps to step v) increases NB and BE and, in case $NB > NB_{max}$ the transmission fails (i.e. node did succeed in accessing the channel), otherwise starts again from step ii). The second operational mode, i.e. *beacon-enabled*, the channel access is managed through a superframe. In this case the node which is appointed to be the network manager, called *coordinator* or *sink*, sends a specific message, i.e. *beacon*, that identifies when a new superframe starts. The superframe structure is shown in figure 2.3. It is composed of: i) Contention Access Period (CAP) which is the portion of superframe where nodes perform CSMA/CA procedure to access the channel; ii) Contention Free Period (CFP), the coordinator allocated a portion of the superframe, aGuaranteed Time Slot (GTS), to a specific node (up to 7 GTSmay be assigned). The standard define GTS use as optional, however it is mandatory to

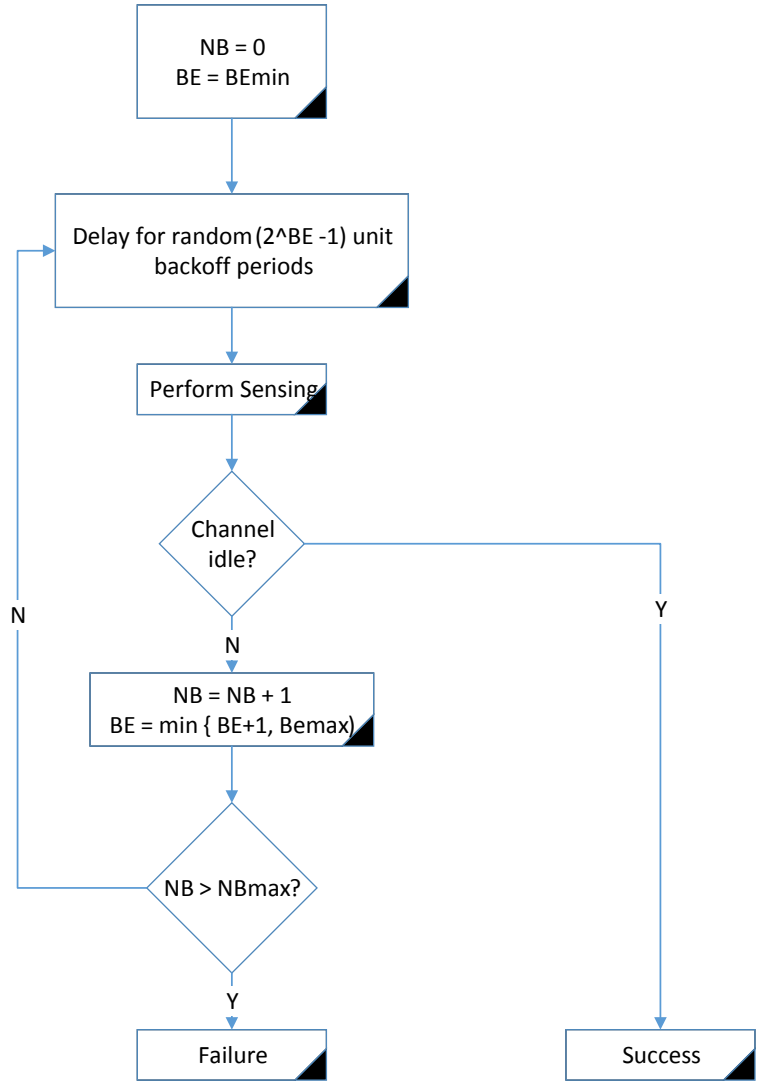

Figure 2.2: IEEE 802.15.4 CSMA/CA algorithm in non beacon-enabled case

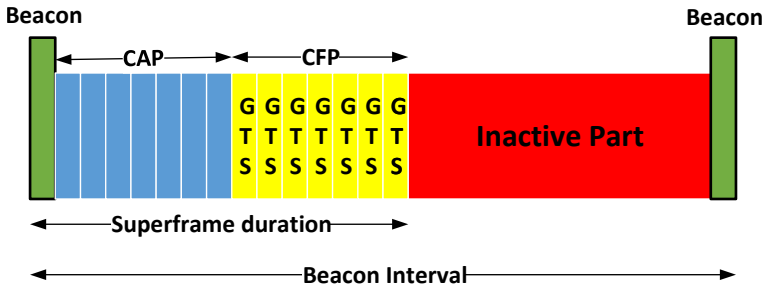

Figure 2.3: IEEE 802.15.4 CSMA/CA algorithm in beacon-enabled case

reserve enough time for CAP phase; iii) in order to reduce nodes' energy consumption an *inactive part* can be reserved. In the last case nodes can switch in sleep mode and saves some energy by turning off some hardware. The CSMA/CA algorithm used in *beacon-enable* mode is slightly different with respect to the former presented. The algorithm it is shown in figure 2.4. In this case the backoff and sensing phase are run $CW = 2$ times.

2.1.2 Zigbee

This section is dedicated to the Zigbee standard, for the scope of this dissertation, here the focus is only on the routing protocols defined by the protocol standard. Other important features, security, application layer are not discussed here. For all those aspects it is suggested to read [10] and [13].

2.1.2.1 Routing: Ad-hoc On-demand Distance Vector (AODV)

ZigBee Alliance proposed a well-known routing protocol as default protocol for IEEE 802.15.4/ZigBee networks: AODV [14]. According to AODV protocol, a node which has data to be transmitted, sends a Route Request (RREQ) using broadcast mode in order to discover the appropriate path. Each device receiving the RREQ packet

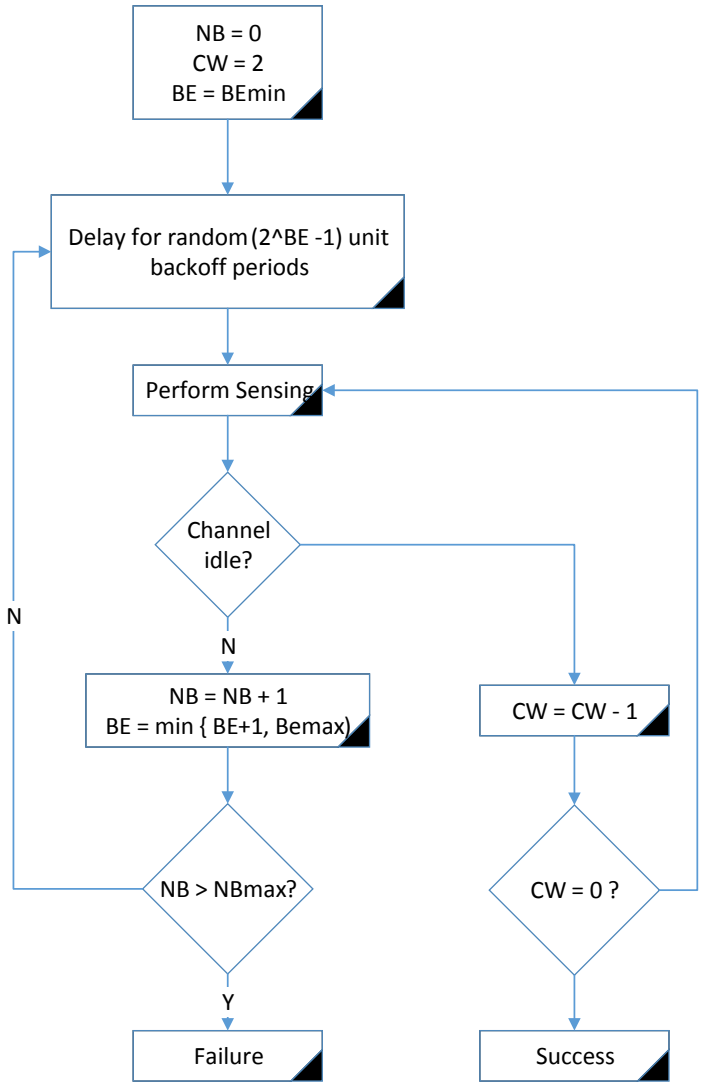

Figure 2.4: IEEE 802.15.4 Superframe structure

retransmits it, by broadcast, until it reaches the destination node. During the process of rebroadcasting the RREQ, intermediate nodes record in their route discovery tables the address of the sender from which the first copy of the broadcast packet was received, and the corresponding link cost (see [13]). The comparison among path costs of packets with the same RREQ allows choosing the best path. Once the destination node receives the RREQ, it responds by sending a Route Replay (RREP) packet in unicast back to the source along the reverse path.

In case of link failures, or expiration of the entry into the routing table, the device repeats the RREQ/RREP transmission in order to refresh the route.

The RREQ/RREP procedure is used only for the transmission of unicast data packets.

In the case of multicast transmission, a path between the coordinator and the multicast group should be established. The standard implementation uses AODV to establish the route between the coordinator and the multicast group; in this case the RREQ packet, sent in broadcast, includes the address of the multicast group to be discovered. Nodes in the network that are linked to the target multicast group, send a RREP back to the coordinator through the selected path. The latter path is used for the transmission of query packets. In the uplink direction, that is from the queried nodes to the coordinator, nodes use the same protocol as for the unicast transmissions.

2.1.2.2 Routing: Many-to-One (MTO)

MTO routing allows to establish a tree topology, rooted at the coordinator. In order to form and maintain the tree, the coordinator periodically sends a Many-to-One

Route Request (MTO-RR) packet in broadcast. Each node, receiving a MTO-RR before retransmitting it, reads the accumulated path cost (i.e., the sum of the costs of the links of the reverse path toward the coordinator) included in the packet, and selects the next hop toward the coordinator. In particular, if a node receives several MTO-RRs from different nodes, it elects as a next hop the node characterised by the minimum total path cost to the coordinator. At the end of this MTO-RR transmission, all nodes in the network are aware of the next hop to be used in order to transmit their data to the coordinator, that is their parents in the tree. However, if the coordinator wants to know the path to reach a specific node in the network (or a set of nodes by multicasting), MTO routing should be combined to Source Routing (SR). After the MTO-RR transmission, once a node has a data packet to be sent to the coordinator, it first sends a *Route Record* (RREC) packet through the selected path. Each node in the path receiving the RREC packet, adds in the relay list field its own address and forwards the new RREC packet toward the coordinator. The coordinator analyses the RREC packet and stores that information in the Source Route Table. Each time the coordinator has to send a packet to a node, it reads the relay list from this table and sends the packet through the selected path.

In order to let nodes compute the link costs to be used in the MTO routing for the selection of the path, each node in the network periodically sends *Link Status* packets in broadcast at one hop. Each node receiving the Link Status packet computes the link cost, being a function of the link quality indicator of the received packet [15].

Even though MTO-RRs are periodically sent by the coordinator and are not generated on-demand (which would make the protocol pro-active), ZigBee saves the re-active feature through the use of Ad hoc On-Demand Distance Vector (AODV)

protocol [14], when needed. In particular, in case of link failure, AODV is used for discovering a new path toward the destination. According to AODV, a node searching for a destination node sends a *Route Request* packet (RREQ) in broadcast, which is retransmitted by all receiving nodes until it reaches the destination. During the process of rebroadcasting the RREQ, intermediate nodes record in their route discovery tables the address of the RREQ sender, and the corresponding total cost of the reverse path to the source. The comparison among paths' costs of packets related to the same RREQ allows choosing the best path. Once the destination receives the RREQ, it responds by sending a RREP in unicast back to the source along the reverse path.

2.1.3 6LowPAN

The IETF IPv6 over Low power Wireless Personal Area Networks (6LoWPAN) working group published first document in August 2007 [16]. Among the several available IPv6 over Low power Wireless Personal Area Networks (6LoWPAN) solutions, in this dissertation is used μIPv6 stack, implemented in Contiki operating system[2] and ported it on the Flextop platform, i.e. the testbed platform used to compare the protocols.

2.1.4 Protocol Stack

The 6LoWPAN protocol stack is shown in Fig. 2.5. Due to the fact that the direct integration between IPv6 and IEEE 802.15.4 lower network layers is not possible, the

[2]Contiki source code, [Online] January 2014, http://sourceforge.net/projects/contiki/files/Contiki/

IETF 6LoWPAN working group has specified an adaptation layer and header compression scheme for transmission of IPv6 packets over IEEE 802.15.4 radio links. The purpose of adaptation layer is to provide a fragmentation and reassembly mechanism that allows IPv6 packets (Maximum Transmission Unit for IPv6 is 1280 bytes) to be transmitted in IEEE 802.15.4 frames, which have a maximum size of 127 bytes of the MPDU. At network layer, the IPv6 routing protocol, RPL, is used (see below for details). At the transport layer, User Datagram Protocol (UDP), providing best-effort quality of service, is applied. Finally, at the application layer, Constrained Application Protocol (CoAP) is present.

2.1.4.1 The Routing Protocol

According to RPL, a Destination-Oriented Directed Acyclic Graph (DODAG), where each node may have more than one parent toward the root, is built [17]. One of the parents is called preferred parent, and it is used for routing toward the root. In the rest of this chapter, the root node is also referred as coordinator.

The topology is set-up based on a *rank* metric, which encodes the distance of each node with respect to its reference root, as specified by the *objective function*. A common metric, used in the performance analysis in the follow sections, is the hop count metric; therefore the rank of a given node represents the number of hops separating the node from the coordinator. Paths in the DODAG are selected in order to minimise the rank.

RPL nodes exchange signaling information in order to setup and maintain the DODAG. The construction of DODAG is initiated by the root that sends DODAG Information Object (DIO) messages to its neighbours to announce a minimum rank

value. Upon receiving a DIO message, an RPL node will: i) update the list of its neighbors; ii) compute its own rank value; iii) select its preferred parent used as next hop to reach the root as the strongest one (i.e., the one from which it received the largest power); iv) start transmitting DIO messages, containing its respective rank in the DODAG (a distance to the DODAG root according to the hop-count). RPL nodes may also send DODAG Information Solicitation (DIS) messages when joining the network to probe their neighbors and solicit DIO messages.

Finally, Destination Advertisement Object (DAO) messages are used to propagate the destination information upward along the DODAG. DAO messages are sent in unicast by the RPL node to the selected parent to advertise its address. When a node receives a DAO, it updates its routing table and then this information is used by the DODAG root to construct downward paths. Each router in the path records the route identifier and the corresponding next hop toward the destination.

RPL uses an adaptive timer mechanism, called the Trickle timer, to control the sending rate of DIO messages. The Trickle algorithm implements a check model to verify if RPL nodes have out-of-date routing information. The frequency of the DIO messages depends on the stationarity of the network, and the frequency is increased when the inconsistency is detected. Once the network becomes stable, the Trickle algorithm exponentially reduces the rate at which DIO messages are emitted.

RPL supports both unicast and multicast traffics. In the case of multicast, one solution is using the Stateless Multicast RPL Forwarding (SMRF) protocol. According to the latter, nodes join a multicast group by advertising its address in their outgoing DAO messages, which only travel upwards in the DODAG. Upon reception of message from one of its children, a router makes an entry in its forwarding table for

this multicast address. This entry indicates that a node in the DODAG is a member of the group. This router will then advertise this address in its own DAOs, and relay multicast datagrams destined to this address.

2.1.5 SDN approaches

The first implementation of SDWN was developed in October 2012 [18]. The main idea behind the protocol is to adapt a centralized approach, such as the one proposed in SDN networks, to a wireless environment, thus giving the opportunity to support the flexible definition of rules and topology changes.

2.1.5.1 Protocol Stack

The SDWN protocol stack is shown in Fig. 2.5: PHY and MAC layers are those of IEEE 802.15.4, while upper layers are inspired by the SDN paradigm.

A typical SDWN network is composed of a *controller* device, a *sink* node, as well as several other nodes. The controller gathers the information from nodes, maintains a representation of the network, and establishes routing paths for each data flow. The sink is the only node that is directly connected to the controller, and it acts as a gateway for nodes. In this implementation, the sink coincides with the network coordinator and its protocol stack is equivalent to that of a generic node.

The stack of a generic node is divided into three parts: the Forwarding Layer (FWD), the Aggregation Layer (AGGR), and the Network Operating System (NOS). The MAC layer provides incoming packets to the FWD layer that identifies the type of the packet. Six different types of packets are defined:

- *Data*: generated (delivered) by (to) the application layer;

- *Beacon*: periodically sent in broadcast by all nodes in the network;
- *Report*: containing the list of neighbors of a node;
- *Rule Request*: generated when it receives a packet for handling which it has no information (i.e., the path);
- *Rule Response*: generated by the controller as a reply to the Rule Request;
- *Open Path*: used to setup a single rule across different nodes.

When a non-beacon packet is received by the FWD layer, it is sent to the NOS that searches for the corresponding rule in an appropriate data structure called *Flow Table*. The Flow Table stores all the rules coming from the controller. For each rule, there are three types of action that could be executed: forward to a node, modify the packet, or drop it. If a packet does not match any of the rules in the table, a Rule Request is sent to the controller.

2.1.5.2 The Routing Protocol

The path between the sink and the node for sending/receiving Rule Request/Rule Response packets must be chosen effectively, considering both reliability of the path and its length. Each node constantly stores its distance (in number of hops) from the sink, and the Received Signal Strength Indicator (RSSI) that is the level of power it receives from the next hop toward the sink. During the network initialization, each node is in a quiescent state waiting for messages. When the sink turns on, it sends a Beacon, containing the number of hops from the sink (zero in this case). When a node A receives the Beacon, it performs the following four operations:

- Add the source of the Beacon and the RSSI received in the list of nodes (neighbours table) that are one hop distant from A.
- Analyse the distance contained in the Beacon and the RSSI of the received message, then compare these values to the corresponding stored values: if the number of hops is lower and the RSSI is higher, the source of the Beacon is elected as the best next hop toward the sink, and the values stored in A are updated.
- The Beacon timer is activated and node A will periodically send its own Beacon in broadcast.
- The Report message timer is activated: the neighbours table of A is sent periodically to the sink node using the best next hop toward the sink. After each transmission, the list of neighbors is deleted in order to have an updated view of the network. The Report period must be greater than the period used to broadcast Beacon messages (Beacon period).

The information included in the Report messages are used by the controller to create a map of the network. Based on this representation, the controller is able to respond to Rule Requests and to decide the routing paths for data packets, while Rule Request will keep following the previously discovered path.

The actual implementation of the controller uses Dijkstra's routing algorithm to solve Rule Requests. The weight of the edges in the topology representation is a function of the received RSSI.

A possible change in the network is notified to the controller using Report messages. As specified above, the controller obtains periodically all the lists of neighbours,

according to the Report period that is bounded by the Beacon period. By decreasing the latter period, a faster responsiveness to environmental changes could be obtained to the detriment of having larger overhead.

In the actual implementation of SDWN, the controller sends a Rule Response only after receiving a Rule Request from a node and rules contained in the nodes expire after a configurable period of time. Therefore, at the end of this period, the controller receives a new Rule Requests for the unmanageable packets.

As previously mentioned, more than one action can be executed for an incoming packet, thus achieving the multicast communication. By performing multiple actions, the controller is able to clone an incoming message into multiple outgoing messages. Unfortunately, a drawback of this approach is that the multicast is locally executed by transmitting a series of unicast messages. In other terms, the broadcast nature of the wireless communication is not exploited.

2.2 Testing platform: EuWIn@UniBO

EuWin is a three site laboratory develop within the FP7 project NoE Newcom#. The three site are: Eurecom - Sophie Antipolis (FR), CTTC - Castelldefels (ES) and University of Bologna - Bologna (IT). Three testbeds are available at UniBO: FLEXTOP, DATASENS and LOCTEST. [19] give an exhaustive description of the entire laboratory, while for the aims of this dissertation only FLEXTOP and DATASENS testbed are described.

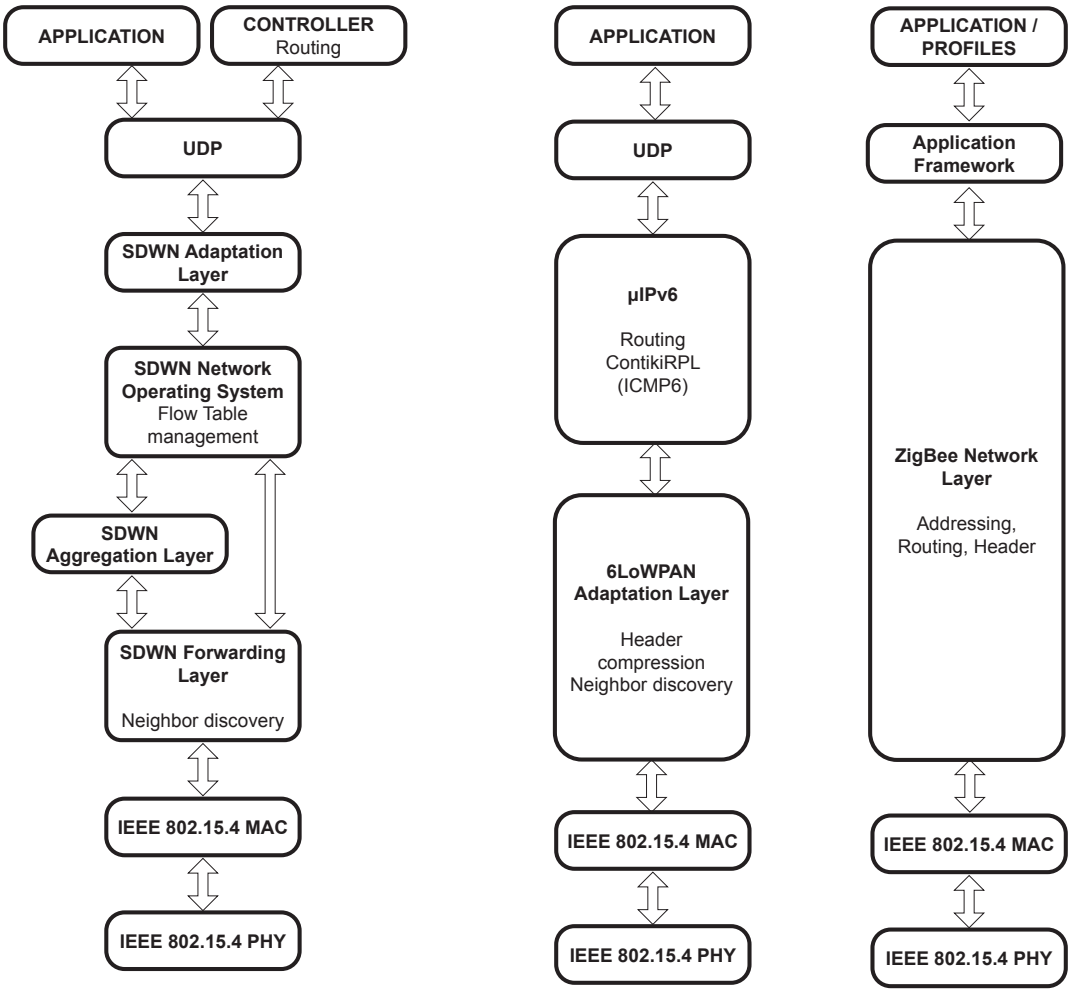

Figure 2.5: Protocol architectures: SDWN (on the left), 6LoWPAN (in the center), and ZigBee (on the right).

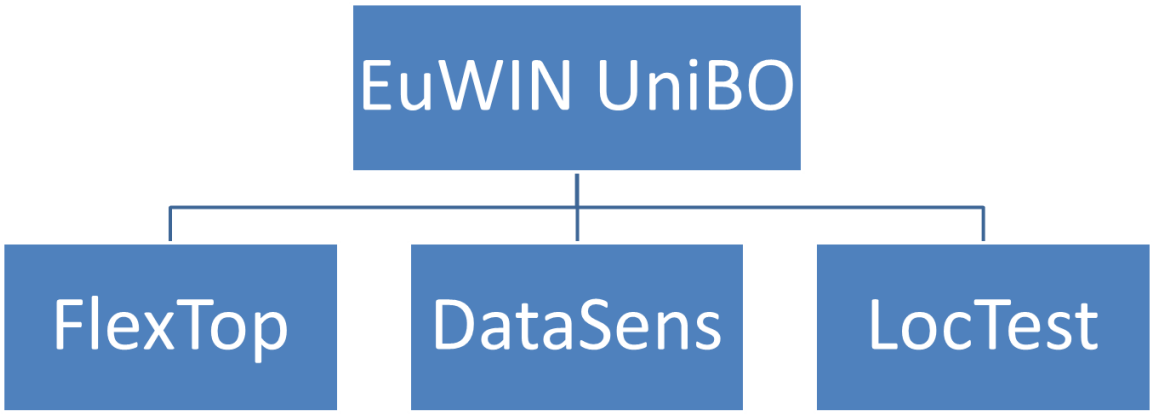

Figure 2.6: The EuWInUniBO site platforms.

2.2.1 The FLEXTOP testbed

The general architecture is shown in Fig. 2.7.

FLEXTOP is a platform composed of (up to) one hundred programmable wireless nodes and a dedicated software environment. The radio transceivers are manufactured by Texas Instruments and are IEEE 802.15.4 compliant (PHY and MAC). The hardware architecture of the wireless nodes have been designed by CNIT/UniBO in collaboration with Embit srl, an Italian SME that acts as design center for Texas Instruments. The nodes have been jointly conceived by CNIT/UniBO and Embit in order to permit Over-the-Air (OTA) programming of the firmware that implements the protocol stack. Through this platform any protocol stack compatible with 802.15.4 can be tested (e.g. Zigbee, or 6lowPAN as proposed by many IoT developers, etc.).

FLEXTOP is a remotely accessible testbed. While it is deployed at the premises of the University of Bologna, researchers are able to upload their firmware implementing the protocol stack (above MAC) on the wireless nodes, run the experiments and

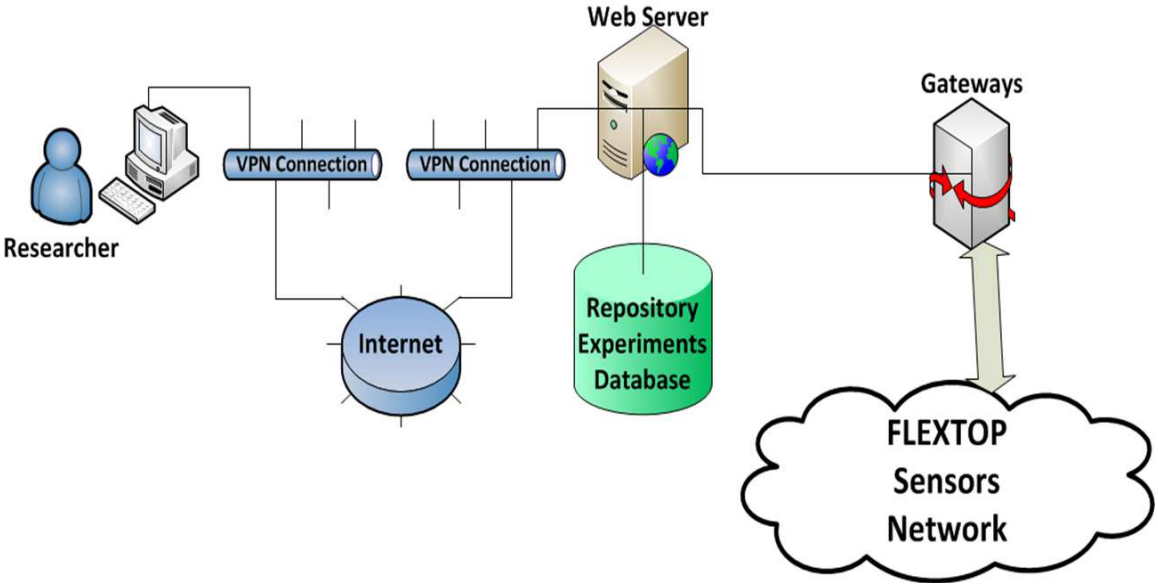

Figure 2.7: Flextop general architecture.

download the log files including all experiments results.

The wireless nodes are deployed according to a fixed grid of positions in a corridor (see Fig. 2.8). However, the researcher using the testbed can set different values of transmit powers achieving very different network topologies (linear, star, double linear, etc.). In particular, nodes can be turned on and off independently during the experiments, and the creation of sub-sets of networks is possible. At start of each experiment, the network automatically measure and generate the matrix of channel gains, which is useful to certify the propagation environment. Experiments run at night, when nobody is allowed to walk in the corridor: therefore the experimental environment is stable for the full duration, making experiment results certified.

The nodes do not carry sensors. However, several types of sensor data can be simulated by programming the application layer of the nodes so as to let them generate data according to specific and realistic environmental conditions. Therefore, the one

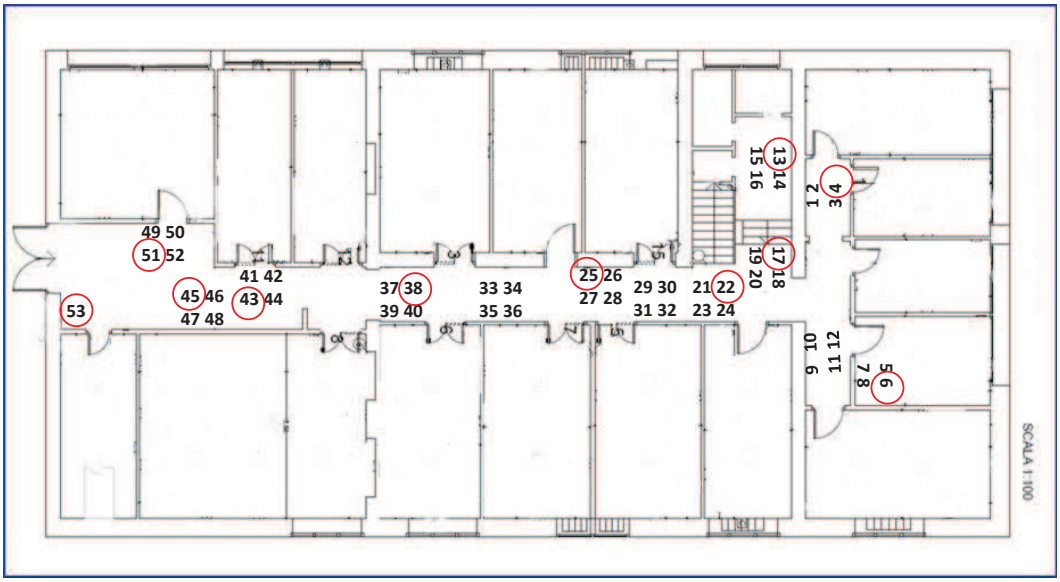

Figure 2.8: Flextop nodes map.

hundred nodes emulate a true and flexible sensor network.

Packet Error Rates, Delays and Throughput are the performance figures that can be captured from the wireless network during the experiments.

Fig. 2.7 represents the architecture of FLEXTOP. Through a VPN connection a researcher can remotely access the lab facilities. Through a web browser it is possible to download the GUI application that is used to send the firmware and send the desired parameters of the experiment. In order to use FLEXTOP a researcher needs a PC with a VPN Client, a browser and a Java Virtual Machine installed.

The server allows the access to the user and it is used as a repository for experiments results; furthermore, on the server there is a database that stores all information related to the experiments (parameters, raw data, firmware, etc.).

Fig. 2.8 shows a map of the building floor and an example of network topology

layout that can be created by selecting specific nodes (52 nodes are active in this case).

Two gateways allow the interfacing between the server and the wireless nodes. They are single board computers based on ARM architecture running on embedded Linux. The aim of these devices is to communicate with the coordinators of the wireless sensor network; the coordinators are connected to the gateways through a wired interface. The gateways also include sniffers which store in log files all information captured from the network (packets sent, source and destination addresses, etc.). The gateways are also responsible for storing the experiments results in a raw file.

Sniffers are TI CC2531 based devices. Through a custom firmware the researchers can directly communicate with the sniffers as well as send commands to them. Coordinators are TI CC2530 based devices. Through the gateways the researcher can send the new firmware to the coordinators. Coordinators manage the firmware performing the OTA download to all devices in the network.

The wireless nodes are also based on TI CC2530. The main specifications of these devices are as follows:

- 256 KB Internal flash + 256 KB external EEPROM
- 8KB of RAM
- Tx power 0 through +20 dBm
- Receive sensitivity tunable from -92 to -102 dBm
- Unique IEEE (extended) address
- Over-the-air programmable

2.2.2 User Interface and remote access procedure

The researchers willing to perform experiments on the FLEXTOP test bed needs to install on them own computer a Java Virtual Machine and a Web Browser; at least 20 MB of free space on the Hard Disk is needed.

A Java Application is used to set the information and parameters of the experiment, as well as to send the firmware image that will be uploaded on the devices using the OTA scheme. In order to obtain the grant to access the FLEXTOP testbed, a researcher has to follow the registration procedure, as described in the following section. Once the user is registered, he receives the private web server URL, which for security reason is accessible from the VPN. The Java application with the installation and user guide will be available on this private web server. This private Web server is also used for sharing some information on the experiments among researchers. The Java Application (GUI) is shown in Fig.s 2.9 and 2.10.

Fig.s 2.9 and 2.10 show some details regarding the Java Application. The researcher has to fill 3 different forms:

- Experiment Meta-data: details about the experiment, title, description, authors and keywords.

- Experiment Setting Data: duration of the experiment in hours, transmission power (in dBm), nodes and coordinator selected to be used in the experiment.

- Firmware upload: this screen will enable the researcher to send the firmware image to the remote server. This image will be OTA uploaded on the FLEXTOP devices.

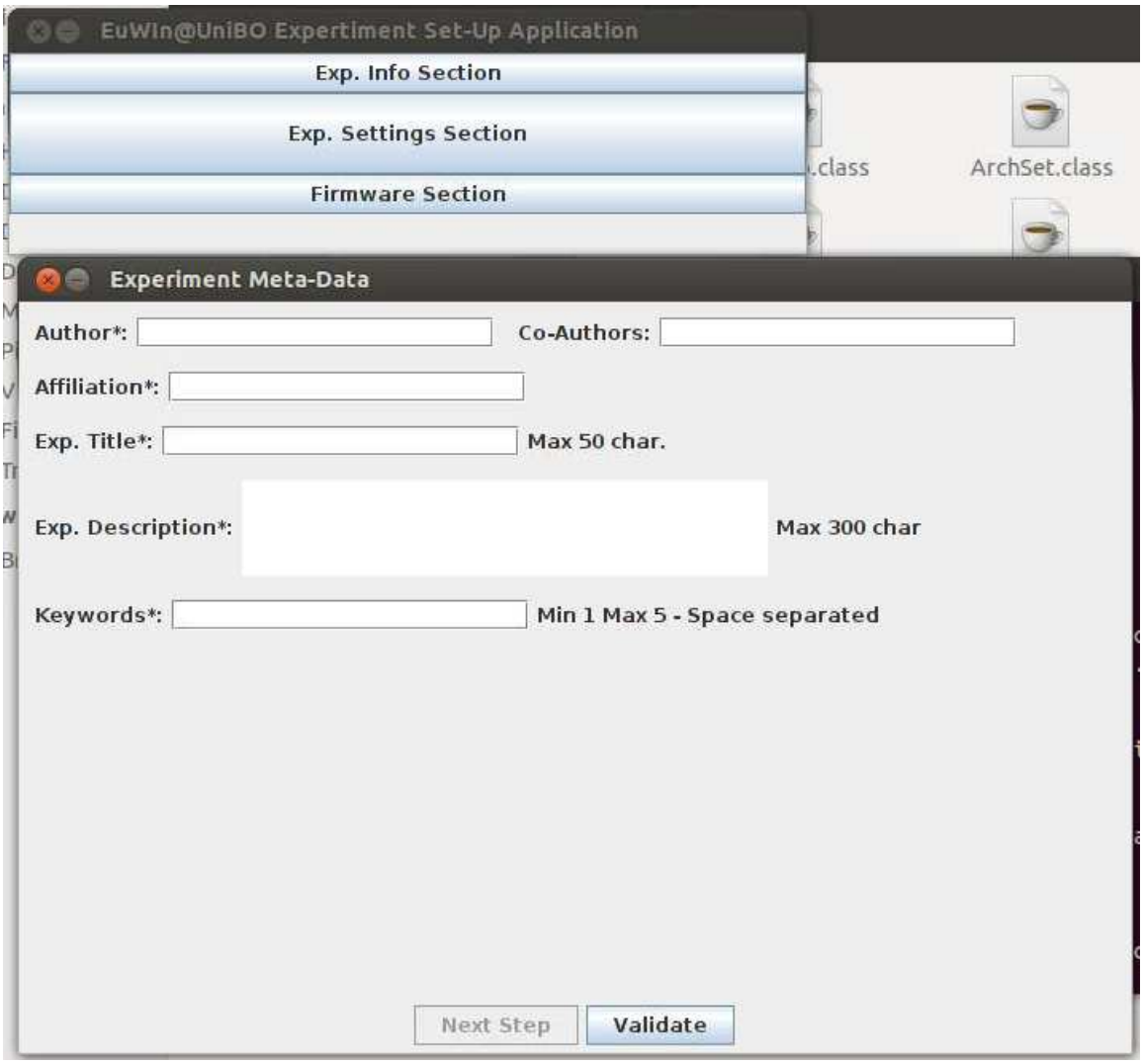

Figure 2.9: Flextop Java Application.

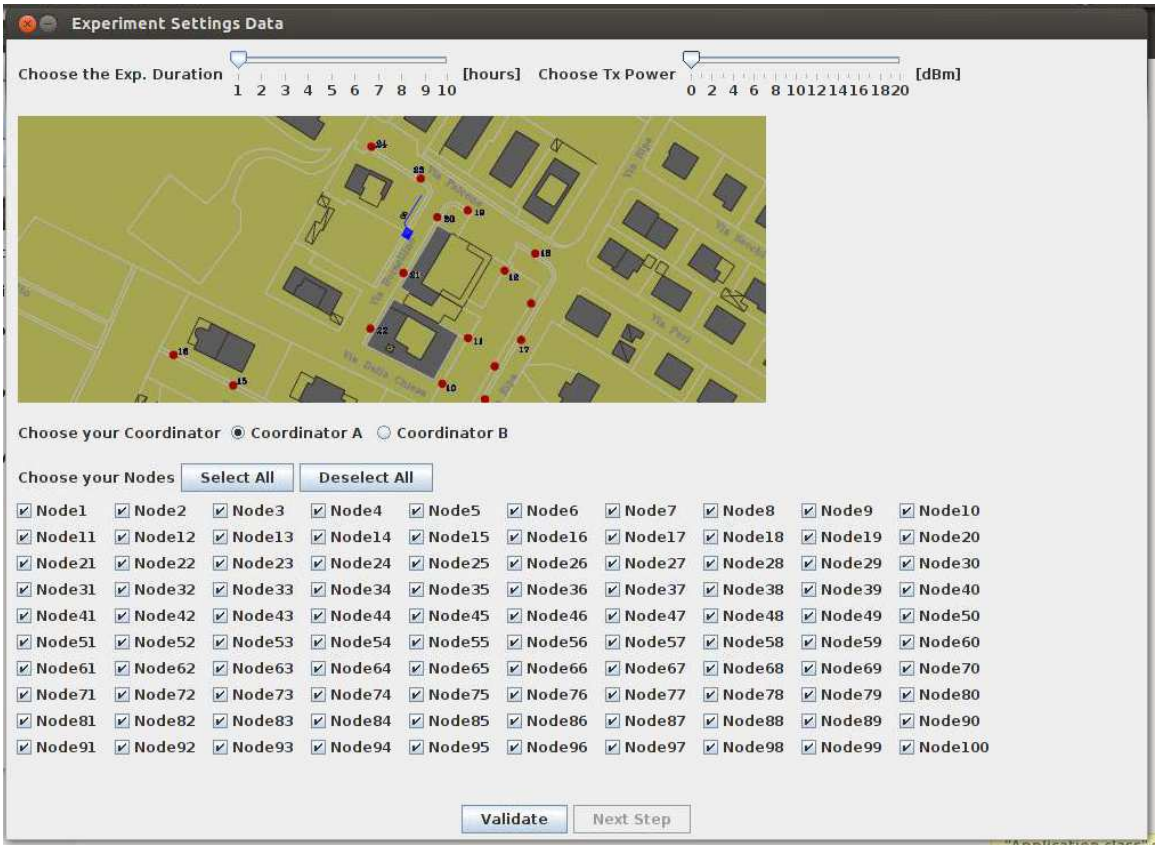

Figure 2.10: Flextop Java Application.

Since the facilities are inside the University network, proper level of security has to be implemented. The researcher who asks for the access grant is responsible for the correct use of his grant. All the accesses are logged and stored in a secure area.

The results are provided on the Private web site and sent via email to the author. The result are given in form of text files as described in the following:

- Coordinator output: the coordinator is directly connected to the gateway via a serial interface. A program running on the gateway is able to store all the data coming from the coordinator. The structure of this file is chosen by the researcher when he/she downloads the firmware.

- Three files are generated by the sniffer

- A file describing the channel and environmental condition; before each experiment, an application runs and provides an output file containing the path loss matrix. The matrix $P^{(r)}$ of size $N^{(r)}\text{x}N^{(r)}$, is obtained as follows. Nodes, one at the time, transmit a burst of 10 000 packets while all other nodes are in the reception mode, measuring the received power and averaging over the total number of packets received from the specific transmitter. When all nodes finish transmitting their burst of packets, they report their array, containing the average received power by each transmitter, to the coordinator. In this way, the matrix $P^{(r)}$ is created and extracted from the coordinator.

2.2.3 Objectives

FLEXTOP is a platform devised in order to achieve separate types of objectives.

1. The platform permits testing of separate protocol stacks in realistic settings,

and their performance comparison under a certified environment, with known propagation conditions. For instance, different routing protocols can be tested, and their suitability to different network topologies measured. The platform constitutes a sort of reference context for comparison of protocols.

2. Besides scientific goals, the platform can be used for performing pre-deployment tests. Industries developing IoT or smart city applications based on 802.15.4 will be allowed to first test their solutions on the FLEXTOP platform, to check their performance under a controlled environment. This will allow establishment of proper liaisons with industry.

3. The platform can be used as a benchmark for those research groups, developing 802.15.4 network simulators, to test their implemented software and certify its adherence to real network environments.

4. Similarly to the previous objective, FLEXTOP can be used as benchmark with respect to mathematical models developed by scientists that provide performance of 802.15.4 networks under specific algorithm implementations.

In the follow sections, the strength of FLEXTOP with respect to these objectives is proved.

2.3 Performance analysis: Short-range protocols comparison

Several approaches have been considered by research community as possible enablers for the Internet of Things (IoT) implementation. In tnis section, results obtained

by testing and comparing three different solutions are presented. In particular, a centralised solution based on SDN approach, i.e. SDWN, is compared with ZigBee and 6LoWPAN, which are two standard and distributed solutions. SDWN uses a centralized network layer protocol, where routing policies are defined by an external controller that can be positioned anywhere in the network. The other two solutions are actually the most common protocol stacks for wireless sensor networks, and they both use a distributed routing protocol. As anticipated above, the comparison is achieved by experimentations performed on the EuWIn platform developed within the Network of Excellence, NEWCOM#. Results show that SDWN is the best solution in static or quasi-static environments, while the performance degrades in highly dynamic conditions. However, ZigBee has a good re-activity to environmental changes. The evaluated performance metrics are several, including packet loss rate, round-trip-time and overhead generated in the network, under different conditions and considering different kinds of traffic.

2.3.1 Related Work

Few works exploit the potential of a SDN approach in wireless networks, especially in sensor networks. [20] presents the idea of exploiting the OpenFlow technology to address the reliability in WSNs. The Authors claim that OpenFlow-based sensors are more reliable than typical sensors, and simulation results show that the proposed approach achieves better performance for large networks. The use of OpenFlow in a wireless mesh network allows a rapid change of forwarding and routing algorithms [21]. A survey on challenges and opportunities in using wireless SDNs is presented in [22].

The paper claims that the SDN technology will have to face problems regarding slicing, isolation, status reporting, and handoffs, whereas it will improve connectivity, QoS, planning, security, and localization. [23] proposes a SDN system, where experimentations show that the proposed solution reduces the energy consumption and provides a higher level of flexibility in network management.

Many research papers deal with the implementation of ZigBee networks. For example, [24–26] refer to the implementation of a ZigBee network for smart home applications. [27] measures the impact of Wi-Fi interference over ZigBee networks, while [28] evaluates the performance of a small ZigBee network (composed of less than five nodes) in terms of throughput and latency. An experimental analysis of star and tree ZigBee networks based on commercially available hardware and software is provided in [29], in order to determine the limitations of technology. Finally, [30] provides a comparison between ZigBee Pro and ZigBee IP, in terms of latency, where a network is composed of five nodes.

Referring to 6LoWPAN, [31] presents an implementation over Texas Instruments (TI) MSP430 devices. A star topology with an edge router and three nodes was deployed, and IP addressability features were tested. In [32], a novel architecture for supporting applications in the field of Intelligent Transportation Systems is presented. The implementation and evaluation of different neighbour management policies applied to RPL are given in [33]; experiments were conducted on the TU-Berlin TWIST testbed with 100 TelosB motes spread over a three floor office building. In [34], the performance of the RPL protocol is evaluated by using the Lille SensLAB testbed composed of 100 TI CC2420 devices, randomly deployed in an indoor environment.

Several papers are also comparing ZigBee and 6LoWPAN: [35] provides a qualitative comparison, without addressing any quantitative evaluation of protocols' performance. In [36], the Authors present a comparative performance assessment of ZigBee and 6LoWPAN protocols for industrial applications. The testbed is composed of four TelosB nodes deployed in a linear topology.

However, there are no works in the literature dealing with the comparison of the SDN approach and the distributed approach represented by ZigBee and 6LoWPAN. The most important aspect, that differentiates this work from the previous ones, is that experimental results have been achieved in a controlled environment, where tests can be conducted and replicated under predictable conditions, thus making the comparison fair.

2.3.2 Experimental Setup

Two network setups are considered: i) a network consisting of 10 nodes (nodes 4, 6, 13, 17, 22, 25, 38, 43, 45, 51, underlined with red circles in Fig. 2.8); ii) a network of 20 nodes, where the following nodes are added: 1, 8, 10, 11, 15, 20, 23, 30, 31, 33. In all cases, the node 53 at the end of the corridor, is used as the network coordinator. Nodes were selected according to their level of connectivity, measured by the matrix P described above, in order to have nodes that could reach the coordinator through different number of hops. The matrix P, characterising the level of connectivity among the selected nodes in the case of ten nodes and the coordinator, is reported in Table 2.1, where values are expressed in dBm and where "-" indicates absence of connectivity. The level of transmit power, set to obtain the matrix and used during experiments, was -5 dBm. In the case of 20 nodes, the matrix is not included for the

Table 2.1: Average Received Powers [dBm] Matrix for -5 dBm.

IDs	4	6	13	17	22	25	38	43	45	51	53
4	-	-74	-54	-63	-62	-66	-	-	-	-	-
6	-73	-	-80	-64	-75	-83	-	-86	50	50	-88
13	-53	-81	-	-55	-60	-69	-83	-	-85	-	-
17	-64	-65	-56	-	-63	-58	-86	-82	-85	-89	-83
22	-64	-79	-62	-65	-	-55	-80	-86	-84	-87	-85
25	-66	-84	-69	-57	-53	-	-63	-67	-69	-79	-74
38	-	-	-82	-85	-78	-61	-	-58	-80	-84	-72
43	-87	-88	-	-82	-83	-68	-60	-	-48	-71	-66
45	-	-	-85	-85	-82	-69	-77	-47	-	-54	-59
51	-	-	-	-	-87	-79	-	-80	-56	-	-65
53	-	-	-	-83	-85	-75	-75	-65	-60	-65	-

sake of conciseness.

2.3.2.1 Data Traffics Generated and Environmental Conditions

A query-based application is considered, where the coordinator periodically sends a query packet to one or several *target* nodes, and waits for the reply from it/them. Both queries and replies are data packets with a given payload that is the same in both cases, and different payload sizes are considered.

Two different communication configurations are evaluated: i) *unicast*, where the coordinator sends the query to one specific node that could be one, two or three hops far from the coordinator; and ii) *multicast*, where the coordinator queries contemporaneously a subset of nodes, and waits for replies from all of them.

As for the environmental conditions, all experiments were performed during the night, when no people were moving around, to avoid uncontrollable environmental changes and to ensure a fair comparison. However, in order to measure the level of reactivity of protocols to possible changes such as in real environments,results in *quasi-static* and *dynamic* conditions were investigated. In particular, experiments were still performed during the night, but a "disturbs" (specified in the follow) was added. In the case of *quasi-static* environment, a day-like situation was emulated, where people move around, by letting two people walk along the corridor at a constant

speed, following a pre-defined path. The comparison among protocols is still fair, since it was reproduced exactly the same situation (same people, path and speed) during all experiments. This case is denoted as *quasi-static*, since only two people were moving without creating huge obstacles and fast fading. In the case of *dynamic* environment, it was emulated the movement of nodes leaving the network and possibly coming back, by switching off and on nodes at random instants. In particular, it was implemented the following procedure: i) once a node switches on, it remains in this state for at least 5 seconds, after which it ii) generates a random and uniformly distributed delay between 0 and 10 seconds at the end of which iii) the node switches off for 1 second, and then it switches on again (back to step i)). The comparison among protocols is still fair, since the above described duty cycling is implemented in the tests identically. Moreover, the channel conditions could be considered as extremely dynamic, since nodes switches off frequently and at random time instants.

2.3.2.2 Parameters setting

All the parameter settings related to PHY and MAC are the same for the three protocols, and they are provided in Table 2.2. It also includes the network layer parameters, different for the three protocols stacks, but set to the same values, when possible. In particular, for the fair comparison the SDWN Beacon packets period was set equal to the ZigBee Link status period, as well as the SDWN Flow tables refreshing time equal to the ZigBee MTO-RR period. Therefore, when the environment is static, routing tables are refreshed and new paths are discovered with the same frequency (i.e., every 150 s). Broadcast packets used to compute link costs/RSSI values are sent with the same frequency (i.e., every 10 s). Obviously, in the presence of changes

in the environment, the two protocols behave differently. In case of 6LoWPAN, as stated above, the frequency of generation of DIO packets is managed by the Trickle algorithm: the RPL router will schedule the emission of a DIO at some time in the future, depending on the events in the network and real-time environment condition. In this study, the default period between two consecutive DIO messages was selected, i.e. equal to 12 s.

The setting of the remaining parameters, since they are standard related, were set to the default values.

In relation to the packet sizes, all protocols use a MAC acknowledgement of 11 bytes and a PHY header of 6 bytes. The MAC header is 18 bytes in the case of ZigBee and SDWN, since short addresses are used, while it is 22 bytes for 6LoWPAN in the case of unicast packets (data packets and DAO), and 14 bytes in the case of broadcast packets (DIO and DIS), due to the use of long addresses. The MAC Service Data Unit lengths for the different packets and the different protocols are presented in Table 2.3.

2.3.2.3 Performance Metrics

In this protocol comparison, the following performance metrics are considered: i) Packet Loss Rate (PLR); ii) Round Trip Time (RTT); iii) overhead; and iv) throughput. In all experiments, the coordinator is sending one query every 300 ms toward the target node(s), and a total number of 5,000 queries are generated at the application layer. To compute the PLR, in each experiment the number of replies received at the coordinator, n_{RX}, from each target node was counted. Therefore, there is a loss if the query or the reply independently from the link in which the packet is lost. In the case

Table 2.2: Parameter Settings

PHY Layer	
Bit Rate	250 kbit/s
Frequency Band	channel 11, at 2.405 GHz
Transmit Power	-5 dBm
Receiver Sensitivity	-92 dBm
PHY layer header	6 bytes

MAC Layer	
BE_{min}	3
BE_{max}	5
NB_{max}	5
Max number of retransmissions at MAC level	3
MAC header for ZigBee and SDWN	18 bytes
MAC header for 6LoWPAN	14 - 22 bytes

NET Layer	
SDWN	
Beacon packet period	10 s
Report packet period	20 s
Flow tables refreshing time	150 s
Maximum number of children per parent	6
ZigBee	
Link status period	10 s
MTO-RR period	150 s
MTO-RR number of retransmissions	3
Maximum number of children per parent	6
Random jitter for broadcast packets	(0, 127) ms
6LowPAN	
Minimum DIO period	12 s
DIO period doublings	8 s
Maximum number of children per parent	6
Random jitter for DAO packets forwarding	(0, 4) s
Random jitter for DIS packets generation	(30 - 60) s

Table 2.3: MAC Service Data Unit lengths

SDWN Packet Type	MAC Service Data Unit length (bytes)
Data	10 + Payload
Beacon	10 + 2
Report	10 + 3 + (3 * No. of neighbors)
Rule Request	10 + Payload
Rule Response	10 + (16 * No. of rules sent)
Open Path	10 + (2 * No. of nodes in the path)

ZigBee Packet Type	MAC Service Data Unit length (bytes)
Data	15 + Payload
MTO-RR	15
RREC	13 + (2 * No. of nodes in the path)
Link Status	13 + (2 * No. of neighbours)

6LoWPAN Packet Type	MAC Service Data Unit length (bytes)
Data	15 + Payload
DIO	85
DAO	48
DIS	6

of unicast transmission $PLR[\%] = (5,000 - n_{RX}) * 100/5,000$, while in the case of multicast it was computed an average PLR, averaged among the target nodes. The resolution of the PLR is approximately 0.5%, since 5,000 packets were transmitted.

The RTT is defined as the interval of time between the transmission of the query at the application layer of the coordinator, and the instant in which the reply is received at the application layer of the coordinator as well. In order to compute the RTT of each packet, a software-defined timer implemented at the application layer of the coordinator was used, this timer has a resolution of 1 ms. Results are then averaged over all packets received in each experiment, and among the target nodes for the multicast case.

Two definitions are used for the overhead: i) the ratio between the total number of packets transmitted in the network (being data packets transmitted for the first time or retransmitted, acknowledgement, or control packets), and the number of queries generated at the application layer of the coordinator; ii) the ratio between the total number of bytes transmitted in the network, and the number of bytes of information included in the generated replies. It was computed the latter by processing the data gathered by two sniffers located at fixed positions at the end (near the coordinator) and in the middle of the corridor.

It was measured the network throughput by counting the average number of payload bits of the replies per second, correctly received by the coordinator.

2.3.3 Numerical Results

In this section are reported the numerical results obtained in the experimental campaign. More specifically, first the results for the static and quasi-static cases are

provided and, then the dynamic case is addressed.

2.3.3.1 Static and Quasi-Static Environments

Fig. 2.11 shows the RTT as a function of the number of hops for the case of 20 bytes of payload, unicast transmission and static environment. The set of target node(s) is different for the different protocols, since different topologies are generated. In particular, the set of target nodes is reported in Table 2.4, with the corresponding number of hops and path connecting the node to the coordinator. It can be observed that the node 51 is always directly connected to the coordinator. For example, the node 4 is connected by three hops in the case of SDWN and 6LoWPAN, while for ZigBee only two hops are needed.

Table 2.4: Target node(s) with the number of hops and paths.

Protocols	1 hop target node	2 hops: target node	2 hops: path	3 hops: target node	3 hops: path
SDWN	51	22	22 - 45 - 53	4	4 - 22 - 45 - 53
ZigBee	51	4	4 - 22 - 53	6	6 - 22 - 46 -53
6LoWPAN	51	13	13 - 43 - 53	4	4 - 25 - 38 - 53

As expected, the RTT increases with the number of hops, since the packet has to pass through more routers. In Fig. 2.12 shows the RTT as a function of the payload size in the case of one hop, considering unicast and static environment. It is possible to observe that the RTT slightly increases with increasing the payload size.

In both figures it can be noticed that SDWN achieves better performance than other solutions, resulting in the lowest RTT in all cases. This is due to the fact that in SDWN, once the path between source and destination is established, forwarding

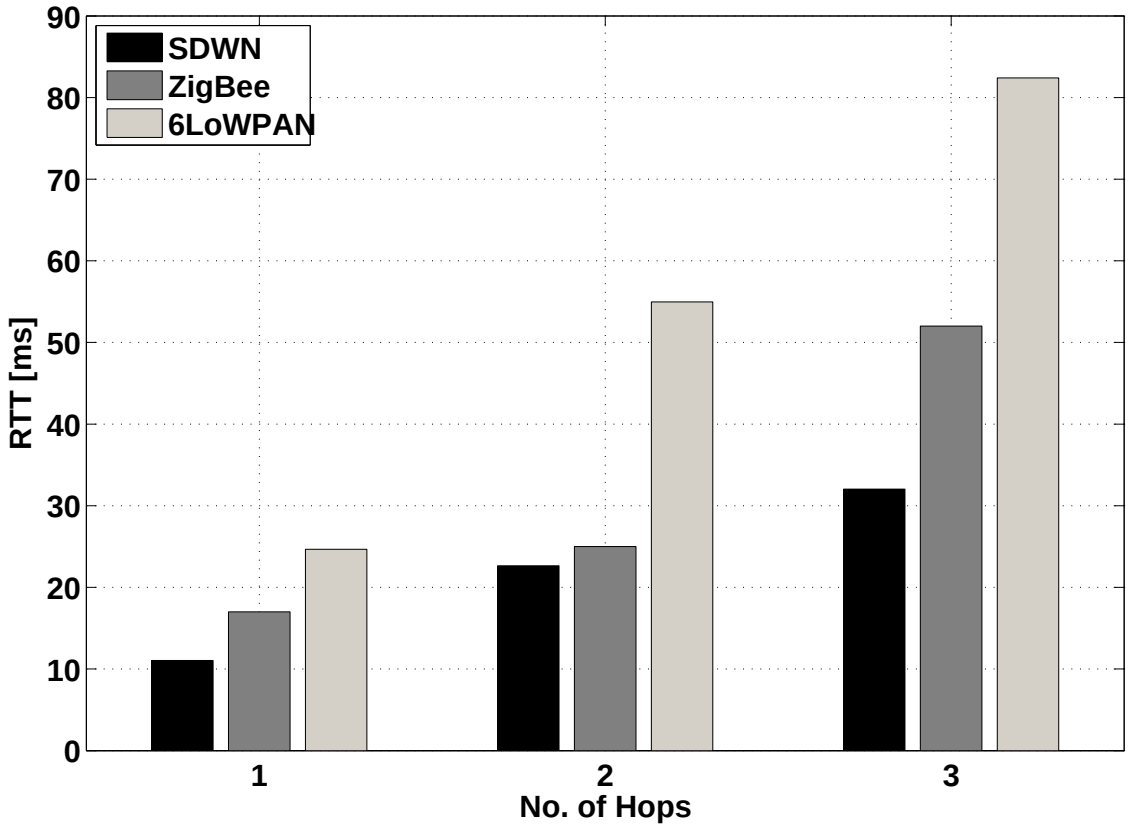

Figure 2.11: Unicast traffic: RTT as a function of the number of hops when transmitting 20 bytes of payload in static conditions.

at intermediate routers is very quick, since intermediate nodes just have to check the action corresponding to the received packet. In ZigBee and 6LoWPAN, instead, routing must be performed at each intermediate node, resulting in increased delay. Moreover, it can be observed that ZigBee notably outperforms 6LoWPAN. The reason is that the protocol stack implemented by 6LoWPAN is more complex, resulting in longer processing time, especially at the adaptation layer (implementing addressing and fragmentation). Finally, the packet size in the case of 6LoWPAN is larger due to the use of IP addresses.

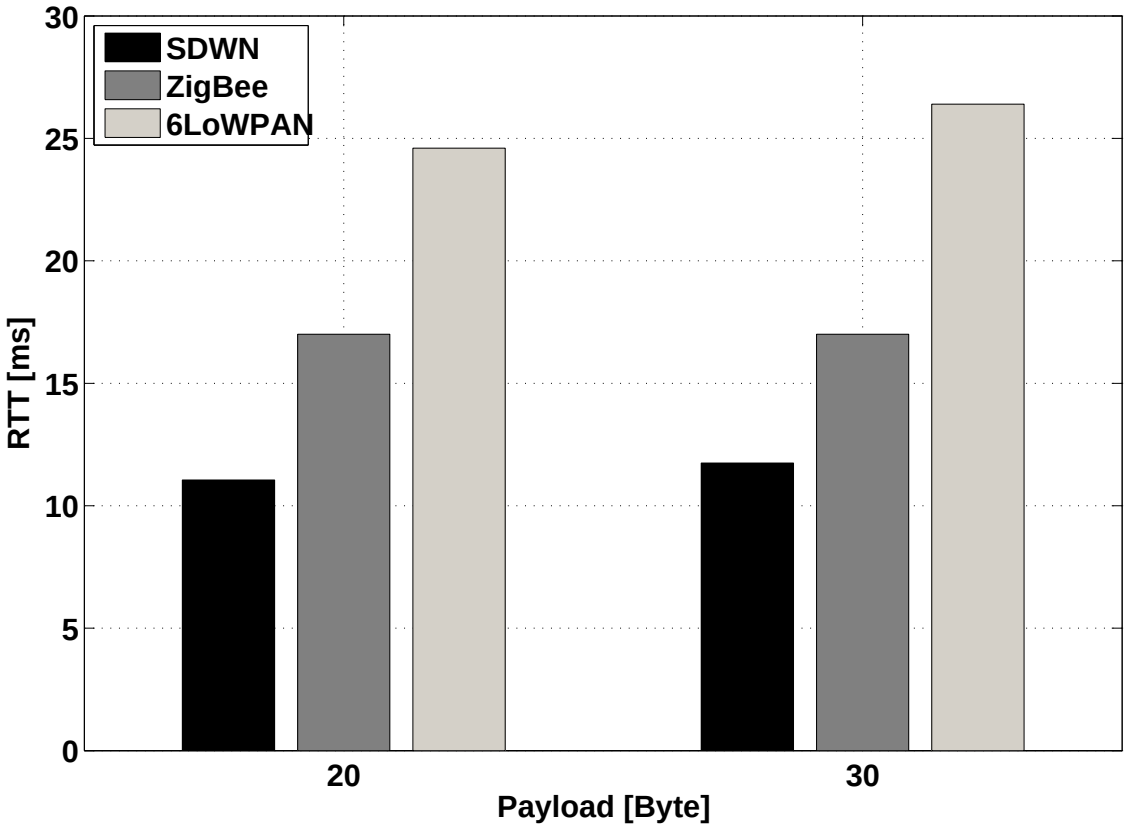

Figure 2.12: Unicast traffic: RTT as a function of the payload size in the case of one hop and static conditions.

In Table 2.5, it is compared the overhead generated by the different protocols by considering a payload of 20 bytes, static environment, unicast traffic and different number of hops. As expected, the overhead is almost doubled by passing from 1 to 2 hops. Moreover, it is increasing by passing from SDWN to ZigBee and to 6LoWPAN solution. This is due to the fact that, in static conditions, SDWN keeps under control the number of packets transmitted during the path formation phase, while optimising paths reduces the number of data retransmissions. Referring to the overhead in number of bytes, the difference is also more notable, since headers in SDWN are

shorter than in ZigBee and 6LowPAN.

It is important to emphasize that, for all protocols and in all cases, the PLR was below 0.5%.

Table 2.5: Overhead: comparison among protocols.

Protocol	Packets:1 hop	Packets:2 hops	Bytes:1 hop	Bytes:2 hop
SDWN	2.6	5.6	2.5	5.6
ZigBee	4.7	8.7	6.5	11.4
6LoWPAN	6.2	9.5	10.9	16.8

Fig. 2.13 compares the RTT achieved in case of static and quasi-static environments, particularly considering the case of unicast traffic, 20 bytes of payload and 2 hops. As can be seen, in all cases, the RTT increases when passing from static to quasi-static conditions, due to: i) the need for searching for new paths when links become unreliable and/or ii) links being unreliable inducing more retransmissions, thus increasing the latency. However, in the considered environment, SDWN still remains the best solution, since the channel fading is still quite low and changes in the environment are slow, such that SDWN could properly react and work. Finally, note that 6LoWPAN shows the lowest performance degradation when passing from static to quasi-static, since the implemented Trickle algorithm allows for better adaptation of routing to environmental changes. Moreover, in the case of quasi-static environment, the PLR remains below 0.5% for all the cases, demonstrating the good reactivity of protocols when the environment changes slowly.

The results related to the multicast traffic are reported hereafter. More in details, when a multicast group that consists of nodes 4 and 6 is triggered. Fig. 2.14 shows the average RTT, averaged between the two trigged nodes, while Fig. 2.15 compares

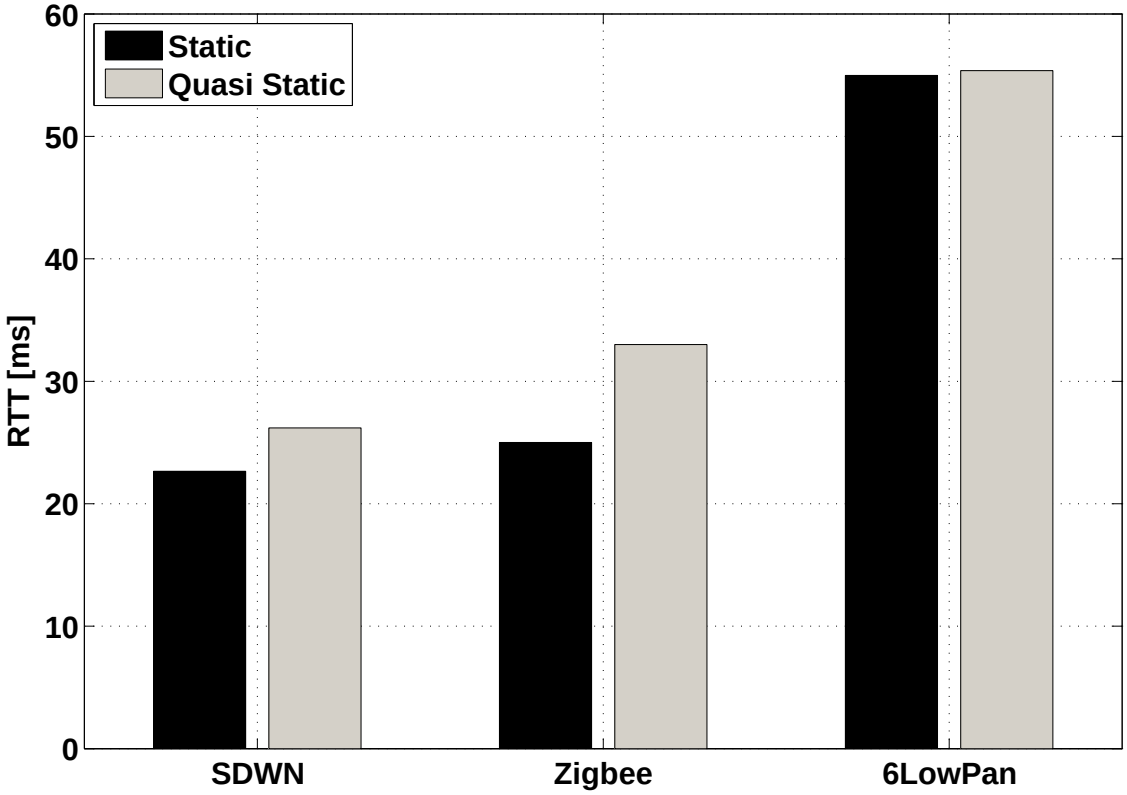

Figure 2.13: Unicast Traffic: RTT for the different protocols in the case of *static* and *quasi-static* conditions, setting 20 bytes of payload and 2 hops.

the average PLR. As can be seen, RTT is much higher than in the unicast case, especially for 6LoWPAN. The latter is due to an increase of the PLR that was below 0.5% in the case of unicast; losses due to collisions between data packets originating from the nodes 4 and 6 that cause retransmissions, and consequently, the increase of delays. However, the multicast traffic increases the network throughput, as shown in Table 2.6. The throughput was computed by considering an offered traffic of one query every 300 ms. Results demonstrate the improvement of the throughput when passing from unicast to multicast, since more than one node is queried at the same

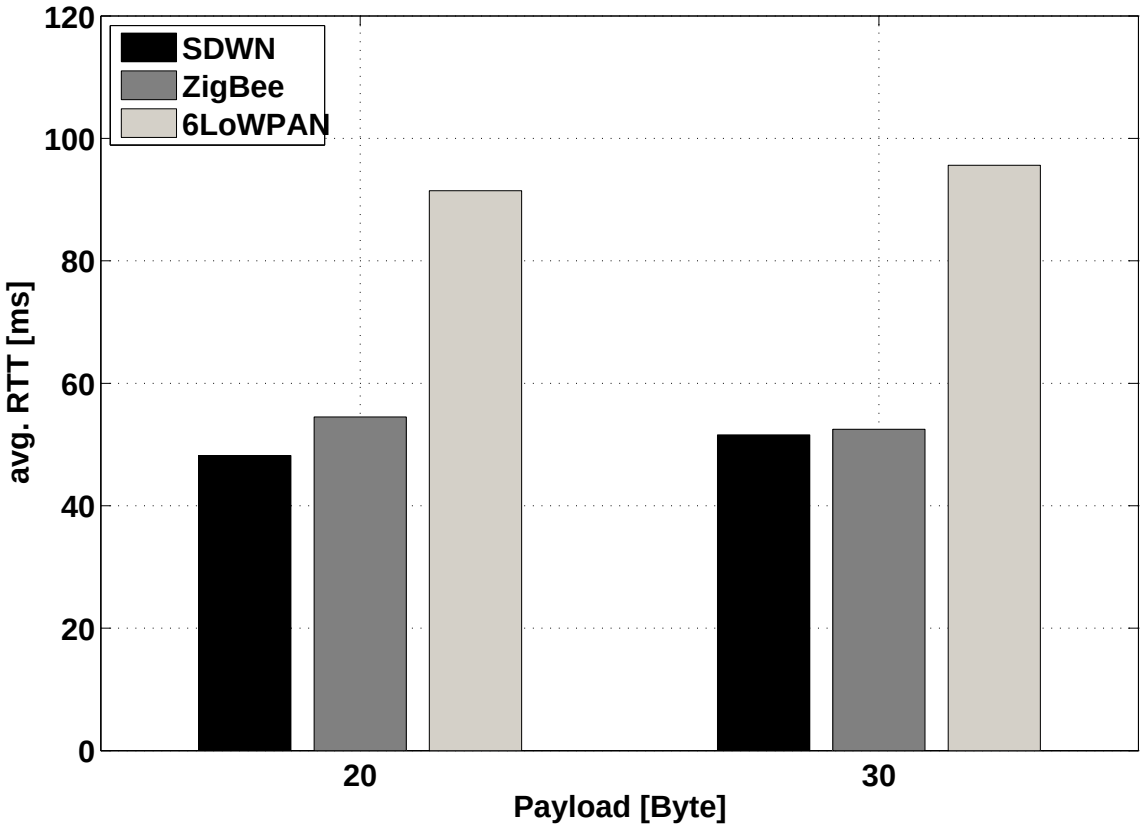

Figure 2.14: Multicast traffic: Average RTT as a function of the payload size.

time. Note that, in the case of unicast, the throughput is the same for all the three protocols, since in all cases the PLR is lower than 0.5%.

Last analysis reported in this section was obtained by considering a network composed of 20 nodes, implementing the unicast application with 20 bytes of payload. The coordinator queries node 4, and static and quasi-static environments were considered. Results are reported in Table 2.7, where only the cases of SDWN and ZigBee are considered, having already demonstrated that 6LoWPAN has the worst performance in all cases. As can be seen, SDWN is again performing better than ZigBee, since environmental conditions are still almost static, therefore for larger networks SDWN

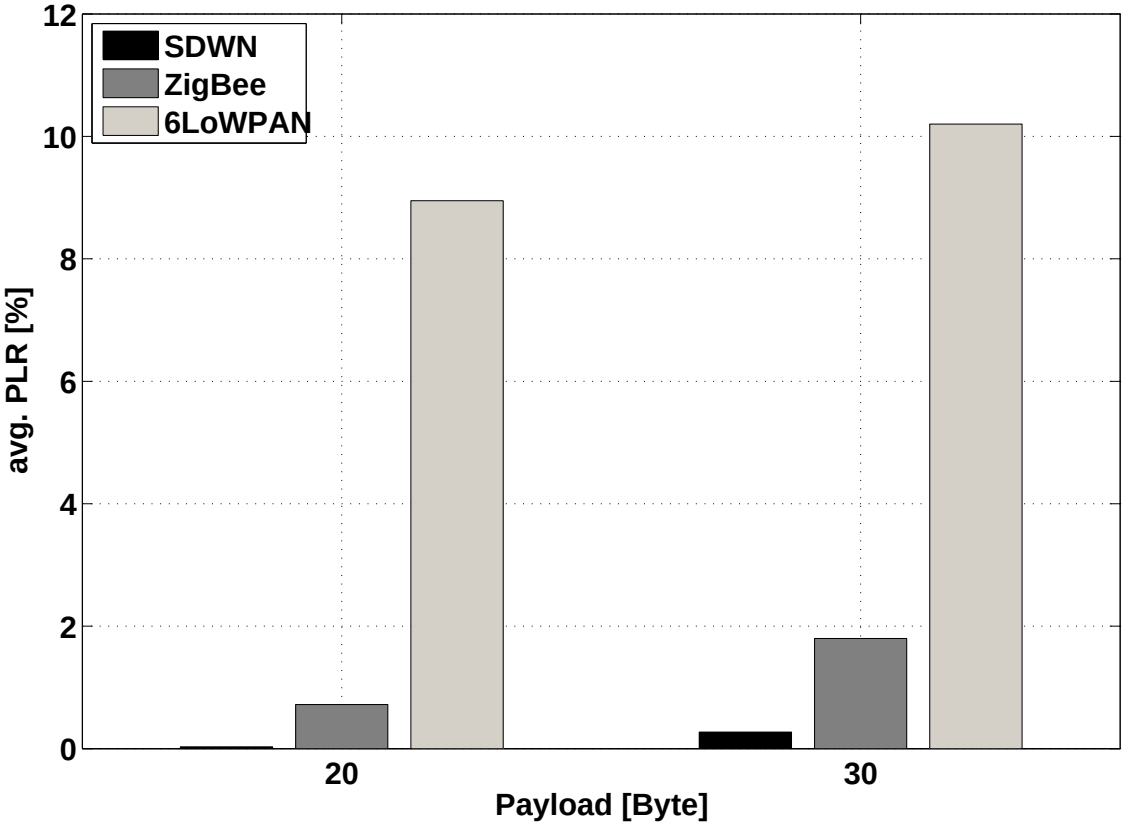

Figure 2.15: Multicast traffic: Average PLR as a function of the payload size.

is also performing well. Obviously, for both protocols, RTT and PLR are larger with respect to the case of 10 nodes network, since more nodes are transmitting packets during the path discovery phase, resulting in more collisions and possibly longer and suboptimal paths.

2.3.3.2 Dynamic Environment

The last considered case is within a dynamic environment, whose performance in terms of RTT and PLR are reported in Table 2.8. Results have been achieved by considering the 10 nodes network, unicast application, and 20 bytes of payload, where

Table 2.6: Throughput [kbit/s] comparison: unicast and multicast.

Protocol	Unicast 20 Bytes	Unicast 30 Bytes	Multicast 20 Bytes	Multicast 30 Bytes
SDWN	0.53	0.8	1.06	1.59
ZigBee	0.53	0.8	1.05	1.57
6LoWPAN	0.53	0.8	0.97	1.43

Table 2.7: 20 nodes network: Comparing RTT and PLR.

Protocol	RTT[ms]: Static	RTT[ms]: Quasi-Static
SDWN	44	49
ZigBee	51	76
Protocol	PLR[%]: Static	PLR[%]: Quasi-Static
SDWN	1.5	2
ZigBee	13	21.5

the coordinator queries node 4. In this case, a highly dynamic environment is emulated by making routers switched on and off at random instances of time. This requires nodes to refresh routes very quickly, because a router in a path already established could switch off and the source should search for a new relay for reaching the destination. All performance metrics have worsened both for ZigBee and SDWN. However, SDWN reaches a very large PLR, since most of the packets cannot find a proper route to reach the coordinator. The average RTT of SDWN still remains lower than in case of ZigBee, since when a packet manages to find a proper route with all routers switched on, forwarding is still very quick. This demonstrates that SDWN presents some issues in the case of highly dynamic environments, as expected.

Table 2.8: Dynamic conditions: Comparing SDWN and ZigBee.

Protocol	RTT [ms]	PLR [%]
SDWN	40	96
ZigBee	61	33.5

2.3.4 Conclusion

The work presented in this section is a comparison among different solutions for the IoT paradigm: ZigBee, 6LoWPAN and a software defined-based solution, SDWN, implementing a centralised routing. Results of an extensive measurements campaign performed over the EuWIn laboratory are reported.

Results show that in static and quasi-static conditions SDWN outperforms the other solutions, independently on the network size, payload size, traffic generated, and performance metric considered. The reason for this is the fact that SDWN allows to optimise paths selection and minimise forwarding time at routers. However, SDWN presents some limitations when high dynamic environments are considered, because of the time needed to refresh paths. As a conclusion, SDWN is more suitable for applications where nodes are in fixed positions and under low mobility scenario, as for the case of smart home and buildings applications. However, when the situation is dynamic and there is a node mobility, a distributed solutions like ZigBee and 6LoWPAN could work better. As an example, the case of smart city applications, where nodes could be mounted over lamp posts in streets where object (e.g., cars and people) are moving around, or where nodes could be directly carried by moving objects, requires solutions characterised by high reactivity rather than lower delays.

2.4 Performance analysis: Coexistence analysis

Wireless technologies used to realise local or personal area networks (i.e., WLANs or WPANs), operate into the unlicensed frequency bands, which can be exploited by multiple users and networks at the same time. In particular, the 2.4 GHz Industrial Scientific and Medical (ISM) band is used worldwide by several technologies, such as IEEE 802.11 [37] and IEEE 802.15.4/Zigbee [26, 38]. However, due to the mutual interference, the coexistence of different devices operating in proximity of each other can be troublesome. As proved by many authors [39, 40], this is especially true for ZigBee networks, whose performance is heavily influenced by the presence of Wi-Fi devices. In fact, even thought Zigbee provides some functionalities which should prevent the network to work on an interfered channel, in many cases it is not easy to completely overcome the problem. In some cases, in fact, there could be a lack of free available channels (e.g., indoor scenarios with many Wi-Fi networks deployed) and in some conditions also the use of channel non completely overlapped with those used by Wi-Fi may cause worsening of performance, as shown in this paper. Moreover, the latest ZigBee (Zigbee Pro [13]) has introduced the support for frequency agility, to allow the Zigbee coordinator to move the whole network to another channel if the one in use is overloaded. However the latter procedure is not fast, reliable, and energy saving, such that the interference problem still remains an issue [41]. Given the latter, the characterisation of the impact of the Wi-Fi interference is fundamental to understand in which conditions the Zigbee network performance strongly degrades.

2.4.1 Related Work

ZigBee performance has been investigated extensively using analysis and software simulation. As an example, in [42] an accurate analytic model to compute the packet error rate (PER) of ZigBee, when affected by Wi-Fi interference, is derived. The model is validated through simulations, but not through experimental activities. In [43], the performance of IEEE 802.15.4 under the effect of IEEE 802.11 interference is analyzed in terms of the bit error rate (BER), without considering the collision time during which IEEE 802.11b packets overlap IEEE 802.15.4 packets. ZigBee performance under WiFi interference has also been measured in empirical experiments. In [44], the received signal strength indicator (RSSI) and the PER of IEEE 802.15.4 are measured using off-the-shelf hardware. [41] reports the outcome of an experimental study involving Wi-Fi, ZigBee, and Bluetooth. The goal of such analysis was to characterize not only the reciprocal interference when pairs of technologies share the same spectrum, but also the coexistence of the three systems when they are all active in the same time and space, an aspect that has always been neglected. In [40] the PER of a ZigBee system under the interference of Wi-Fi devices, Bluetooth devices, and also of a microwave oven is reported. However, the study is limited to a single source of interference and considering only a unidirectional transmission.

In contrast with the above works, the aim of this section is to show the impact of Wi-Fi interference on a Zigbee network implementing a query-based application, where the Zigbee coordinator (ZC) periodically sends queries to a Zigbee device (ZD) and waits for replies. As never done in the literature, it shows the impact of interference over routing, by measuring the increasing of the overhead generated by the network layer. Moreover such overhead is evaluated for different types of traffic used

for the down-link transmission (from the ZC to the ZD), that are: i) *unicast transmission*, where the query is sent through CSMA/CA (carrier sense multiple access with collision avoidance) and using the Ad-Hoc On-Demand Distance Vector (AODV) routing protocol defined by Zigbee to search for the destination; ii) *broadcast transmission*, where the access to the channel is managed through the application of a random jitter and the packet is directly transmitted by the ZC, without the need to search for a path to reach the destination. The two approaches are fairly compared in this section.

2.4.2 Wi-Fi network setup and traffic

An IEEE 802.11 network can operate over one of the 14 channels defined for the 2.4 GHz ISM band (see Fig. 2.16). In the case of IEEE 802.11b each channel is 22 MHz wide, while in the case of IEEE 802.11n it is possible to use also a 40 MHz band. In the 2.4 GHz band the maximum transmission power is 20 dBm in Europe, which is the transmit power used during the experiments. Finally, the modulation scheme is complementary code keying with DSSS (Direct-sequence spread spectrum) for 802.11b and OFDM (orthogonal frequency division multiplexing) for 802.11n.

The latest IEEE 802.11 standard [37] defines two medium access schemes: a random CSMA/CA scheme and a polled scheme. In practice, however, the latter is not implemented by any card manufacturer, thus leaving the former as the sole scheme actually employed by Wi-Fi devices. In short, according to the CSMA/CA algorithm, every Wi-Fi device shall listen to the medium before transmitting. The transmission is allowed only if the medium has been sensed idle for a pre-defined time period. In

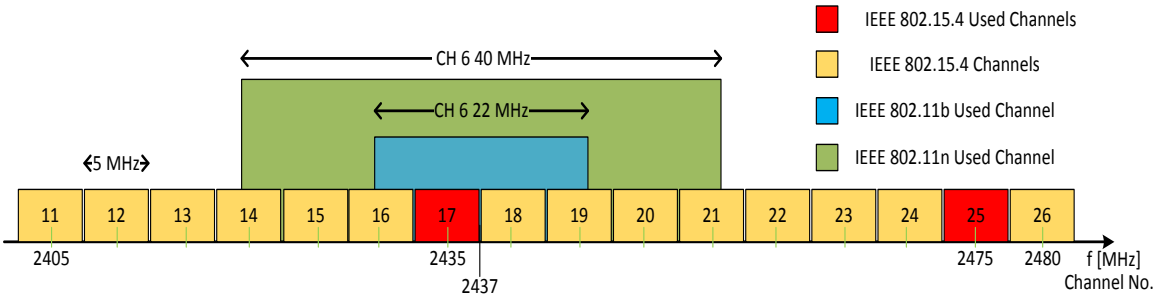

Figure 2.16: The carrier frequencies of IEEE 802.11 and IEEE 802.15.4.

case the medium is sensed busy, or after a collision, the device shall refrain from transmission for a period whose length is determined by a random variable (exponential backoff).

Figure 2.17 shows the setup of the Wi-fi network. The implementation details are given in the following.

Video Streaming Server The video streaming server is a linux machine running Ubuntu 12.04 LTS, where Video LAN Client (VLC) is installed. The latter offers a feature, i.e., Video Lan Server (see http://www.videolan.org/streaming-features.html) (VLS), that allows the machine to run as a streaming server. During these experiments, a HTTP server was set-up. This HTTP server broadcasted the video in on-demand fashion. The latter is a mp4 video with an average bit-rate in the order of 10 Mbps, moreover an on-the-fly trans-coding was applied (MPEG2 + MPGA(TS)). The video streaming feeds through an 100 Mbps Ethernet switch the access points (APs), two or three depending on the configuration.

Access Points The devices used as access points are TP-Link TL-WA830RE. These devices can act both as range extender as well as access point. In the used set-up, they act as access point without any "smart" feature (e.g., smart DHCP). Each device has 2 antennas (+4 dBi omnidirectional) vertical oriented. The receive sensitivity is

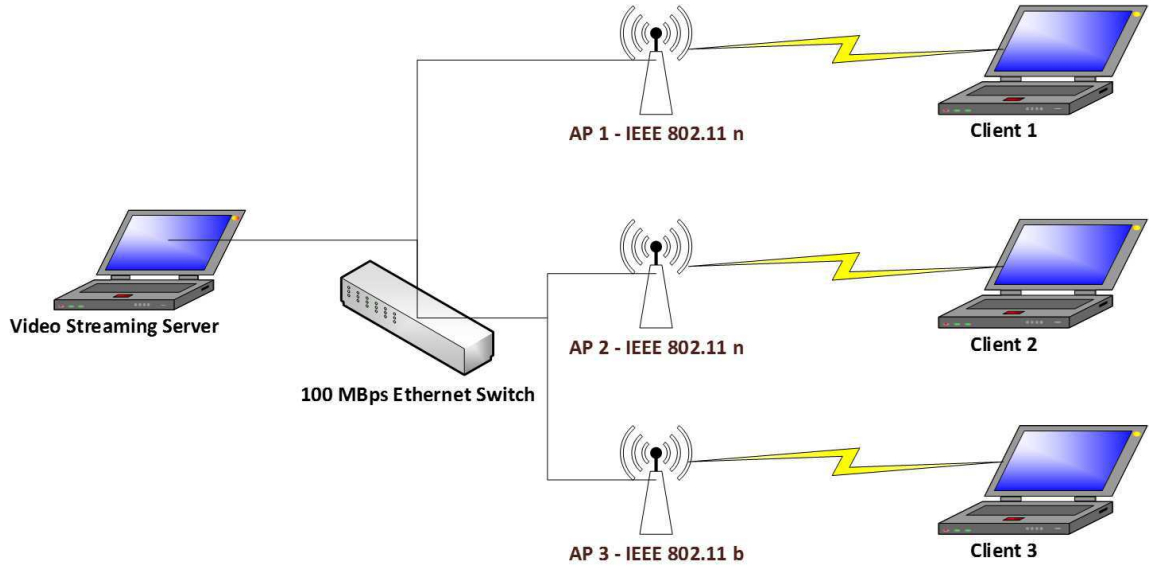

Figure 2.17: Set-up of the IEEE 802.11 Network

-68 dBm assuming a PER in the order of 10 % (in the case of IEEE 802.11n) and receive sensitivity of -85 dBm assuming a PER in the order of 8% (in the case of IEEE 802.11b). The most important feature of those devices is that it is possible to set independently the mode (b, g, n or mixed mode) and the transmission bandwidth. The APs set 3 different Wireless LAN with 3 different ESSID.

Clients The Clients are laptop running MS Windows XP or MS Windows 7. Each client is connected to an AP. On the clients is running VLC in client mode, firewalls are disabled.

2.4.3 Zigbee network setup and traffic

The Home Automation Zigbee profile has been used and a query-based application is implemented using two modalities: i) *unicast* and ii) *broadcast*. In both cases the coordinator periodically sends a query packet to the target device (implemented as a

Zigbee router), and waits for a reply from it.

In the case of unicast transmission, the query is sent as a unicast data packet (i.e., CSMA/CA is used at the MAC level for transmitting the packet), from the ZC to the ZD. In order to know the path to reach the ZD, the ZC coordinator starts the RREQ transmission, waiting for the RREP, before the transmission of the first data packet. The procedure is repeated in the opposite direction, that is from the ZD to the ZC, before sending the reply. Since the experiments are using the Zigbee upper layers, nodes do not know the path to reach each other and a RREQ/RREP procedure needs to be used to discover it. The latter procedure is performed before the transmission of the first data packet, when the entry in the routing table expires, and each time the path is detected to be unreliable, due to losses on the link. The latter situation happens very frequently when interference is present, causing large increasing of the delays.

In the case of broadcast transmission, the query is sent in broadcast, applying a random jitter before the transmission of the data packet (i.e., without using CSMA/CA). Moreover, since passive acknowledge is not used, each broadcast packet is sent three times, according to the standard. In uplink (i.e., from the ZD to the ZC), on the other hand, the Zigbee standard requires that the AODV routing protocol be used. According to the latter, the device sends a RREQ packet in broadcast in order to discover the path toward the ZC and the coordinator then replies sending a RREP. Upon receiving the RREP, the ZD will send the reply data packet.

2.4.4 Numerical Results

Results have been derived by averaging over 1.000 different transmissions. For the Wi-Fi network is considerd the following set-up: i) 2 APs using 802.11n (bandwidth 40 MHz); ii) 3 APs, where 2 APs are as in case i) and the other one is IEEE 802.11b AP (bandwidth 22 MHz). All APs use channel 6, centered at 2.437 GHz (see Fig. 2.16) and transmit at 20 dBm. APs are located at a distance d from the ZC. The cases d =3 m and 10 cm are considered. The clients are always located at 3 meters far from APs in all the cases (see Fig. 2.8). For the Zigbee network the period of time between two subsequent queries was set equal to 1 s, the payload size of the query and of the reply equal to 10 bytes and the transmit power of the Zigbee network equal to -5 dBm. The MAC and network layers parameters were set to the default values. Finally, two channels are considered for the Zigbee network (see Fig. 2.16): i) *Overlapped Channel*, that is channel 17 (centered at 2.435 GHz), completely overlapped with the one used by the IEEE 802.11 network; ii) *Non Overlapped Channel*, that is channel 25 (centered at 2.475 GHz).

2.4.4.1 Performance Metrics

As far as the metrics are considered:

- *Packet loss rate (PLR)*: The percentage of packets lost. A packet is considered as lost if either the query, or the reply is lost and independently from the link in which the packet is lost. When unicast packets are transmitted, up to three retransmissions at MAC level (i.e., at link level) are allowed.

- *Average Round Trip Time (RTT)*: The interval of time between the transmission

Table 2.9: Average Received Powers Matrix

	ZC	Device 22	Device 33	Device 45
ZC	0	-48	-60	-84
22	-49	0	-78	-79
33	-65	-75	0	-68
45	-81	-77	-66	0

of the query at the application layer of the coordinator and the instant in which the reply is correctly received at the application layer of the coordinator too. The average is performed (if not otherwise specified) over the correct packets received at the coordinator.

- *Overhead*: the ratio between the number of RREQ/RREP packets transmitted in the network and the total number of packets (including data packets transmission and retransmissions, acknowledgements and network layer control packets) transmitted in the network.

2.4.4.2 Environment Certification

Table 2.9 reports the average received powers matrix, P, where values are expressed in dBm. As expected by increasing the distance between the device and the ZC the average received power decreases. Tables 2.10 and 2.11 report the ED measurement results for the cases no-interference, overlapped and non overlapped channel, respectively. Each device stayed 500 ms over each channel. As can be seen, by decreasing the distance between the ZC and APs and the number of APs, the measured interference increases. Moreover, the ZC and device 22 always measure a larger interference with respect to devices 33 and 45, located in farer positions with respect to the APs.

Table 2.10: ED Measurement: No Interference and Overlapped Channel

Device	No-Inter.	2APs@3m	2APs@10cm	3APs@3m	3APs@10cm
ZC	-89	-41	-13	-32	-12
22	-75	-34	-36	-36	-33
33	-76	-66	-50	-64	-53
45	-88	-86	-70	-76	-66

Table 2.11: ED Measurement: Non Overlapped Channel

Device	2APs@3m	2APs@10cm	3APs@3m	3APs@10cm
ZC	-88	-15	-91	-52
22	-92	-27	-92	-88
33	-92	-54	-92	-92
45	-92	-61	-92	-92

Table 2.12 shows the channel utilization for all the considered cases. The utilization for the case of no-interference was equal to 0.1%. Note that in the case of overlapped channel was reported the value of utilization of channel 6 of 802.11, overlapped to channel 17 of 802.15.4, while for the case of non overlapped channel was reported the utilization of channel 13 of 802.11, overlapped to channel 25 of 802.15.4.

2.4.4.3 Packet Loss Rate Results

In the case of no-interference, considered as a benchmark and evaluated in the case of unicast transmission, any loss was registered, since all devices are well connected to the ZC (see Table 2.9). In the case of non overlapped channel the utilization is very low, bringing to a PLR always lower than 10%. This last figure of merit is due to the fact that only 1.000 packets are transmitted, so the statistics was not sufficient to show PLR lower than 10%. In Fig. 2.18 it is shown the PLR for the different devices and the different Wi-Fi network settings (i.e., different number of APs and distance from the ZC) for the case of unicast transmission and overlapped channel. As can be seen the PLR is strongly affected by the percentage of utilization of the Wi-Fi: when

Table 2.12: Wifi Utilization [%]

	2APs@3m	2APs@10cm	3APs@3m	3APs@10cm
CH 17	14	11	48	60
CH 25	0.70	10.40	0.60	1.30

Wi-Fi APs occupy the channel for less than 15% of time, which happens when only two APs are present, the PLR remains below 10%. When three APs are set-up the utilization strongly increases (up to 60%) and the PLR strongly increases too.

In Fig. 2.19 the case of broadcast is shown. The PLR is still strictly related to the utilization values: by increasing the utilization the PLR increases too. It can be noted that the use of broadcast transmission in downlink, instead of unicast, improves the performance, since the ZC does not need to find the route toward the ZD, which generates overhead and losses (see the subsection below).

2.4.4.4 Overhead and Average Round Trip Time Results

Table 2.13 shows the overhead for the different cases. In the case of no-interference the overhead was equal to 11%.

In Fig. 2.20 the average RTT, $\overline{RTT}$, averaged among devices, in the case of unicast transmission for the different cases, no-interference, channel 17 and 25. The logarithmic scale is used for the sake of readability. For the case of no-interference, being the PLR null, the average RTT is almost constant and it is around 16 ms (8 ms per link, as expected). For the case of overlapped channel, instead, it is almost constant in all cases (about 600 ms) and it is extremely larger with respect to the no-interference case. This is due to the routing protocol: when some packets are lost over a link, due to the interference, the link is considered unreliable and the device will search for a new path to reach the destination. The latter is performed by sending

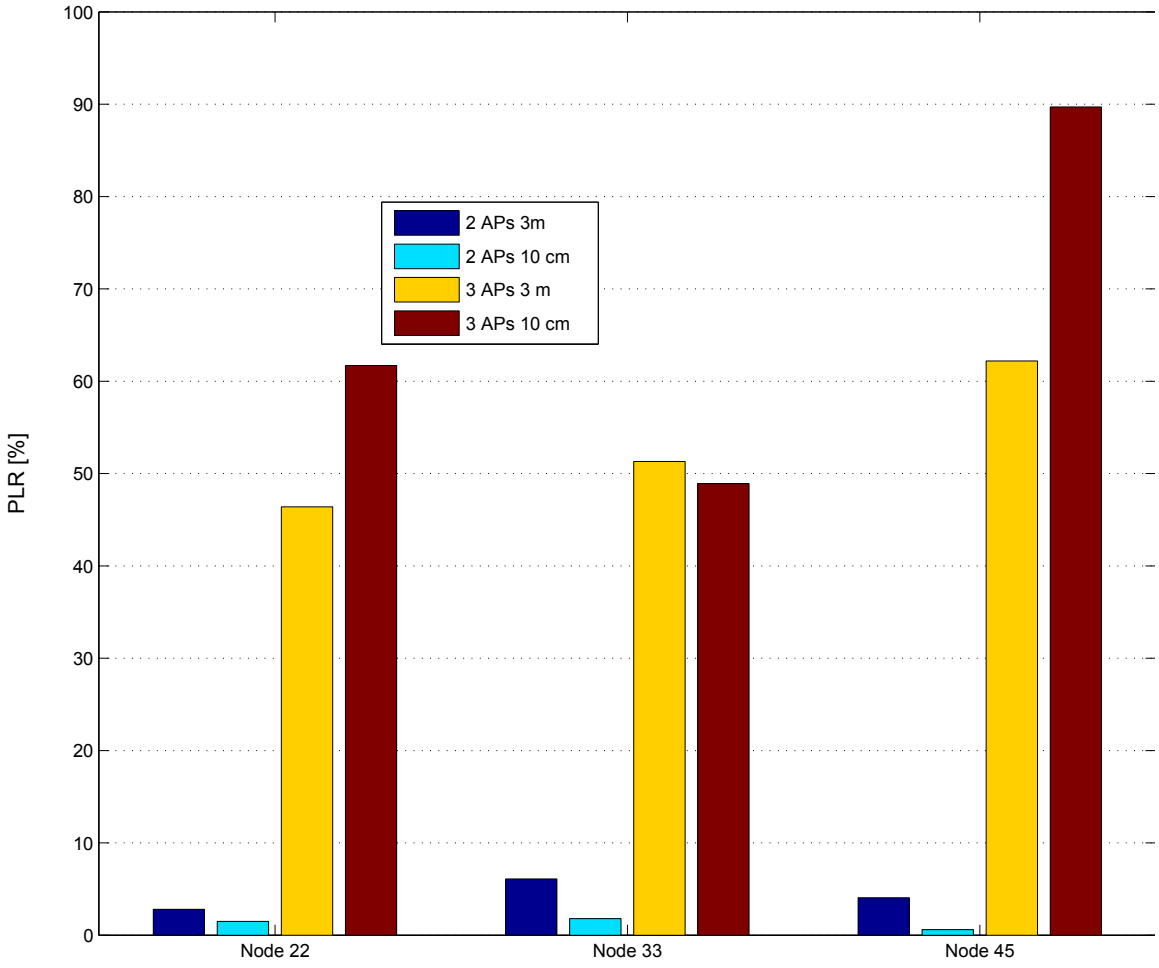

Figure 2.18: PLR for the different devices for overlapped channel and unicast transmission.

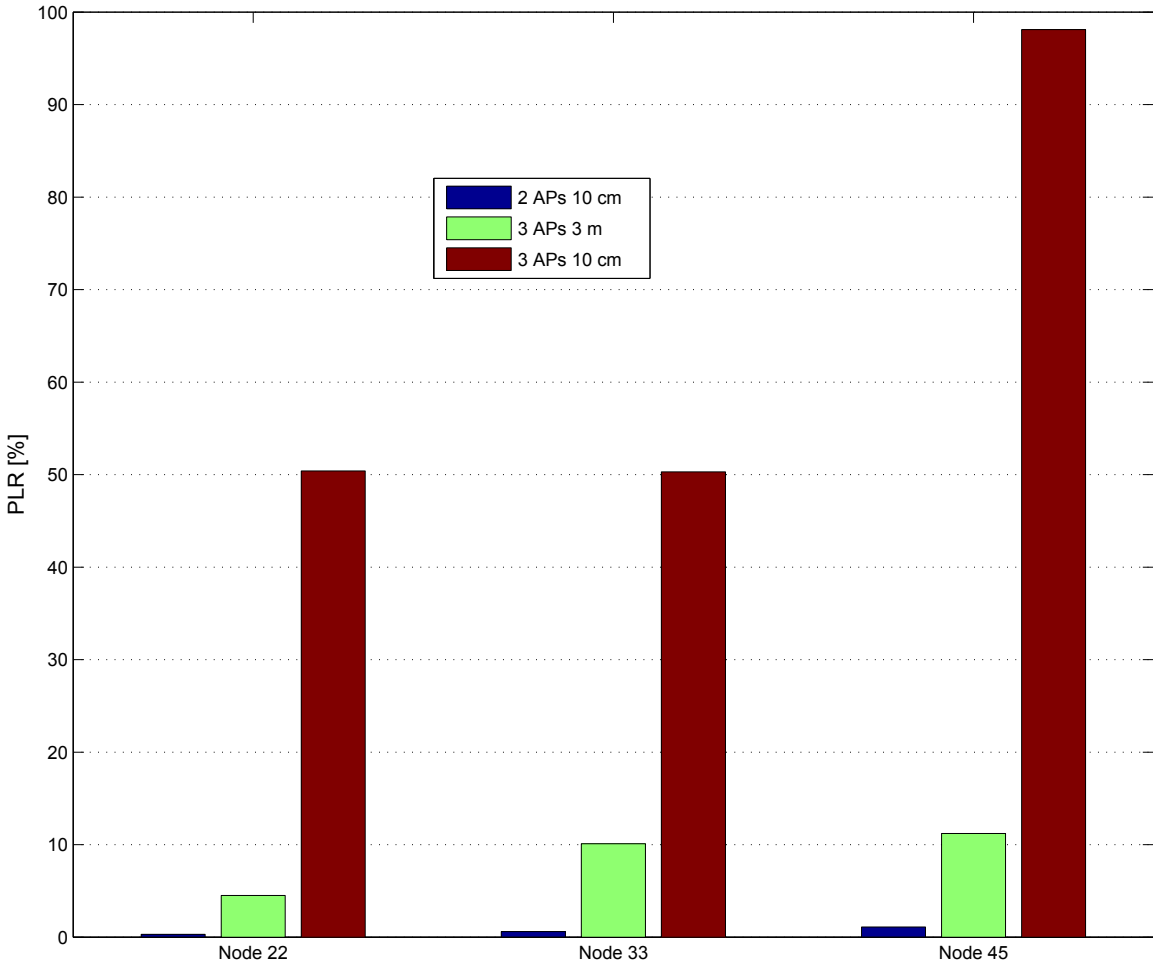

Figure 2.19: PLR for the different devices for overlapped channel and broadcast transmission.

Table 2.13: Overhead [%] for the different cases

	2APs@3m	2APs@10cm	3APs@3m	3APs@10cm
CH 25	11.1	32.9	12.1	36.9
CH 17 unicast	34.8	36.3	34.9	36.9
CH 17 broadcast	4.5	7.1	8.7	N.A.

a burst of RREQs, until a reliable RREP is received and only at that point the data packet is transmitted. Therefore, a lot of overhead is generated and many time passes before the device can send the data packet. This is demonstrated by results in Table 2.13: the overhead in the case of overlapped channel is much larger than the case of no-interference, and it is almost constant for the different cases, causing an increase of the RTT, which is constant too.

In the case of non overlapped channel the overhead is low when the APs are at 3 m, resulting to a RTT of approx. 16 ms, as in the case of no-interference. When the APs are at 10 cm, instead, the ZC suffers of a larger interference (see also the ED measure in Table 2.11) and resulting in an increase of the overhead, which on its turns generates an increasing of the RTT, again almost constant and around 600 ms.

The average RTT for broadcast and overlapped channel is reported in Table 2.14. The strong decrease of the overhead with respect to the unicast case, shown in Table 2.13, brings to a decrease of the RTT, which now increases with the number of APs and their proximity to the ZC. Again, the use of broadcast, avoiding the search for the path in downlink, results in better performance in the presence of interference.

Finally, the relationship between the RTT and the overhead is also underlined in Fig. 2.21, where the average RTT for device 22 is shown as a function of the overhead for the different cases.

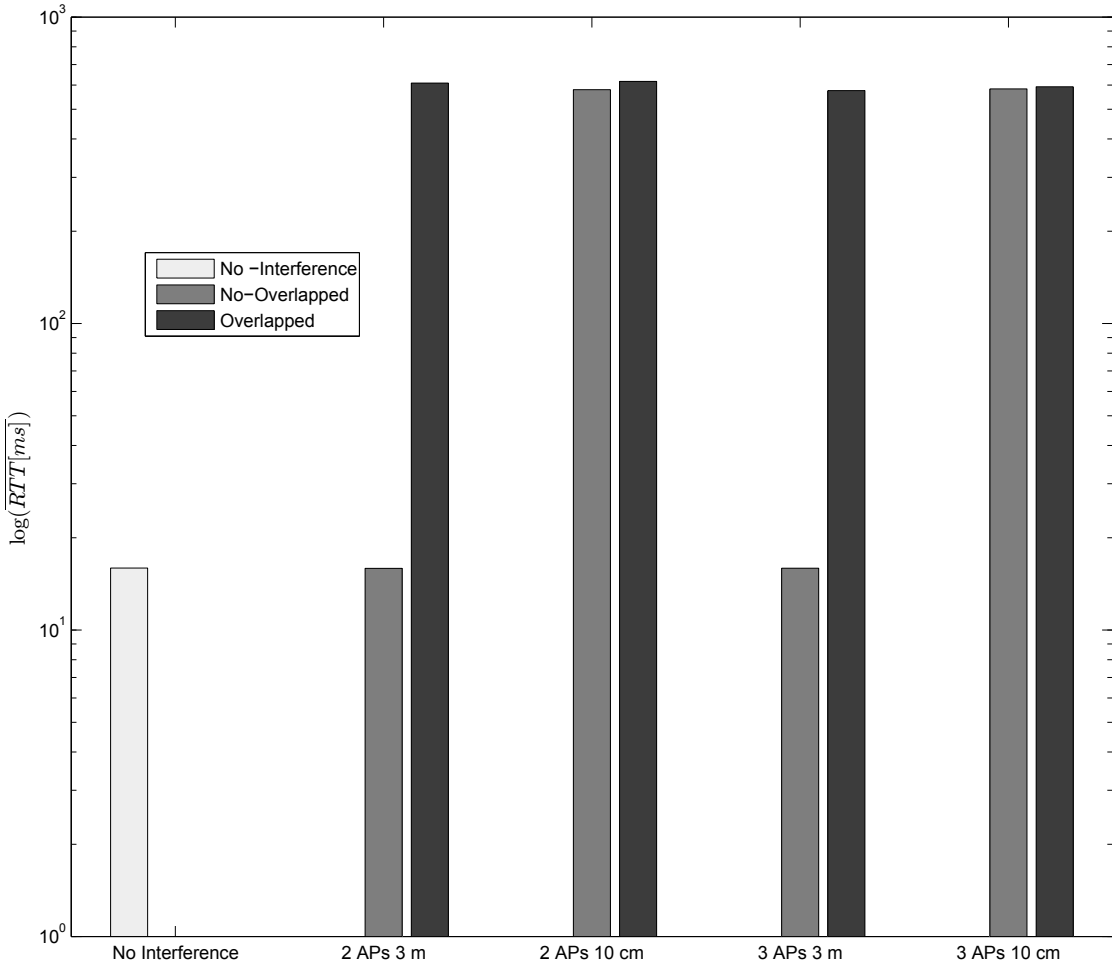

Figure 2.20: RTT averaged among devices for unicast transmission.

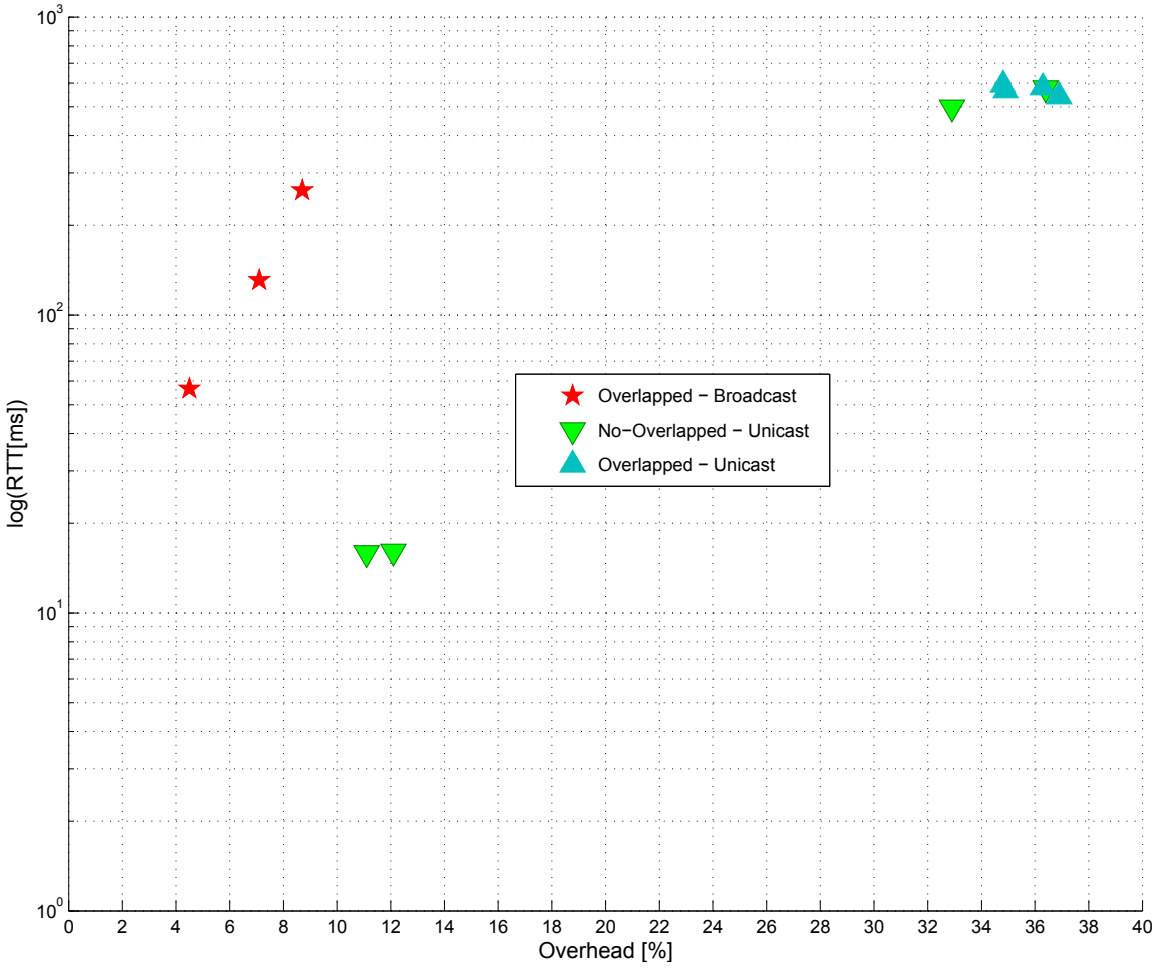

Figure 2.21: RTT as a function of the overhead for device 22.

Table 2.14: RTT [ms] for broadcast transmission and overlapped channel

Device	2APs@3m	2APs@10cm	3APs@10cm
22	56.61	130.86	261.87
33	119.14	244.44	316.7
45	179.03	325.7	N.A.

2.4.5 Conclusion

In this work, the problem of coexistence of IEEE 802.11 and IEEE 802.15.4/Zigbee was addressed. Results, based on a measurements campaign, are derived in different interference conditions and using different transmission strategies. Some conclusions are drawn below. Performance is strongly affected by the routing protocol: when AODV is used in both direction, the overhead increases and worst performance are obtained with respect to the case of broadcast transmission. The RTT is strongly affected by the overhead: when the overhead is lower than 10% the RTT is in the order of 16 ms; when the overhead becomes larger than 40% the RTT strongly increases (up to hundreds of ms). While the PLR is mainly affected by the utilization of the Wi-Fi network: when the utilization is lower than 15% the PLR is lower than 10%; when the utilization is larger than 40% the PLR becomes larger than 50%. In the case of non overlapped channel, when a distance of 10 cm is considered the ZC still receives some energy over channel 25, generating some interference and causing an increase of the overhead and of the RTT.

2.5 Fast Deploying tools

This section presents two tools useful for fast deployment of a real WSN. The first one is a methodology proposed to spatial downscaling an outdoor testbed/network

onto the FLEXTOP testbed. This procedure is intended to be used in all the case where fine-tuning of network parameters is needed or in case an outdoor application could be tested on a easier accessible environment. As example, this tool has been used to downscale an outdoor smart lighting testbed deployed on lamp post in the city center. Downscaling tool, therefore, shows is usefulness in a fast-deployment and agile development cases that are key factor for a business success in the current digital market for smart cities.

The second and tool is a proof-of-concept where low-cost and low-complexity devices can be used for fast deployment of a wireless network. In fact, in this section a device for create multi-radio Radio Enviromental Map (REM) is presented. Exploiting the REM concept is, for instance, a useful tool,The utility of the developed device is demonstrated through some experimental results reported in the following.

2.5.1 Downscaling

According to FIRE+ (Future Internet Research and Experimentation), one of the components of Horizon 2020, experimentally-driven research and innovation is a key mechanism towards advancement in Internet technology and applications[3]. In addition, the topic clearly emphasises that running experiments under controlled and replicable conditions, as well as reducing the time for experiments, by performing them on reliable and benchmarked infrastructure is fundamental. Testing communication protocols on benchmark platforms, in fact, can strongly reduce the time-to-market, avoiding complex, demanding and expensive tests in the real environment. Furthermore, small to medium size companies cannot afford deploying testbeds only

[3]http://ec.europa.eu/research/participants/portal/desktop/en/opportunities/h2020/topics/85-ict-11-2014.html

for product testing purposes, as it is a financially demanding and time consuming task. Moreover, significant human resources should be invested, as testbeds require a careful planning, deployment and maintenance.

This section replies to the latter needs, by proposing a methodology to realise the downscaling (in space) of a real testbed deployed in an outdoor scenario on a benchmark testbed deployed indoor,for benchmarking IEEE 802.15.4-compliant networks.

The aim of downscaling is to reproduce a testbed, denoted as *target* testbed hereafter, over an indoor and controllable testbed, denoted as *benchmark* in the following. Reproducibility is the ability of an entire experiment to be reproduced, but also refers to the degree of agreement between observations or measurements conducted on replicate specimens in different locations [45]. With reference to the latter definition, the aim of this procedure is to identify the proper subset of nodes on the benchmark testbed, such that experiments run over these nodes are in agreement with those observed on the target testbed in terms of performance and obtained results. It is denoted as *downscaled* testbed the subset of nodes of the benchmark testbed identified through the downscaling procedure, properly reproducing the behavior of the target testbed. Fig. 2.22 further clarifies the concept: a real world deployment (a) with $N^{(r)}$ nodes and a coordinator can be reproduced on the downscaled testbed (b) having the same number $N^{(r)}$ of devices; the latter is part of the controllable testbed that, for the sake of flexibility, is made of a larger number $N^{(c)}$ of nodes, and is compact in space. The selection of the subset must be such that the performance of the protocols/solutions implemented and tested on the downscaled testbed, will be similar to those that would be measured in the real world deployment.

The problem of selecting the best possible subset of nodes on the benchmark

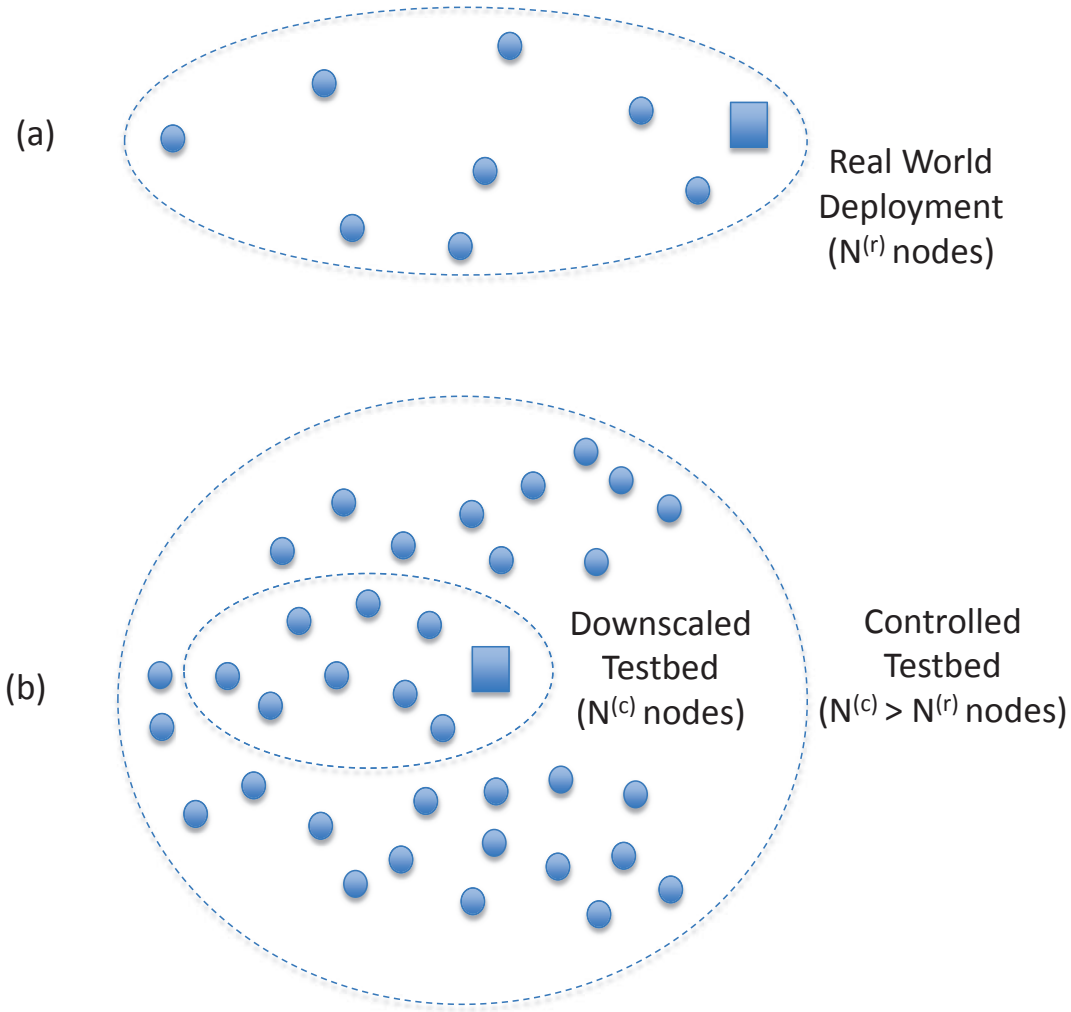

Figure 2.22: Downscaling description.

testbed is formulated as a 0-1 Linear Program in this paper, and solved to optimality using a state-of-the-art MILP solver.

In order to reproduce the same results obtained over different testbeds, it is of outmost importance to reproduce the level of connectivity among nodes in the testbeds, since connectivity affects network topologies and possible interference among nodes. Therefore, being able to reproduce the connectivity levels among nodes in the target, over the downscaled testbed allows to obtain the same results, with large probability. Thanks to this, protocol optimisation such as parameters tuning could be performed on the downscaled testbed, avoiding inconvenient and complex outdoor tests.

2.5.1.1 Related Work

The MiNT [46] and Orbit [47] testbeds attempt to shrink a wireless network into a smaller space while maintaining link characteristics through power control. Authors reduce transmission power via software and/or radio frequency components, and received power via augmented environmental noise and/or controllable attenuators. The work presented in [48] focuses on the reliability of spatial scaling of wireless networks as well. [49] presents a work dealing with the emulation of the performance of real world networks on an indoor wireless testbed. In particular, they tend to replicate each link from the real network on the indoor testbed, focusing on the downlink signal-to-noise-ratio mapping.

In contrast to the above works, the method presented here deals with 802.15.4-based networks and it proposes a different algorithm to select nodes to create the downscaled testbed. The proposed methodology however is not specific only for the described testbeds, but it is general and independent on hardware and environment.

While in the scientific literature, there are no other similar works dealing with downscaling of real world deployments to an indoor testbed, there are plenty of works dealing with experiments exploiting indoor or outdoor testbeds, which deserve citation here as they inspired the motivation for this work. [50] describes a testbed having a dual purpose: on one hand it allows real world experimentation of IoT related technologies and, on the other hand, it supports the provision of smart city services aimed at enhancing the quality of life in the city of Santander. [51] provides a comprehensive survey of the enabling technologies, protocols, and architecture for an urban IoT referring to a practical implementation of this concept, named Padova Smart City. The target application consists of a system for collecting environmental data and monitoring the public street lighting by means of 300 wireless nodes deployed in the city of Padova. The work [52] presents the VESNA wireless sensor network platform and its role in experimentally-driven research and development.

In [53], authors propose an indoor testbed which is built on the ceiling board of the demonstration room. The purpose of this testbed is to evaluate various types of algorithms and protocols before using them in real world applications. The work [54] gives an overview of all aspects concerning the feasibility of large scale wireless sensor network deployments. Authors refer to a testbed deployed in the buildings of the Department of Information Engineering at the University of Padova. The paper describes different hardware and software architectures for large scale wireless sensor networks, but also efforts that have to be made in terms of communication protocols and strategies for the organization of large testbeds. Twist [55] is a scalable and flexible indoor testbed supporting experiments with heterogeneous node platforms. The testbed consists of 100 TelosB motes spread over a three floor office building. The

SensLAB [56] is a testbed consisting of 1000 sensor nodes available for distributed embedding sensor network applications and distributed systems research.

2.5.1.2 The downscaling methodology

The aim is to reproduce a real world deployment, being characterised by a given number of nodes located in given positions and transmitting at a given power level, on an indoor controllable testbed. Reproducibility refers to the degree of agreement between measurements or observations conducted on separate specimens in different locations [45]. Therefore, the aim of this procedure is to identify the proper subset of nodes of the controllable testbed, their respective locations and the level of transmit power they have to use, such that results obtained through experiments running over the downscaled testbed are in agreement with those observed in the real world.

The procedure is based on the following premise: if one is able to reproduce the channel gains between each nodes pair in the network, he will be able to obtain the same network performance with a good approximation. In the following, channel gains will be used to define the *connectivity level* between two nodes, that is the probability that the data transmitted by one node is correctly received by the other (and viceversa). The level of connectivity among nodes has a strong impact on: i) the topologies formed in the network, that is the set of paths connecting transmitters and the respective receivers; ii) the number of nodes each node can "hear", that is the set of nodes that are not hidden to the given one and with which it will not interfere; iii) the level of interference possibly generated by each node on the other nodes in the network. All the above mentioned items strongly affect the performance of the network, therefore reproducing the connectivity brings to reproducing the network

performance, with large probability.

It is important to underline that this downscaling approach is intended in terms of space and that it is possible when the controllable testbed provides the following degrees of freedom: i) a number of available nodes, $N^{(c)}$, larger than the number $N^{(r)}$ of nodes in the real world deployment, so that a large number of options for the subset selection is possible; ii) the possibility to set different levels of transmit power (or any other parameter affecting the connectivity among nodes) to be used by the nodes in the downscaled testbed.

Moreover it is important to underline that this downscaling methodology could be applied to whatever an hardware platform, provided that the two platforms used in the real deployment and in the downscaled testbed are compatible. In fact, it had been applied to testbeds (real and controllable) using exactly the same hardware and radio.

The proposed methodology is shown in Figure 2.23, where are underlined in white the steps that require programming of devices and running of experiments, and in grey the processing and design tasks. The methodology consists of two parts: i) the identification of the downscaled testbed and ii) its utilization. The first part is composed of the following steps:

1. Estimation of the level of connectivity among nodes in the real world deployment;

2. Measurement of the level of connectivity among nodes in the controllable testbed;

3. Selection of the downscaled testbed nodes, which is the subset of nodes of the

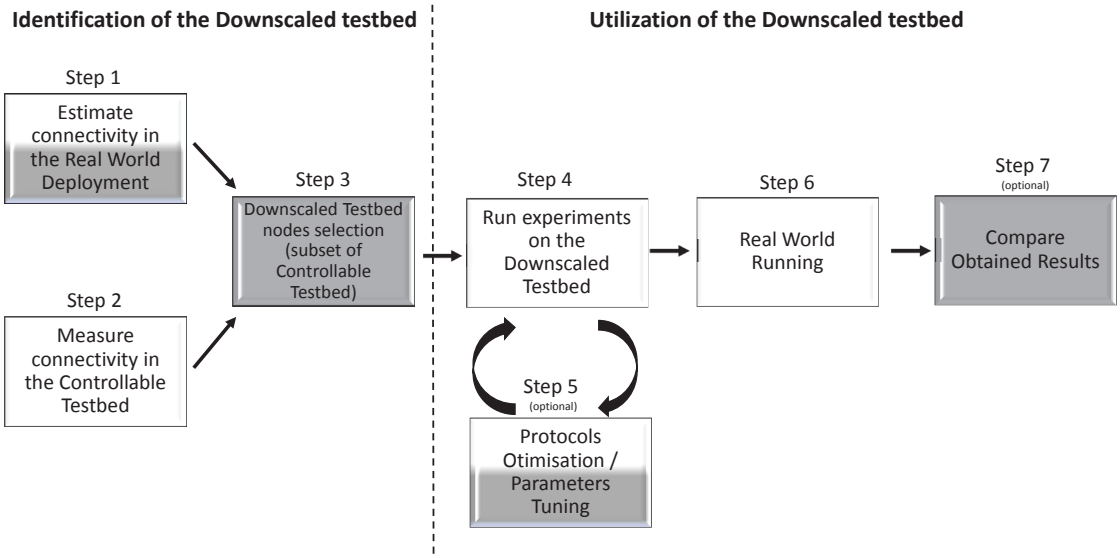

Figure 2.23: Downscaling methodology.

controllable testbed properly reproducing the real world network.

The second part is composed of the following steps:

4. Run experiments on the identified downscaled testbed;

5. (Optional) Optimise the protocols and/or parameters tuning;

6. Real world running, which refers to running the application on the real world deployment;

7. (Optional) Compare results achieved on the two testbeds (real world and downscaled).

2.5.1.3 Identification of the downscaled testbed : Downscaled testbed nodes selection

For each node of the real world deployment a counterpart in the controllable testbed has to be selected with the aim of reproducing the same connectivity properties. More precisely, denoting with $\phi(i) : I \rightarrow J$ a function mapping each node of the real world deployment to a node of the controllable testbed, i.e., for each $i \in I$, $\phi(i)$ is its counterpart in the controllable testbed and $\phi(i) \neq \phi(k)\ \forall i, k \in I$.

In the ideal case, it is likely to have $P^{(r)}_{ik} = P^{(c)}_{\phi(i),\phi(k)}$ for all pairs of nodes $i, k \in I$. Usually this is not achievable, but it is reasonable to get as close as possible to the ideal case by finding the mapping function ϕ that minimizes the sum of the distances

$$D = \sum_{i \in I} \sum_{k \in I} \left| P^{(r)}_{ik} - P^{(c)}_{\phi(i),\phi(k)} \right|.$$

The problem can be modeled as a Rectangular Quadratic Assignment Problem (RQAP) [57], which calls for the determination of an assignment of each element of I to a distinct element of J (with $|I| < |J|$), so that the objective function, D, representing the distance between the two connectivity matrices, is minimised.

More precisely, if node $i \in I$ is assigned to node $j \in J$ and node $k \in I$ is assigned to node $l \in J$, their distance, d_{ijkl}, is defined as

$$d_{ijkl} = |P^{(r)}_{ik} - P^{(c)}_{jl}| + |P^{(r)}_{ki} - P^{(c)}_{lj}|.$$

Quadratic assignment problems are among the most difficult and studied Combinatorial Optimization problems found in the Operations Research literature. RQAP is strongly NP-hard, i.e., it does not have an approximation algorithm running in polynomial time for any factor, unless $P = NP$ [58]. By introducing a set of $|I|$x$|J|$

binary decision variables

$$x_{ij} = \begin{cases} 1 & \text{if node } i \in I \text{ is assigned to node } j \in J \\ 0 & \text{otherwise.} \end{cases}$$

RQAP can be formulated as the following Integer Program with a quadratic objective function.

$$\min D = \sum_{i \in I} \sum_{j \in J} \sum_{k \in I: i<k} \sum_{l \in J} d_{ijkl} x_{ij} x_{kl} \tag{2.5.1a}$$

$$\text{s.t.} \sum_{j \in J} x_{ij} = 1 \qquad \forall i \in I \tag{2.5.1b}$$

$$\sum_{i \in I} x_{ij} \leq 1 \qquad \forall j \in J \tag{2.5.1c}$$

$$x_{ij} \in \{0, 1\} \qquad \forall i \in I,\ j \in J \tag{2.5.1d}$$

Constraints (2.5.1b) impose that each node in I is assigned to a node of J and constraints (2.5.1c) impose that each node of J is assigned to at most one node of I.

According to preliminary computational experience, model (2.5.1) turned out to be not solvable in reasonable computing time by state of the art quadratic programming solvers for the size of the instances arising in practical cases. Therefore it is adopted a standard linearized integer programming model for RQAP.

Consequently, a second set of decision variables is introduced:

$$y_{ijkl} = x_{ij} x_{kl} \quad (i < k \in I,\ j, l \in J).$$

and then RQAP can be written as the following 0-1 linear program:

$$\min D = \sum_{i\in I}\sum_{j\in J}\sum_{k\in I:i<k}\sum_{l\in J} d_{ijkl}y_{ijkl} \tag{2.5.2a}$$

$$\text{s.t.} \sum_{j\in J} x_{ij} = 1 \qquad \forall i \in I \tag{2.5.2b}$$

$$\sum_{i\in I} x_{ij} \leq 1 \qquad \forall j \in J \tag{2.5.2c}$$

$$x_{ij} + x_{kl} - y_{ijkl} \leq 1 \qquad \forall i < k \in I, j, l \in J \tag{2.5.2d}$$

$$x_{ij} \in \{0, 1\} \qquad \forall i \in I,\ j \in J \tag{2.5.2e}$$

$$y_{ijkl} \in \{0, 1\} \qquad \forall i < k \in I,\ j, l \in J \tag{2.5.2f}$$

The new constraints (2.5.2d) link the two sets of variables, forcing $y_{ijkl} = 1$ if node $i \in I$ has been assigned to node $j \in J$ and node $k \in I$ has been assigned to $l \in J$. Such formulation is valid since in the problem all the coefficients d_{ijkl} are non negative. Thus, it is never convenient to set $y_{ijkl} = 1$, if not imposed by constraints (2.5.2d).

Model (2) brings to the selection of a different subset of nodes, for each of the connectivity matrices $P^{(c)}$. The final subset, identifying the downscaled testbed, is selected by comparing the values of D obtained for the different matrices $P^{(c)}$, taking the case with minimum D.

2.5.1.4 Conclusions

In this section, a methodology to reproduce a real world deployment on a downscaled testbed deployed in an indoor and controlled environment have been presented. This

methodology allows replication of experiments for optimisation purposes. The downscaled testbed is represented by a subset of nodes of a controllable platform. The described procedure is based on solving an optimization problem, namely a RQAP, where the objective function is the minimization of the total connectivity difference between the real world deployment and the downscaled testbed. The methodology can be applied to any real IoT world deployment, provided that a controllable testbed is available, having a number of nodes at least two or three times larger than the size of the real world deployment, and allowing to set different levels of transmit power. An exhaustive description of this fast deployment tool can be found at [59].

2.5.2 REM device

The IoT market players expect a fast deployment of networks and applications, hence a huge role is played by wireless technologies which are faster to install with respect to wired solutions. Due to the scarce of spectrum resources and to the cost of licensed radio bands, different standards should coexist in the same band. For instance, in the Industrial Scientific and Medical (ISM) band at 2.4 GHz different standards, like IEEE 802.11, IEEE 802.15.4 and IEEE 802.15.1 and other proprietary solutions should compete for the radio resource.

This work addresses the issue of coexistence by presenting a prototype device, able to measuring the level of interference generated by different technologies over a given bandwidth and to create a multi-standard Radio Environmental Map (REM) [60]. Hence, the multi-standard REM can be used to: i) properly selecting the least interfered channel to be used by a given technology; ii) create coverage maps, in the

presence and in the absence of interference; iii) detect the presence of possible frequencies characterised by a low level of interference, which could be opportunistically exploited by other new technologies.

The problem of coexistence has been widely studied in the literature (e.g., [61]-[62]). Most of the works presented in literature are related to software defined network and cognitive radio [63], some apply the REM concept on WiFi network limited to localization [64]. However, in the scientific literature, there are no works presenting a multi-standard device for creating REM to be used as tool for fast network deploying and low-cost monitoring. In particular, in this section a low-cost device able to analyse the environment is presented. This devise can measure the electromagnetic activity and discriminate among standards. The considered standards are working in the ISM band at 2.4 GHz and are: IEEE 802.11 [37], 802.15.4 [12] and 802.15.1 [65]. Under the REM concept, the device senses the spectrum, analyses the data and provides information to a central database. In the rest of this section, since it describes an experimental activity based on real applications, the terms Wi-Fi, Bluetooth and Zigbee identify applications running on IEEE 802.11, 802.15.1 and 802.15.4 respectively.

2.5.2.1 Problem statement

Fig. 2.24 shows the entire ISM band, having a bandwidth of 80 MHz, and its occupancy by the three considered standards, using channels of 22 MHz (802.11), 5 MHz (802.15.4) and 1 MHz (802.15.1). The overlap among the different channels of the different technologies can be clearly seen in the figure, and justify the need of REM to manage interference. As anticipated above, in this section the relevant standards

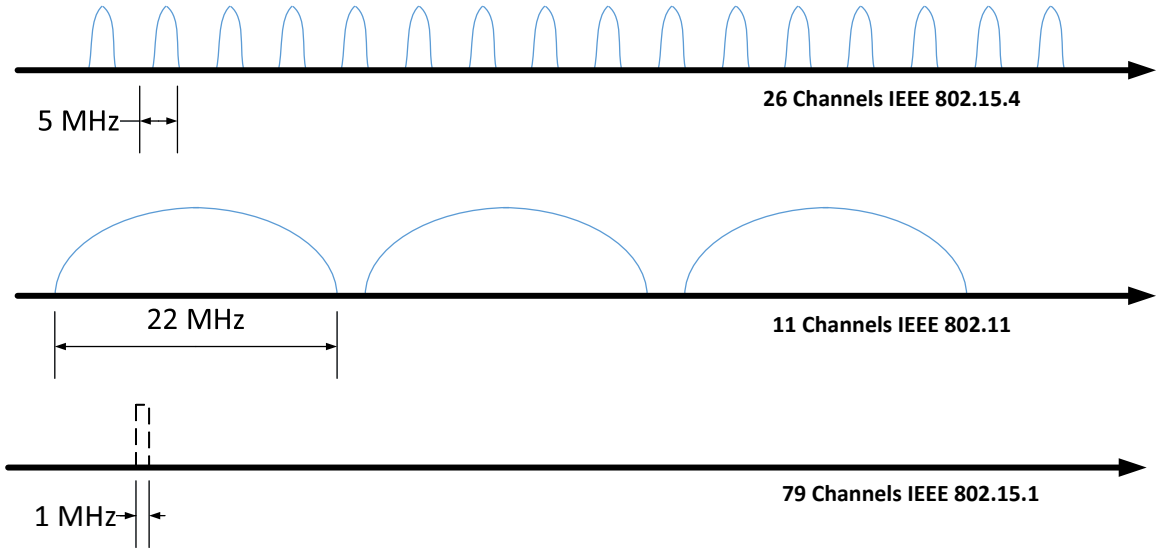

Figure 2.24: Channels overlapping within the 2.4 GHz band.

are: IEEE 802.15.4 [12], IEEE 802.11 [37], IEEE 802.15.1 [65].

2.5.2.2 The REM Device Developed

Hereafter it is described the device, denoted as *measurement unit*, its hardware and software components; then the measurement procedure implemented are discussed.

Hardware and Software Characteristics The control unit is an Intel Galileo, based on the Intel Quark SoC X1000 Application Processor, a 32-bit Intel Pentium-class system on a chip (SoC) [4]. The control unit runs a minimal Linux distribution. Since this operating system native support Python, the air interface are querying by using python scripts. It also runs a local database to store and process data gathered over air interfaces. The IEEE 802.15.4 air interface is a Flextop device connected through USB interface to the control unit. It runs a customize firmware that allows

[4]http://www.intel.com/support/go/galileo

us to send command from the control unit, e.g. define scan type, scan duration and so on. The other two air interfaces are integrated in a mini-pci express card, i.e., Intel N-6205 [5]. The control unit is connected with the frontend, which is a laptop used to visualize the measurement outcomes. For prototyping reason, the frontend and control unit are connected through a serial interface, however the measurement unit can be connected on internet to be remotely controlled.

Measurements Procedure: IEEE 802.15.4 Scan The standard provide two method to sense the specturm: Energy Detection (ED) scan and Active Scan (AS). In this context both are available and used. ED provides an estimate of the RSSI within the bandwidth of an IEEE 802.15.4 channel. No attempt is made to identify or decode signals on the channel, therefore it could be used to detect presence of all possible technologies working into a given 802.15.4 channel (being 802.15.4, 802.11 or 802.15.1). The ED time shall be equal to 8 symbol periods, where a symbol period has a duration of 16 μs. At the end of the scan a list of the channels and associate RSSI list is returned. In particular, the peak values measured in each channel are returned.

AS is used by 802.15.4 devices, to locate all 802.15.4 coordinators transmitting beacon frames. The active scan is performed on each channel by first sending a beacon request command, waiting for a beacon. The scan returns the list of the Personal Area Network (PAN) coordinators found out, the corresponding channels used and the RSSI received from each of them.

[5]http://www.intel.com/content/dam/www/public/us/en/documents/product-briefs/centrino-advanced-n-6205-desktop-brief.pdf

Measurements Procedure: Wi-Fi Scan It is directly available by the operating system, i.e. *iwlist*. It is a Linux utility that provides the list of Access Point (AP)s in range and many information, such that MAC address, Channel, Extended Service Set Identification (ESSID), RSSI, etc. This command set the air interface on each channel for 200 ms. This value is chosen because the maximum beacon broadcasts interval is 100 ms, hence 200 ms ensure that at least a beacon is received.

Measurements Procedure: Bluetooth Scan The bluetooth scan was implemented by using a python module, i.e. pybluez. The outcome of this command is a list of bluetooth device MAC address and their corresponding RSSI values.

2.5.2.3 Experimental Setup

This work shows measurement results obtained with both: UniBo premises, the corridor (see Fig. 2.25) , and a 200 m^2 flat located in a residential area (see Fig. 2.26). The former is a controlled environment, where the presence of interference could be controlled, by switching on and off the different networks on demand. While the latter scenario is less controllable, due to the presence of possible interfering networks located in apartments nearby. Both environments are divided in pixels of 6,25 m^2 (2,5x2,5 m) (see Fig.s 2.25 and 2.26). In this work the measurements are provide on pixel base.

In the rest of this section, the application used over the different air interfaces are presented. Fig. 2.27 shows the application setup for the case of 802.15.4 and Wi-Fi networks. An 802.15.4 coordinator sends a data packet of 30 bytes to an 802.15.4 end device with a periodicity of 300 ms, using channel 26. In the case of Wi-Fi an AP sends a video stream to a laptop connected in the same network. If not otherwise

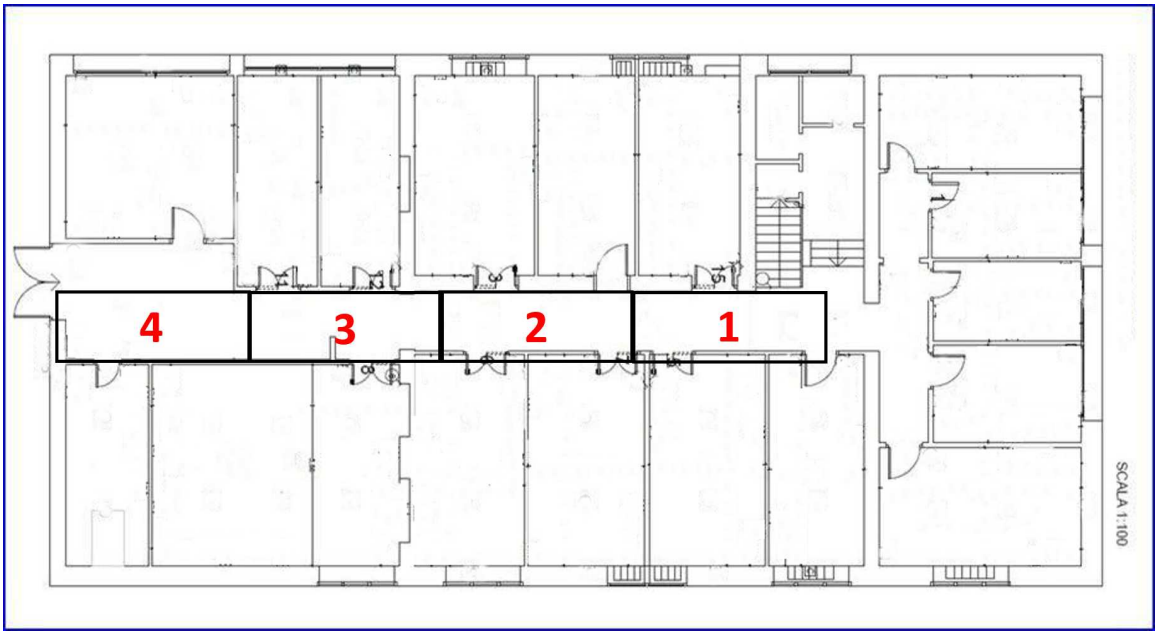

Figure 2.25: Map of the devices located in the corridor, with the corresponding pixels.

specified the AP is setup on channel 1 using mixed mode, i.e., both IEEE 802.11b and IEEE 802.11g are enabled. As application running over Bluetooth was selected an audio streaming between a stereo headphone and a laptop.

2.5.2.4 Experimental Results

The aim of this study is to demonstrate three possible applications for the measurement unit: i) properly selecting the least interfered channel to be used by a given technology; ii) create coverage maps, in the presence and in the absence of interference; iii) detect the presence of possible frequencies characterised by a low level of interference, which could be opportunistically exploited by other new technologies.

First aim: Selecting the least interfered channel A scenario where other networks are present in the environment is considered in the case of a new technology

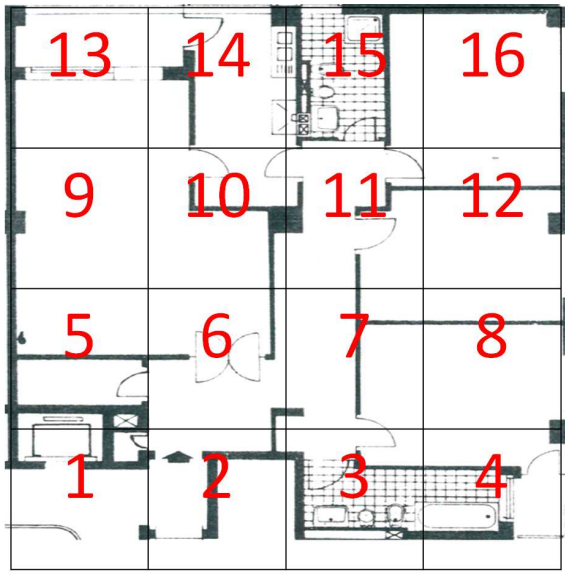

Figure 2.26: Map of the devices located in the flat, with the corresponding pixels.

installation(or a new network of an already present technology). In other words, the foreseen application scenario is: fast deploy a new network on the least interfered channel. Fig. 2.28 refer to the case where one 802.15.4 network is working on channel 26, one BT network and one Wi-Fi AP on channel 3 (figure on the left) or two Wi-Fi APs on channels 3 and 11 (figure on the right). Both results are related to the corridor scenario, where all the above networks were deployed in pixel 1 of Fig. 2 and the measurement unit is located in the four pixels. The measurement unit was performing energy detection scan over the available 16 channels in each pixel. More in details, 10 measurements per pixel have been performed and the average RSSI values computed. Figures show the average value of RSSI measured in each pixel and in each channel and the corresponding mean value, by averaging among the different pixels. Values are reported in dBm. Results show that the least interfered channel was channel 25.

A similar measurement have been done in the flat, by just setting up one Wi-Fi

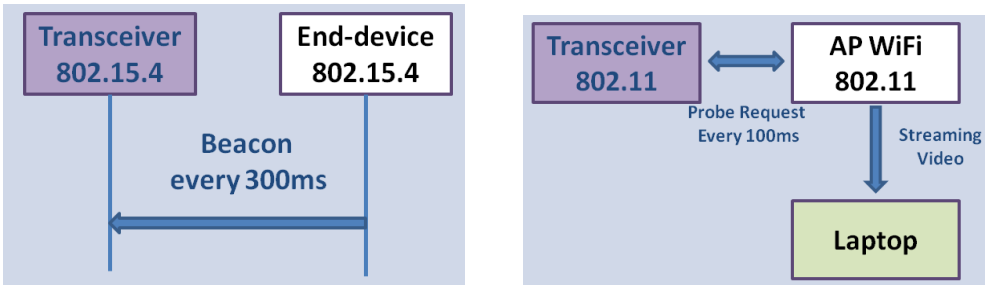

(a) (b)

Figure 2.27: Zigbee and Wi-Fi networks setup: a) IEEE 802.15.4 network, b) WiFi network.

Ch\Px	1	2	3	4	Mean value
11	-78	-69	-66	-53	-67
12	-76	-68	-66	-55	-66
13	-63	-70	-66	-47	-62
14	-51	-64	-70	-55	-60
15	-52	-67	-71	-77	-67
16	-61	-77	-81	-80	-75
17	-50	-74	-77	-77	-70
18	-53	-75	-77	-77	-71
19	-58	-79	-87	-84	-77
20	-68	-77	-84	-87	-79
21	-50	-62	-74	-77	-66
22	-50	-60	-73	-66	-62
23	-49	-61	-74	-66	-63
24	-52	-62	-83	-84	-70
25	-87	-84	-90	-92	-88
26	-65	-76	-86	-81	-77

(a)

Ch\Px	1	2	3	4	Mean value
11	-77	-67	-67	-61	-68
12	-74	-67	-66	-57	-66
13	-53	-67	-67	-68	-64
14	-43	-65	-68	-68	-61
15	-48	-69	-78	-73	-67
16	-58	-76	-84	-80	-75
17	-48	-64	-77	-80	-67
18	-47	-65	-77	-78	-67
19	-53	-76	-79	-82	-73
20	-49	-76	-77	-81	-71
21	-45	-64	-74	-76	-65
22	-35	-63	-69	-73	-60
23	-35	-66	-71	-69	-60
24	-50	-74	-78	-82	-71
25	-77	-92	-92	-86	-87
26	-66	-77	-90	-86	-80

(b)

Figure 2.28: REM in the corridor scenario: a) One Wi-Fi net, one 802.15.4 net, one BT net; b) Two Wi-Fi net, one 802.15.4 net.

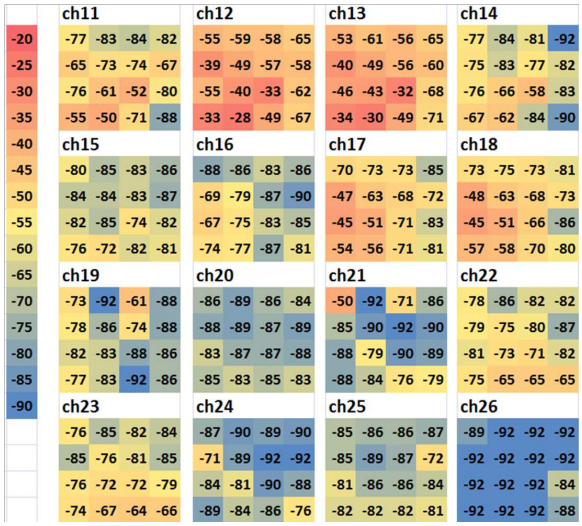

Figure 2.29: REM in the flat: values for the different pixels.

network using channel 12 and located in pixel 2 of Fig. 2.26. Fig. 2.29 shows the ED measurement values on pixel base, for the different 802.15.4 channels, while Fig. 2.30 reports the average RSSI per channel, averaged among the measurements performed in the different pixels. In this case, the least interfered channel was 25. As stated above, the environment was uncontrollable, meaning that possible other sources of interference could be present around. As an example, in pixel 13 on channel 21 where an unexpected high value (-50 dBm) was received.

Second aim: Coverage Maps Another possible use of this measurement unit is creating coverage maps, both in the presence and in the absence of interference. The flat scenario and channel 26 are considered, no other interferences were present during experiments.

Coverage in the absence of interference In this case the aim was to evaluate the level of coverage generated by an IEEE 802.15.4 coordinator in the absence of interference. The coordinator was located in pixel 2, and the measurement

ch11	ch12	ch13	ch14
-71	-50	-51	-77
ch15	ch16	ch17	ch18
-82	-81	-66	-67
ch19	ch20	ch21	ch22
-82	-86	-83	-77
ch23	ch24	ch25	ch26
-77	-86	-84	-91

Figure 2.30: REM in the flat: mean values.

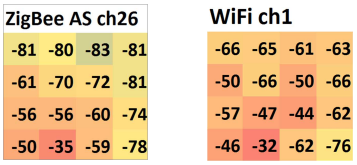

(a) (b)

Figure 2.31: REM in flat scenario: a) IEEE 802.15.4 Active Scan REM on channel 26; b) WiFi scan.

unit have been moved from pixel to pixel, in order to perform active scan. In fact in this case the aim of the measurement was to derive the average level of power RSSI that could be received by an 802.15.4 end device from the 802.15.4 coordinator. In Fig. 2.31 on the left AS results are shown, representing the coverage map in the absence of interference. Received power level is very high in the pixel 2 (-35 dBm) where the coordinator was located. All others power levels are substantially high, with a little drop in the pixels of the upper perimeter of the map.

Coverage in the presence of interference In this case a Wi-Fi AP working on channel 11 and located in pixel 2 was activated, in order to derive the level of interference that could be suffered by an IEEE 802.15.4 end device located on the different pixels. The 802.15.4 network (i.e., the coordinator) was switched off in this measurement. In this case ED scan was performed by the measurement unit, again in the different pixels. Fig. 2.29 shows the ED results. The AP was on channel 1, hence channels 11, 12 and 13 of 802.15.4 show high values, as expected since those channels are completely overlapped with Wi-Fi channel used. Meanwhile, on channel 26 there is no any kind of activity, in fact the measured values are basically the receive sensitivity.

Measurement results in Fig. 2.31 have been used to derive the coverage map in the presence of interference. In particular, a pixel have been considered as *covered* if the signal to interference ratio (SIR), C/I, is larger than a given threshold, called capture threshold, α. Results in Fig. 2.31 on the left, have been obtained by switching on only 802.15.4 and performing AS, therefore they provide the average received useful power, C, for the different pixels. While results on the right have been derived by switching on only interferences, therefore they measure the aggregated interference, I, coming from Wi-Fi. By comparing the SIR with the capture threshold, it can be derived the coverage map in the presence of interference. The resulting map for the different 802.15.4 channels is shown in Fig. 2.33, where $\alpha = 2$ dB was set and white for pixels where $C/I >= 2$ dB (coverage) was used, while black for pixels where $C/I < 2$ dB (no coverage) was used. As expected, channel 26 is the best channel for 802.15.4 transmissions; in fact, it is the only one not overlapped with 802.11 channels. On the contrary, there are no pixels covered in channels 12 and 13, completely overlapped

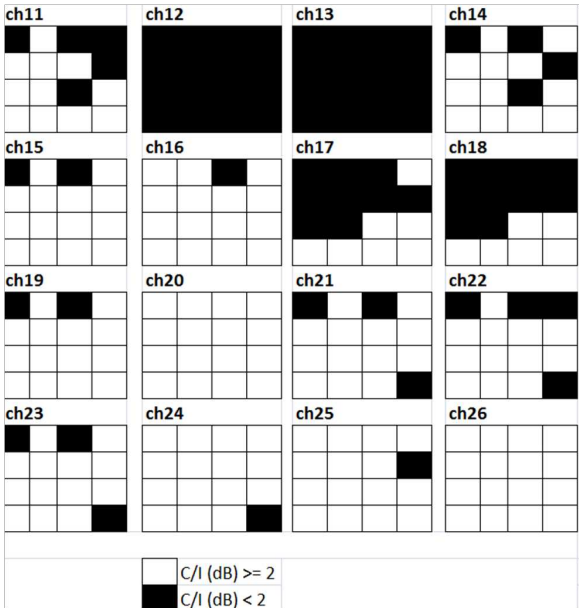

Figure 2.32: Coverage map in the presence of Wi-Fi interference.

with channel 1 of WiFi.

Third aim: Opportunistically exploiting low interfered channels In this third application example the use case is to quickly find the best channel, i.e., the lowest interfered, that can be used to install a new technology. In this latter case the corridor scenario is used, where the 802.15.4 network is setup, one BT network and one Wi-Fi network working on channel 3 (as in the case of Fig. 2.28 on the left). It was assumed that the new technology to be deployed uses a 5 MHz channel in the 2.4 GHz band.

The ED scan results for the different channels and pixels are reported again in Fig. 2.33 where also the maximum level of interference over the different channel are shown, i.e. I_{max}.

By considering different capture thresholds, α, it can be derived different values

Ch\Px	1	2	3	4	Imax	Cmin(α=2)	Cmin(α=4)
11	-78	-69	-66	-53	-53	-51	-49
12	-76	-68	-66	-55	-55	-53	-51
13	-63	-70	-66	-47	-47	-45	-43
14	-51	-64	-70	-55	-51	-49	-47
15	-52	-67	-71	-77	-52	-50	-48
16	-61	-77	-81	-80	-61	-59	-57
17	-50	-74	-77	-77	-50	-48	-46
18	-53	-75	-77	-77	-53	-51	-49
19	-58	-79	-87	-84	-58	-56	-54
20	-68	-77	-84	-87	-68	-66	-64
21	-50	-62	-74	-77	-50	-48	-46
22	-50	-60	-73	-66	-50	-48	-46
23	-49	-61	-74	-66	-49	-47	-45
24	-52	-62	-83	-84	-52	-50	-48
25	-87	-84	-90	-92	-84	-82	-80
26	-65	-76	-86	-81	-65	-63	-61

Figure 2.33: REM in corridor scenario for the case of 1 Wi-Fi net, 1 802.15.4 net and 1 BT net.

of the minimum useful power, C_{min}, that should be guaranteed by the new deployed network, in order to work properly. The results (see Fig. 2.33) show that best channel, i.e. the channel that ensure a corrected reception with the lowest C_{min} is channel 25.

Conclusions In this section, a low-cost low-complexity device for multi-standard REM analysis was presented. This device allows REM generation on different air interfaces, in this version the focus was on the unlicensed band ISM at 2.4 GHz and on IEEE 802.15.4, IEEE 802.11 and IEEE 802.15.1. The device could be used both in fast deployment and fast delivery techniques; and also for continuous monitoring. The usefulness of this approach have been shown through three different use cases: i) selecting the least interfered channel; ii) creating coverage maps, in the presence and in the absence of interference; iii) detecting free channels for deploying new technologies. In all cases it was demonstrated that even with simple measurements the device could be useful.

2.6 Conclusions

In this chapter, three different short-range protocol standard for IoT applications have been presented. Those are standard solutions with distributed approach, i.e. Zigbee and 6LoWPAN; and a centralized approach based on Software Defined Network (SDN) approach - SDWN. All those solution rely on IEEE 802.15.4 standard that is the 'de facto' standard for WSN. The different solutions have been tested and evaluated using FLEXTOP, a testbed platform developed within Newcom# at University of Bologna. Furthermore, an analysis of coexistence between Zigbee and Wi-Fi networks have been presented.

Finally two development tools for WSN have been shown. The first one is a methodology to spacial downscaling a testbed or an application onto FLEXTOP. While, the second one, is a device able to identify different wireless standards within the ISM band at 2.4 GHz. Both development tools are useful in agile and fast development of smart cities and more in general IoT applications. Both solutions have been tested using FLEXTOP.

Chapter 3

IoT in the Cellular world - MTC

This chapter studies the IoT in cellular world. In particular, the main research challenges will be presented and the 3GPP architecture from Machine Type Communications (MTC) will be described. The concepts introduced in this chapter together with the M2M traffic model already presented in Chapter 1 are preparatory to the next chapter, where the Radio Resource Management (RRM) for M2M application in LTE network will be discussed.

3.1 Challenges

In this subsection we analyze the main challenges related to how using the 3GPP cellular infrastructure as a communication support for M2M traffic. In addition we provide an overview of how they have been approached up to date by the state of the art. There are a number of important differences between MTC and Human to Human (H2H) communications. MTC involves several entities which do not necessarily need human's operation. Three use cases have been identified in 3GPP Technical Report 37.868 [66]. Those uses cases are metering, road security, and consumer electronic and devices. Taking those cases as examples, it gets clear that there are

main differences from H2H communications: 1) different market scenarios, 2) supported services: unlike traditional H2H services, such as voice and web streaming, M2M services often have very different requirements due to their specific feature (e.g. group-based communications, low or no mobility, time controlled operation, delay tolerant, small and infrequent data transmission, secure connections, MTC monitoring, priority alarm messages, extra low power consumption, high reliability, etc.), 3) lower costs, 4) a very large number of end devices, 5) little traffic from every device. These differences make that 3GPP standards need to be revisited to be adapted to support the advent of this new technology. The future challenges are multiple and can be summarized in the following points:

- *Low cost M2M devices*: In order for LTE to be a successful platform for the support of M2M communications, the cost of LTE devices needs to be reduced [67]. A 3GPP RAN1 group is currently working on this topic.

- *QoS management*: In literature few schemes have been proposed to deal with the multiplexed access of machines to the Evolved UMTS Terrestrial Radio Access Network (E-UTRAN) network, such as [68]. To achieve successful M2M communications, QoS is the most important requirement. Some applications require hard constraints and disasters may occur if those are violated. Other applications have more relaxed constraints. Different from applications in classical cellular communications, based on human-to-human relations, where packet arrival periods can range from 10 ms to 40 ms, in MTC they can range from 10 ms to several minutes. This is referred to as infrequent transmission in 3GPP. Thus, how to successfully multiplex and schedule massive accesses with enormously different QoS characteristics turns out to be the most challenging task.

A proposal in this sense is given in [69]. A study on latency requirements and bottlenecks across the whole architecture is given in [70].

- *Resource Allocation and scheduling*: Packet scheduling constitutes the key RRM mechanism to minimize the overall resource usage, while guaranteeing individual QoS requirements. As a result, resource allocation and scheduling are expected to play a crucial role to deploy M2M communications through LTE. In general, scheduling is not part of the standardization work, but it is an implementation specific issue. However, signaling is standardized, thus any scheduling proposal should be in line with the set of control requirements. Toward this purpose, a generic packet scheduling framework has been proposed in 3GPP. Leaning on this, several schemes have been devised for dynamically allocating resources with heterogeneous QoS requirements. However, with M2M scenarios coming into play, the scheduling entities have to deal with extremely diverse QoS criteria. For example, delay tolerance may span from tens of ms (vehicle collision) to several minutes (environmental monitoring), and the error rate tolerance, scale similarly. As a result, defining QoS classes is not an easy task. The literature is in general very limited in addressing the scheduling for M2M traffic in LTE systems. Schedulers designed for LTE cannot be applied for M2M, mainly due to the fact that H2H communications consider a limited amount of services which can be delivered through the network, and consequently a reduce set of QoS requirements for the different applications, compared to those that should be considered for M2M traffic. In [71] the authors propose a grouping-based technique for LTE-A stations to manage radio resources for MTC devices, according to which they form clusters with respect to their packet arrival rate and

maximum jitter. Channel quality os not considered here, but it is instead in this other contribution [68], where two uplink scheduling schemes are presented, taking into account channel conditions and maximum allowed delay of each device that requests transmission. In [72] semipersistent scheduling is applied to Voice over IP (VoIP) traffic which presents similar characteristics to the MTC.In particular, LTE is supposed to support hundreds of VoIP users that generate small amounts of periodic data traffic. In the literature, semi-persistent scheduling schemes have been proposed to deal with this special traffic characteristic [72], as they make allocation decisions for a longer time period than usual, thus making it unnecessary to inform the UEs on a Transmission Time Interval (TTI) basis. An overview of scheduling for M2M traffic over LTE state of the art is provided in [73], while a performance comparison between three delay-aware scheduling algorithms for M2M traffic over an LTE system is given in [74].

- *Need for improvement in efficiency in radio resource utilization*: H2H and MTC have to be handled in the framework of the same spectrum, for spectral efficiency requirements. In particular, time and frequency resources are to be shared between H2H users and MTC devices, thus resulting in co-channel interference among them. Such co-channel interference plays a detrimental role in degrading the performance of the LTE-A network with M2M communications. Furthermore, different types of users are characterized by different interference tolerance. Some work on this is initiated in [72].

- *Analysis of impact of M2M utilization on LTE performances*: Due to the differences in features between H2H and M2M traffic, there is the need to evaluate the impact that has to deal with these transmissions on the same LTE network.

Typically, M2M applications receive or transmit only a small amount of data or require very low data rates, leading to an unreasonable ratio between payload and required information and nonoptimized transmission protocols. Hence the impact of small packets transmitted periodically needs to be analyzed. In [73] this is studied by means of a Markovian model, which is parameterized by laboratory measurements and ray tracing simulations. In [74] Coverage and capacity analysis for Machine type communications in LTE are analyzed.

- *Management of Random Access Load*: Related to the scheduling problem is also another important design consideration, which is how to design an efficient method for handling the Random Access (RA) load generated by a possibly huge population of M2M nodes attached to the network. Network congestion in Random Access Channel (RACH) can lead to long delay and possible network access failure. To solve this problem, several solutions have been studied including time controlled access, staggered access, overload indicators to prevent MTC devices from access attempts, etc. In the RA process, the User Equipment (UE) shall go through a preliminary stage, called Access Barring Check (ABC), where the UE should check whether the access to the network is prevented or not, based on the received System Information and its random-generation number. Once passed the ABC procedure, the UE starts transmitting a preamble to the evolved Node B (eNB), which will be the actual load to the RACH. In 3GPP it is still on the table how to design the ABC mechanism, and some proposals can be found in literature. Some preliminary work can be found in [75]. A more mature proposal is proposed in [76], where two most probable candidate

methods for RA preamble allocation and management are discussed for LTE-A network protocol. The first method proposes to completely split the set of available RA preambles into two disjoint subsets, one for H2H customers and the other one for M2M devices. The second method again splits the set into two subsets, but while one of the two sets is devoted to H2H communications, the second one is split for both H2H and M2M customers. In [77] a novel congestion scheme, which takes advantage of existing congestion schemes, is proposed to curb the severe congestion problem and reduce the impact on QoS of existing H2H devices.

3.2 LTE/LTE-A architecture

As already discussed in Chapter 1, 3GPP devoted a lot of effort to standardization of MTC in order to support M2M applications. This section is intended to present the typical MTC scenario foreseen by 3GPP. Fig. 3.1 shows the scenario addressed by 3GPP. Each element of this scenario are defined as follow:

- Machine Type Communications Device (MTCD): this is the device responsible to gather information from the real environment, it could be a data logger for sensor, an actuator, a camera for record and stream video, etc. This device could be part of the 3GPP network or not. In fact it can use LTE to talk with the Machine Type Communications Gateway (MTCG) or not. In real application most of the time, MTCD are low-cost devices using different standard span from WiFi to Bluetooth or IEEE 802.15.4 based protocols.

- MTCG: from the 3GPP network point of view it can be seen as a UE. As

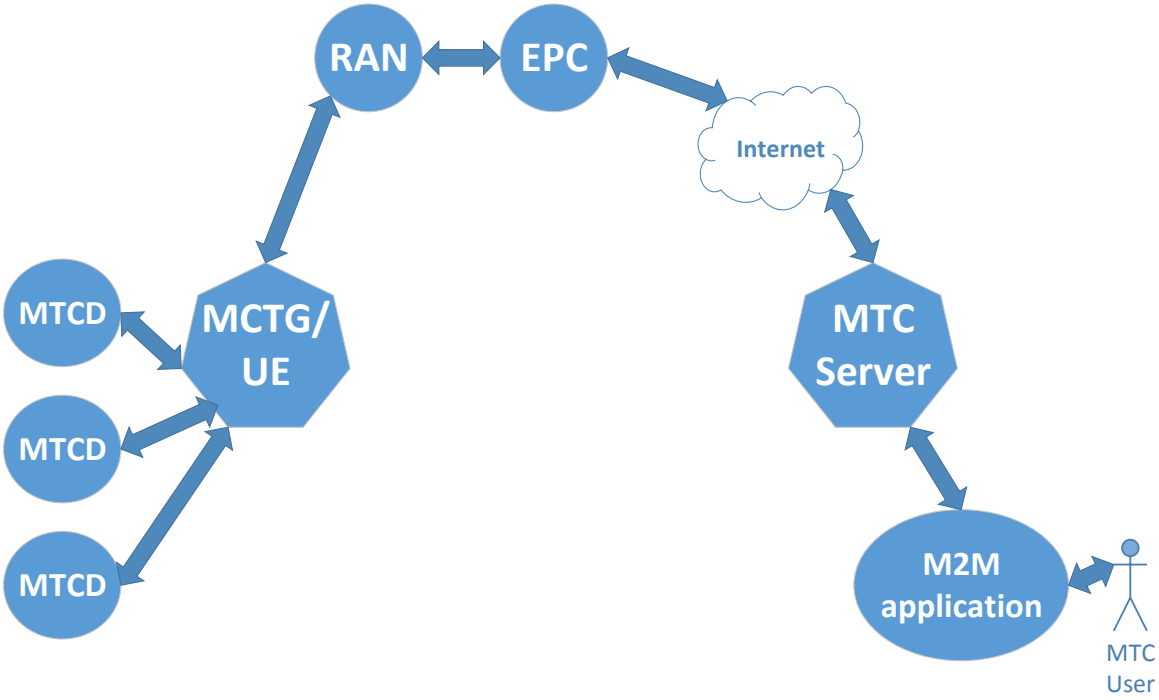

Figure 3.1: M2M application through a LTE network

the name suggests, it is responsible to forward information to and from the MTC server. Of course, even if from the hardware viewpoint this device is very similar to an UE, at least from 3GPP network prospective, this device produces a total different kind of traffic that affects the way the Radio Resource Assignment (RRA) procedure. MTCG could work both in transparent and not transparent mode. Where transparent meaning that information coming from a MTCD is directly forward through the network. While, the latter is realized when MTCG is aggregating data before transmitting. Indeed both solutions have advantages and disadvantages and use one or the other strongly depend on the application. MTCG is always part of the 3GPP network.

- Radio Access Network (RAN): as it is well known it is the part of LTE network

dealing that allows devices to be connected to the Internet. In LTE the concept of heterogeneous network is exploited. Hence, the RAN is composed of different kind of elements, i.e. macro and micro cell, Small Cell (SC)s, Radio Remote Head (RRH), femto-cell and so on. RAN is responsible of the RRM, hence it has a role in the definition of QoS given to the users

- Evolved Packet Core (EPC): it is the core of LTE network. Most of the time it uses high data-rate and highly reliable link; those are realised through optical fiber most of the time, however, due to the densification of RAN also wireless solutions are used. EPCset the boundaries of 3GPP network and it is responsible of minimizing delay on the wired network and maintain the QoS assigned to users.

- MTC server: it is connected to the LTE network through the internet. It is responsible of the communication with the MTCGs. Moreover, it contains the data collected from several devices in the network. It is responsible to send alert to user and to check the status of MTCD, maintain the QoS required by the applications and in case it is not possible, takes consequent actions.

- M2M application represents the front-end toward the final user. The M2M application are build on top of MTC servers, it can exchange information with more than a single MTC server, using data fusion and data analysis techniques.

- As last part of this chain, the MTC user is human. He is responsible of the observation of the network. He set the threshold to have the alert and can take actions and query the network. Most of the time the human intervention is not needed till an alarm is raised.

3.2.1 Uplink in LTE

Due to the increasing data-rate demand from users, 3GPP standard are mainly focusing on the downlink of the cellular network and this is true also for LTE. However, in the last 3-5 years the symmetric applications are growing and the demand in term of throughput in uplink is increasing, also due to the M2M applications that nowadays generate mainly uplink traffic. Hence the uplink bottleneck is not solved in the 4G cellular network, but it will be a key factor in the design of the 5th cellular network generation. In order to satisfy the user data-rate demand, when LTE was standardized Orthogonal Frequency Division Multiple Access (OFDMA) multiple access scheme was used. This has many benefits for high speed data services. However, one disadvantage is that the instantaneous transmitted Radio Frequency (RF) power can vary significantly within a single Orthogonal Frequency Division Modulation (OFDM) symbol, leading to large Peak to Average Power Ratio (PAPR), which entails a distortion problem in the linear devices. This drawback has a major impact in the uplink, since power consumption is an important consideration for mobile handsets. To address this drawback, a pre-coded version of OFDMA, i.e. Single Carrier Frequency Division Multiple Access (SC-FDMA), has been adopted. This different access scheme imposes different constraints with respect to OFDMA, which strongly affect the resource allocation, interference management policy and the scheduling of traffic. In particular, SC-FDMA requires contiguous Resource Block (RB) allocation to the same user.

3.3 Conclusions

In this chapter a brief introduction on the 3GPP vision of MTC has been given. The main research challenges have been addressed and the LTE architecture for M2M application have been presented. Finally, the uplink access scheme adopted in LTE and LTE-A systems has been recall, highlighting the main characteristics and drawbacks.

Chapter 4

RRM for M2M traffic in cellular networks

This chapter presents a framework for supporting multiple policies in scheduling M2M traffic on cellular networks. More in details, the reference network architecture is 4G to 5G networks,in particular the releases 9-10 of 3GPP standard, i.e. Long Term Evolution (LTE) and LTE-A. The models and results have been obtained within a joint research activity between UniBO and CTTC (ES) under the umbrella of the NoE Newcom♯.

The advent of MTC, together with the demanding Quality of Experience (QoE) requirements of data applications, generates a need for capacity increase, which can only be satisfied by a fundamental rethink of the radio access network, where heterogeneous nodes like, Remote Radio Heads (RRH), femto, pico, micro, SCs in general, and traditional macrocells coexist in the same area, with an extremely high density [78]. In these densified scenarios for future 5G networks, neighboring Base Station (BS)s most likely operate on the same channel due to the scarcity of spectrum resources, which makes RRM decisions tremendously complex.

In this chapter, the focus is on a densely deployed network, where neighbouring

base stations operate on the same channel, providing service to a urban scenario in a near future smart city. More in details, the focus is on a big boulevard, equipped with a dense street light small cell deployment, able to support both H2H and M2M traffics. This cost-efficient and self-organized solution has been recently proposed by multiple vendors [78] in order to increase dramatically the density of nodes and to address morphologies from dense urban to suburban. M2M traffic generated by most services/applications is bi-directional, and the network must be designed to support great amount of uplink traffic. Furthermore, different applications have different requirements in terms of throughput, maximum tolerable packet loss rate, maximum delay, etc., which requires the implementation of intelligent scheduling algorithms to meet the requirements of all applications.

In this challenging dense scenario, where multiple M2M applications require satisfaction of their heterogeneous QoS requirements, the LTE scheduling functionality, located at the BS within the LTE MAC layer, plays a crucial role. It manages the limited radio resources at the access level, in a way that optimizes system performance in terms of a variety of criteria, such as throughput, fairness, etc. The bandwidth is organized onto groups of sub-carriers, denoted as RBs, which are the minimum scheduling resolution in the time-frequency domain. The scheduling functionality performs the RB-to-UE assignment in each TTI, handling shared radio resources among neighbour BSs. Decisions are based on scheduling policies, taking into account network conditions, wireless channel quality and the QoS experienced by users at the service level. Considerable work has been devoted in literature to scheduling Downlink (DL) traffic in densely deployed heterogeneous networks, considering also Inter-Cell Interference

Coordination (ICIC) approaches [79]. The study of the Uplink (UL), which is expected to be much more important in 5G scenarios, with M2M communications, even if it has been approached in traditional macrocell scenarios [80], is much less explored in dense networks where the component of interference plays a disruptive role.

In the follows, it is provided a solution for the LTE uplink scheduling problem, taking into account interference coordination issues and the constraint of adjacency of RBs allocated to a single user. To solve the problem: i) first a three-steps model is created, taking into account criteria such as the overall throughput, radio resource usage and Intercell Interference (ICI); ii) then, a more compact model is proposed, referred in the following as "unified", which solves the scheduling optimization in just one round; iii) finally, a greedy algorithm that solves the model and performs UL scheduling is introduced. To solve the problems already mentioned IBM ILOG CPLEX optimization software [81] has been used. A comparative study between the proposed models and the greedy algorithm is presented, in order to evaluate the difference between the heuristic and the optimal solutions. Particular attention it is paid to the feasibility of implementation in the standard, and to the time required to achieve a solution, considering that the scheduler has to be executed every TTI ($1ms$). Also, the heuristic approach is characterized by low computational requirements, and so it can be easily implemented in devices with reduced computational capability, as it can be the case for BSs in future 5G scenarios [82].

The designed heuristic algorithm has been implemented in a 3GPP compliant network simulator, NS3 LENA [83]. Simulation results carried out in NS3, show the promising performance of our scheme for different M2M applications and with respect to state of the art approaches.

4.1 State of the Art Uplink RRM for M2M

The Table 4.1 provides a comparison of recent proposals for scheduling LTE UL, based on the following criteria:

- *Scenario*: it indicates whether the proposed algorithm has been applied in traditional LTE macrocell, single or multicell, scenarios, or if it has been designed for application in heterogeneous dense networks.
- *ICI*: it indicates whether ICI is realistically taken into account. This is important, because dense deployments can cause many RBs not to be available for allocation.
- *Model*: it denotes if the solution is based on a model and which one.
- *Allocation metrics*: it indicates the driving scheduling criteria.
- *QoS*: it defines the QoS supported by the algorithm.
- *Algorithm*: it indicates if the solution is optimal or heuristic.
- *Contiguous RBs*: it denotes whether the model considers the constraint imposed by the implementation of SC-FDMA over the adjacency of RBs assigned to the same user. This is important, because this condition ensures consistency with 3GPP. Notice that some authors consider OFDMA in the UL, and consequently they do not account for the condition on the adjacency of the RBs.
- *Solving Time estimation*: it indicates that the contribution evaluates the time to solve the problem, providing an analysis of the same model. This is important to establish the performances of the algorithm and its practical feasibility.

- *Numerical Evaluation*: it indicates whether the proposed model has been evaluated as a function of, e.g. the number of variables and constraints, the memory occupancy and the complexity.

- *Performance Evaluation*: it indicates if the system performance of the proposed algorithm have been evaluated on a standard compliant network simulator implementing the complete protocol stack.

- *M2M support*: it indicates if the proposed scheduling model and algorithm takes into account the peculiarity of M2M traffic.

As it can be observed, the great majority of the works investigate the traditional macrocell scenario, where only single or multiple cells are considered. Only one work refers to a macro-femto scenario, but heterogeneous dense network deployments have not been considered in literature, for the specific problem tackled in this paper. Currently, these dense scenarios, e.g. stadium [84] [85] or street light small cells, are of great interest for industry and standardization bodies, and consequently innovative solutions have to be studied in these contexts. The ICI issue has only been marginally considered in the literature related with the UL schedulers. It has been studied only in macrocell scenarios, where consequently the interference problem is less critical than in dense deployments. As for the model, the allocation metrics and QoS parameters involved in the optimization procedures, the literature offers many interesting readings. Many of them consider SC-FDMA and provide algorithms fulfilling the RB adjacency constraint imposed by this access scheme, but others do not, either because they neglect this issue, or because they actually focus on OFDMA as access scheme for the LTE UL. The condition of contiguous RBs makes the problem NP-hard, so that

only heuristic solutions can be provided. [86] provides a solution based on search tree model applied to groups of RBs. This solution is optimal, but the algorithm requires fulfilling constraints on the tree. Regarding the M2M support, [87] - [88] support MTC, and only a part of them are also supports H2H traffic, e.g. [89] and [90]. The remaining contributions are specific solutions for M2M scheduling, like [91], which presents a RRA method for video-survaillance systems. Among these works, only few of them have evaluated the performance of the proposed appriaches in a 3GPP-oriented simulator. Finally, the works presented in literature only focus on system performance analysis without providing numerical evaluation of the performance of the proposed models. As a result, it is impossible to evaluate whether the solutions proposed in literature are, e.g., characterized by a reasonable solution time, which makes them actually implementable in the standard.

Taking into account the above observations, here are highlighted the novelties introduced in this chapter with respect to the state of the art:

1. It proposes a scheduling solution for an extremely dense scenario;

2. It provides support to M2M traffic;

3. It proposes two MILP models for scheduling LTE UL of a dense heterogeneous network, characterized by high frequency reuse and high ICI;

4. The two proposed models aim at maximizing the overall throughput, optimizing the radio resource usage and minimizing the ICI;

5. The SC-FDMA and its implementation constraints are considered;

6. The proposed models are analyzed and solved, and the performance are compared to a greedy solutions, the solving time is evaluated, in order to deduce the real feasibility of the proposed approach;

7. The greedy solution, i.e. the proposed heuristic algorithm, has been implemented in NS3 and evaluated against the state of the art algorithms;

8. Two versions of the greedy algorithm are presented and implemented in NS3. Those algorithms are compared with Maximum Fairness (MF) and Round Robin (RR) algorithms.

4.2 System Model

It is considered a heterogeneous dense cellular network composed of a set of $\mathcal{M}$ nodes, ranging from traditional macro to SCs. The $M{=}|\mathcal{M}|$ cells provide coverage over a highly capacity demanding 5G network. All the cells operate in the same frequency band, which allows to increase the spectral efficiency per area through spatial frequency reuse. A SC-FDMA 3GPP Release 9 LTE UL is considered, where the system bandwidth B is divided into m RBs, with $B = m \cdot B_{\mathrm{RB}}$. A RB represents one basic time-frequency unit that occupies the bandwidth B_{RB} over a TTI, equal to $1ms$. The RB is the smallest resource that can be assigned to a UE. Associated with each BS are n UEs, which at every TTI have to be scheduled onto the set of available RBs.

The aim is to design the multi-user resource assignment that distributes the m RBs among the n users, focusing on a Frequency Domain Packet Scheduling (FDPS) scheduling model. A generic user j generates a profit p_j, the aim is to satisfy it by

Ref	*Scenario*	*ICI*	*Model*	*Allocation metric*	*QoS metric*	*Algorithm*	*Contiguous RBs*	*Solving Time estimation*	*3GPP Compliant Sys. level Simulator*	*M2M support*
[92]	M/Mu	Y	MIP	Channel Aware	fairness	H	Y	N	N	N
[93]	M/S	N	N	Channel Aware	QoS class	H	Y	N	N	N
[94]	M/F	Y	Markov chain	Max. Throughput	fairness	H	Y	N	N	N
[95]	M/Mu	Y	N	Multi-cell Channel Aware	fairness	H	N	N	N	N
[96]	M/S	N	N	Channel Aware	Many	H	Y	N	N	N
[86]	M/Mu	N	Search Tree	Fairness	Max. profit	O	Y	N	N	N
[97]	M/Mu	N	MIP	Channel Aware	Maximization profit	H	Y	N	Y	N
[98]	M/S/Mu	N	Y	Channel Aware	QoS class	H	N	N	N	N
[99]	M/S	N	Game theory	Max. Throughput	Max. Throughput	P	N	N	N	N
[100]	S	N	N	Max. Throughput	Max. Throughput	H	Y	N	N	N
[87]	Mu	N	N	Group-based	Delay	H	N.S.	N	N	Y
[101]	S	N	N	Channel Aware	Delay	H	N	N	N	Y
[89]	S	N	N	Semi-static	Max. Throughput	H	Y	N	Y	Y
[90]	S	N	N	Aware bit-rate	QoS class	H	N.S.	N	N	Y
[91]	S	N	N	App specific parameters	Quality of Video (QoV)	H	N.S.	N	N	Y
[88]	S	N	N	Channel-aware M2M/H2H	QoS	H	Y	N	Y	Y

Table 4.1: Related Work comparison. M=Macrocell, F=Femtocell, S=singlecell, Mu=Multicell, H=heuristic, P=polynomial, O=optimal, N.S.=Not Specified

maximizing the overall profit. It is assumed that the coherence time of the channel is than a TTI, so that channel conditions are constant over a TTI. The condition of contiguous RB allocation to the same user is imposed as required by the standard. The number of assigned RBs per user is flexible and spans between 0 and m.

The scheduling is carried out taking into account information transmitted by the user in the UL over the Signalling Radio Bearers (SRB): Scheduling Requests (SR), to distinguish active users with data in buffers, from idle users; Buffer Status Reports (BSR), to inform the BS about the amount of data needed to be transmitted; Power Headroom Reports (PHR), to inform the BS about the available power at the user for the scheduling; Sounding Reference Signal (SRS), used to provide information on the UL channel quality; Channel Quality Indicator (CQI), to measure the channel quality between UE and BS.

In addition to this, and in order to take into account the high level of interference present in a dense network with high frequency reuse, are proposed that:

- *ICI phase*: based on measurements carried out by the same BS and on those of the users, the BS evaluates the blocks of contiguous available RBs, according to the measured interference. Other information exchanged over the X2 interface, such as the High Interference Indicator (HII) or the Overload Indicator (OI) [102] [103], can also be used to extract this information.

- *Scheduling phase*: based on the availability of contiguous RBs, on the quality of the channel and on the QoS requirements of the traffic to be scheduled, RBs are properly allocated to the users.

4.3 MILP approaches, model and results

This section describes a proposed approach to schedule LTE UL in a dense heterogeneous network. It is a three-steps optimization process, driven by multiple objectives: the maximization of the overall throughput, the minimization of the radio resource usage, and the minimization of the ICI. In the follows, it is presented a one step model, which considers all the previous objectives. These optimizations can be stated as MILP problems, as they contain integer and continuous variables, linear constraints and a linear objective function. Complexity-wise the problem was already demonstrated to be NP-hard [94] and, although each MILP is not extremely hard in practice, solving many of them might not be compatible with real-time packet scheduling. Consequently, here it is proposed in the next section a greedy algorithm, which solves the optimization problem in computing times that are compatible with the application at hand. This algorithm has been designed paying special attention to the feasibility of implementation in the LTE-LTE-A standard and to its solving time, considering that it has to be executed every TTI. In addition, the computational cost is low, which assures that it can be implemented also in devices with reduced computational capability, as it may be the case for BSs in future dense 5G deployments [82]. Instead, the MILP approach is used as a reference to evaluate the effectiveness of the greedy algorithm, see Section 4.4.2.

Before describing in details the MILP models and approaches, in section 4.3.1 are introduced a set of definitions common to both the MILP models.

For sake of clarity, in the algorithms' pseudo code (Algorithms 1, 2 and 3), are used capital letters to reference matrix and arrays, e.g. F is a matrix and F_i is an

array i extracted from the same matrix identify by cu; while scalar variables are identified by lower-case letters, e.g. $f_{i,j}$ represents the element identified by i and j in F matrix.

4.3.1 Definitions

Hereafter a binary variable $x_{i,j}$ is introduced to define the allocation of RB i to user j. Namely,

$$x_{i,j} = \begin{cases} 1 \text{ if } RB\ i \text{ is the first assigned to } UE\ j \\ 0 \text{ otherwise} \end{cases} \tag{4.3.1}$$

In addition, it is constructed the bi-dimensional matrix F whose (constant) entry $f_{i,j}$ gives the minimum number of contiguous RBs (h) needed by user j to satisfy its traffic, under the hypothesis that RB i is assigned to user j as a first RB, i.e. if $x_{i,j} = 1$. Otherwise, i.e. if it is not possible to use RB i as first RB for user j, then $f_{i,j} = -1$.

$$f_{i,j} = \begin{cases} h : \sharp\text{of contiguous RBs assigned to UE j if } x_{i,j} = 1 \\ -1 \text{ otherwise} \end{cases} \tag{4.3.2}$$

The value of $f_{i,j}$ depends both on channel conditions and user demand. The procedure used to compute $f_{i,j}$ is described in Algorithm 1. This algorithm requires knowledge about (i) the number of contiguous RBs available starting from RB i, which is summarized by vector Av_{RB}, and which depends on the ICI conditions, and (ii) the maximum Modulation and Coding Scheme (MCS) allowed in each RB, which is contained in vector MCS_{RB}. The ICI phase allows to derive the Signal to Interference plus Noise Ratio (SINR) associated with each RB, and assuming a Block Error Rate (BLER) lower than 10%, the MCS_{RB} can be easily calculated [83] [104].

The function $g(mcs, h)$ is used to determine the capacity c_i, of the contiguous RBs starting in i, i.e. Transport Block (TB) size. This is defined by 3GPP through a lookup table [105] [106]. Finally, it is defined

$$b_{i,k}^{j} = \begin{cases} 1 \text{ if } UE\ j \text{ uses } RB\ i \text{ and } x_{k,j} = 1 \\ 0 \text{ otherwise} \end{cases} \tag{4.3.3}$$

where, the procedure to compute each element of $b_{i,k}^{j}$ is defined in Algorithm 2. In particular, Algorithm 2 generates the elements of the three dimensional matrix B, which can only take 0 or 1 values. For each user j, a two-dimensional matrix is obtained where the $k-th$ column has $f_{k,j} = h$ values set to 1 and all the other values set to 0. In other words, if $x_{k,j}$ is equal to 1, all the values in the range $[b_{k,k}^{j}, b_{k+h-1,k}^{j}]$ must be set to 1. Notice that entries $f_{i,j}$ (4.3.2) and $b_{i,k}^{j}$ (4.3.3) are constant, and they are calculated every TTI before solving the model.

4.3.2 MILP Models

The three-step optimization process based on the first MILP model is described as follows:

1. *Throughput maximization:* The first objective is set by eq. (4.3.4), where the aim is to maximize the overall served traffic, i.e. the amount of bytes transmitted during each TTI. The optimization is then characterized by three scheduling constraints: (i) *exclusivity*, i.e. each user j can start being allocated in at most one RB. This is captured in constraints (4.3.5); (ii) *interference avoidance*, a user cannot be allocated to an unfeasible RB, where an unacceptable level of interference has been detected. This is reflected in constraint (4.3.6); (iii)

Algorithm 1 algorithm to create $f_{i,j}$

{Initialization}
$AV_{RB} \leftarrow$ array of available RB
$MCS_{RB} \leftarrow$ array of maximum available mcs per RB
Define $D \leftarrow$ array of the demand
Initialize $f_{i,j} = -1 \leftarrow$ for all $f_{i,j}$
for $j = 1$ **to** n **do**
  for $i = 1$ **to** m **do**
    $mcs = MCS_{RB}[i]$
    $h = 1$
    while $h \leq AV_{RB}[i]$ **do**
      $mcs = min\{mcs, MCS_{RB}[i + h - 1]\}$
      $c_i = g(mcs, h)$
      if $d_j \leq c_i$ **then**
        $f_{i,j} = h$
        BREAK
      else
        $h \leftarrow h + 1$
        CONTINUE
      end if
    end while
  end for
end for

Algorithm 2 algorithm to create $b_{i,k}^{j}$

```
{Initialization}
for j = 1 to n do
  for k = 1 to m do
    for i = k to m do
      if f_{k,j} ≥ 0 then
        if k + f_{k,j} ≥ i then
          b^j_{i,k} = 1
        else
          CONTINUE
        end if
      else
        CONTINUE
      end if
    end for
  end for
end for
```

adjacency, RBs cannot be used by more than one user. This is described by constraint (4.3.7). The formulation of the first optimization step is then given by:

$$max \sum_{j=1}^{n} p_j \sum_{i=1}^{m} x_{i,j} \tag{4.3.4}$$

subject to:

$$\sum_{i}^{m} x_{i,j} \leq 1,\ j = 1, \ldots, n \tag{4.3.5}$$

$$f_{i,j} x_{i,j} \geq 0; \quad j = 1, \ldots, n; \quad i = 1, \ldots, m \tag{4.3.6}$$

$$\sum_{j=1}^{n} \sum_{k=1}^{i} b_{i,k}^{j} x_{k,j} \leq 1,\ i = 1, \ldots, m \tag{4.3.7}$$

2. *Minimization of allocated RBs*: Once the first optimization has been carried out, and the served throughput maximized, the second aim is to minimize the number of allocated RBs, and consequently the radio resource usage. This

optimization is described in eq. (4.3.8). The optimization is characterized by four constraints, three of them are the same as for the previous optimization. (1) *exclusivity*, (2) *interference avoidance*, (3) *adjacency*, (4) *satisfied profit*, i.e. the optimization has to satisfy at least the same profit P, as achieved by the first optimization. This is captured in constraint (4.3.9). The formulation of the second optimization step is then given by:

$$min \sum_{j=1}^{n} \sum_{i=1}^{m} f_{i,j} x_{i,j} \tag{4.3.8}$$

subject to: (4.3.5)-(4.3.7) and

$$\sum_{j=1}^{n} p_j \sum_{i=1}^{m} x_{i,j} \geq P \tag{4.3.9}$$

3. *ICI Minimization*: Once an optimal traffic has been served, through the assignment of the minimum number of RBs, the third step aims at finding the best possible configuration in terms of ICI through the minimization of the *utilization factor* $r_{i,j}$ defined as

$$r_{i,j} = \frac{d_j}{\sum_{k=i}^{i+f_{i,j}-1} c_i} \tag{4.3.10}$$

This is defined as the ratio between the demand of user j, d_j, and the corresponding TB size (i.e. c_i). This assures that the demand of the scheduled users is transmitted through the best TB, in terms of MCS and/or number of RBs, so as to achieve a reduced Power Spectral Density (PSD) per RB. The optimization is characterized by five constraints, four of them have been defined in the two previous steps: (1) *exclusivity*, (2) *interference avoidance*, (3) *adjacency*, (4) *satisfied profit*, (5) *minimum number of RBs*, i.e. the profit P has to be

served through the same amount of RBs R, as computed through the second optimization process.

$$min \sum_{j=1}^{n} \sum_{i=1}^{m} r_{i,j} x_{i,j} \tag{4.3.11}$$

subject to: (4.3.5)-(4.3.7), (4.3.9) and

$$\sum_{j=1}^{n} \sum_{i=1}^{m} f_{i,j} x_{i,j} \leq R \tag{4.3.12}$$

Finally, here it is presented a unified model that aims at summarizing all the features of the three-step optimization procedure defined above. It uses a set of positive integer coefficients to weight the three components of the objective function. The optimization can still be stated as a MILP problem.

$$max \sum_{j=1}^{n} \sum_{i=1}^{m} (\alpha p_j - \beta f_{i,j} - \gamma r_{i,j}) x_{i,j} \tag{4.3.13}$$

subject to: (4.3.5)-(4.3.7) This unified MILP model has some computational advantages in terms of compactness with respect to the three-step MILP approach. Computational experiments show that it is not significantly more difficult than each of the three MILPs in isolation, thus it is clearly preferable because only one solution step is needed. Nevertheless, it is worth noting that the two methods are equivalent if and only if parameters α, β and γ are carefully selected so as to determine a lexicographic order for the three objective functions. The introduction of the above parameters offers a novel flexibility to the model, which allows also to give combined levels of priority to the different objectives. All these aspects are evaluated through the use of the IBM-CPLEX MILP solver [81].

4.4 Algorithm and algorithm execution performances analysis

4.4.1 Proposed Algorithm

As anticipated, solving MILPs might not be computationally feasible in the real-time scheduling application at hand. As a result, a greedy solution is proposed to solve the optimization problem described in the previous section. The pseudo-code is reported in Algorithm 3. The algorithm's inputs are the same as those defined by the model, i.e. the profit of user j, p_j, and the matrix F, computed by using Algorithm 1; other inputs are the queues PS and FS, handling the users to be served, sorted by their profit, and extracted vectors from matrix F respectively. The function *sort()* takes care of sorting the elements of a queue. The function *pop()* extracts the first element of the queue. Finally, the function *isFeasible()* verifies the exclusivity constraint, i.e. whether a set of contiguous RBs can be assigned to a user. The outer cycle is performed until all users are scheduled or until all RBs have been assigned. On the other hand, the inner cycle is performed until it is proven that it is not possible to assign a set of feasible and contiguous RBs to a certain user j. In this case, the user is not scheduled. In this section are discussed the most important numerical results obtained evaluating the proposed MILP models and the greedy algorithm. The approach that has been followed is first to evaluate the proposed models, by solving the corresponding MILP problems through an optimization software, the IBM ILOG CPLEX Optimization Studio [81]). Then, the results obtained through the solution of the MILP problems are compared to those obtained by the Greedy algorithm, in

Algorithm 3 Greedy algorithm

{Input:}
$P \leftarrow$ array of the profit
$F \leftarrow$ Matrix defined in Algorithm 1
{Variables:}
Define int $rb_{availables} \leftarrow$ total available RBs
Define int $rb_{assigned} = 0 \leftarrow$ assigned RBs
Define $PS, FS \leftarrow$ Queues
$DS = sort(p_j, descending)$
while $DS \neq$ empty **or** $RB_{used} \neq RB_{available}$ **do**
  $cu = pop(PS)$
  $FS = sort(F_{cu}, ascending)$
  while $FS \neq$ empty **do**
    $cc = pop(FS)$
    if $isFeasible(cu, cc)$ **then**
      $rb_{assigned} += cc$
      BREAK
    else
      CONTINUE
    end if
  end while
end while

order to evaluate the actual performance of the heuristic approach in relation to the optimal solution. Optimization Programming Language (OPL) was used to create a script that writes the mathematical models presented in section 4.3.2 and test them on CPLEX. The first aim of this step is to show computationally the equivalence of the unified model (5.4.1),(4.3.5)-(4.3.7) with the three-steps approach. As mentioned, such an equivalence depends on the selection of the values for the parameters α, β and γ, which have been set to 100, 10, and 1, respectively. Operatively, some preliminary tests have been run in order to prove that the value chosen for α, β and γ are appropriate. In other words, α should be large enough to ensure that the first term of the objective function has higher priority than the others, i.e. no solution with a smaller value of the first term in (5.4.1) can be optimal. In the same way, β is chosen to be large enough to have priority over the third term of the objective function.

The results summarized in Table 4.2 are averaged over 6000 channel realizations, where n=100 RBs and m=60 users. This high number of users has been selected to consider a 5G aligned scenario, where e.g. also M2M traffic is allowed.

Table 4.2 compares the two MILP approaches (namely the unified model and the three MILPs of the three-step approach) in terms of (1) number of instances solved by branching; (2) number of instances solved at the root node; (3) average number of needed branches; (4) average gap over the instances. The gap is defined as the difference between the upper bound of the problem (obtained through constraints relaxation) and the optimal feasible solution. A small gap indicates a good model, since the feasible solution is closer to the upper bound. It can be observed that the models are of very good quality in practice, i.e. for most of the instances there is no need to branch, and the optimal solution is found at the root node.

Table 4.2: CPLEX Analysis results

Models	$\geq 1 Branches$	Root Solved	Avg. No. of Branches	Avg. gap
Unified	49	6452	75.79	0.371
1st Step	109	6692	7.07	0.391
2nd Step	75	6726	65.07	2.537
3rd Step	33	6768	9.34	0.939

Table 4.3: CPLEX Analysis results: details over an instance

Models	Unified	1st Step	2nd Step	3rd Step
Obj value	863589.9274	8640	39	20.0726
No. of Branches	19	10	13	18
Red. Variables	1158	1158	1158	1158
Presolve Time [s]	0.2	0.2	0.2	0.1
Total Time [s]	0.06	0.19	0.09	0.08

For a deeper analysis and as an example, the results obtained for one specific instance are reported in Table 4.3. Here, the results indicate the value of the objective functions at the end of the execution; the number of branches; the reduced number of columns characterizing the model after the presolve phase; the pre-solve time; finally, the total time. Observing the unified model behaves with respect to the three step approach (it obtains the same objective function value), so that it is possible to solve our scheduling problem in just one step. In particular, the dimensions of the reduced problems are exactly the same, but the unified approach allows to slightly reduce the execution time and to reduce the memory usage (although not shown in the table).

4.4.2 Algorithms Comparison

In this section the results obtained applying Algorithm 3 are compared to those obtained by CPLEX. The metric metric used is gap, calculated over 150 instances. In this section, the gap is redefined as the difference between the solution provided by the

greedy algorithm and the optimal feasible one provided by CPLEX. More in details, the focus is on the gap's statistic distribution, in particular, on its Probability Mass Function (PMF). Fig. 4.1 shows the PMF of the gap when considering the unified model. It can be observed that in about 50% of the cases the heuristic algorithm provides a solution equivalent to the optimal (0% GAP), and in 90% of the cases, the greedy solution lowers the performances with respect to the optimum, by less than 10%.

Fig. 4.2 shows the empirical Cumulative Distribution Function (eCDF) of the solving time of the greedy algorithm. It can be observed that the proposed algorithm achieves the solution in less than $0.75ms$ in more than 80% of the instance, and in less than $1ms$ in 100% of the cases. These numbers have been obtained by running the algorithm 100 times for every instance. The code has been run on Ubuntu 13.10 operating system, CPU Intel Core i7 3.90 GHz and 8 GB of RAM. This makes the algorithm compliant with the standard's scheduling requirements. It is reasonable to foresee better results in terms of execution time on a dedicated hardware.

4.5 NS3 - simulation tool

NS3 is a discrete event simulator. It is an open source software supported by a large community of developers and the NS consortium[1]. NS3 provides a large set of modules that allows developers to simulate different scenarios and the main IP and no-IP based networks. Since both on the web and in the scientific literature can be found tons of information about this network simulator, the aim of this section is not to present NS3, but it is given an inside on the NS3 LTE module, i.e. LENA [83]. LENA is

[1] http://www.nsnam.org

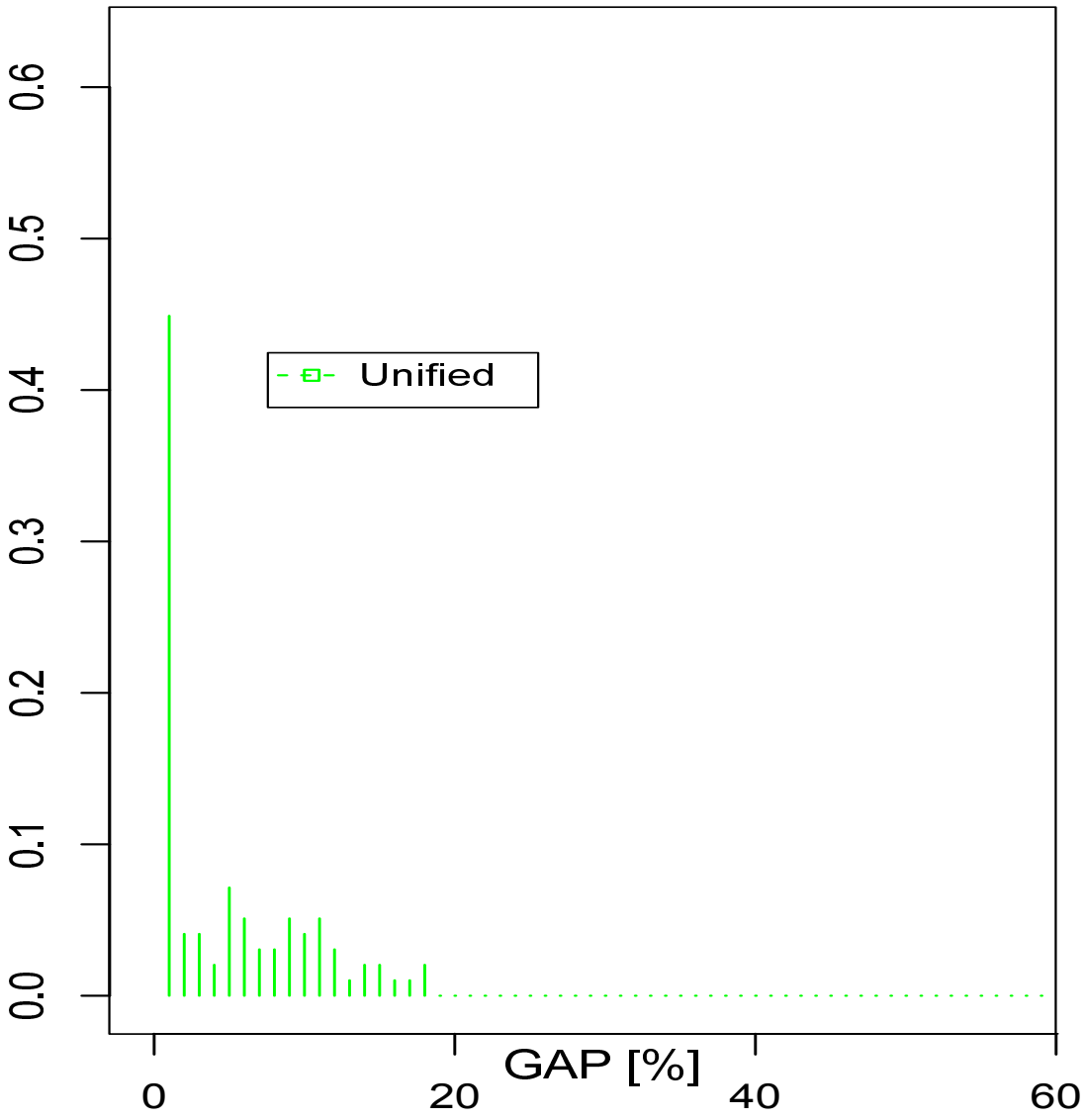

Figure 4.1: PMF GAP wrt optimal solution

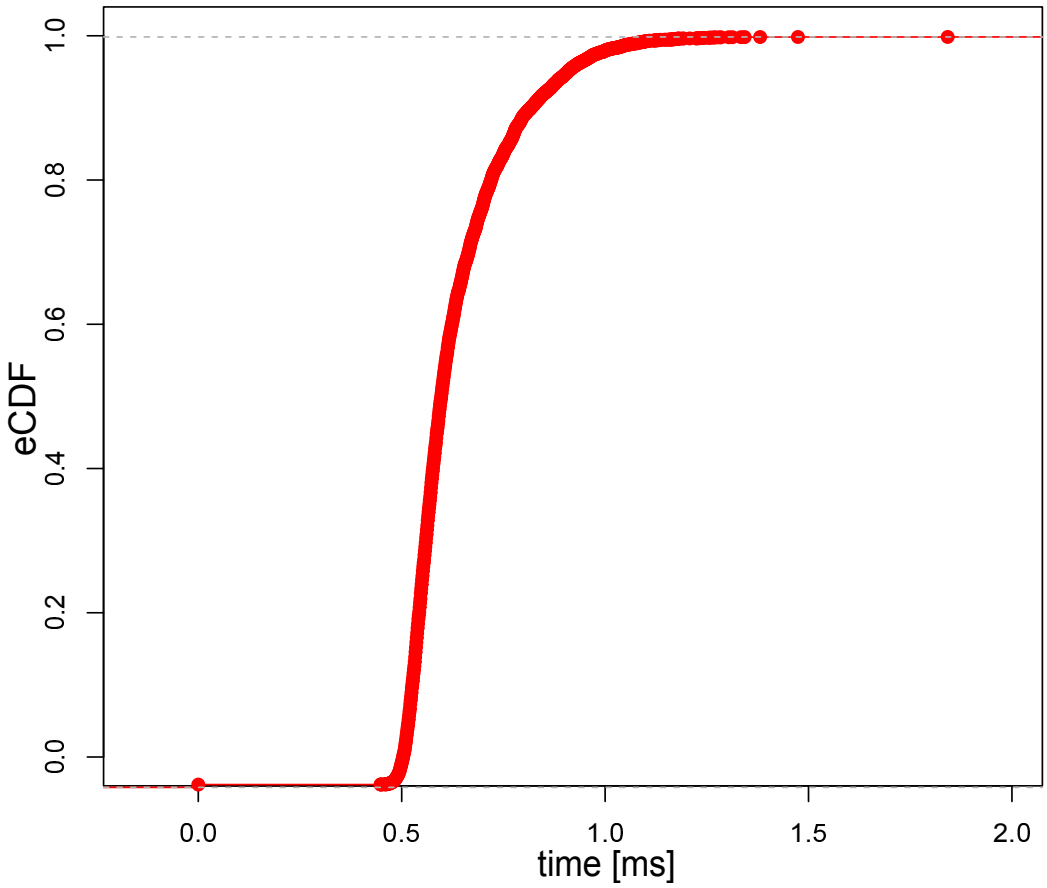

Figure 4.2: ECDF of Solving time

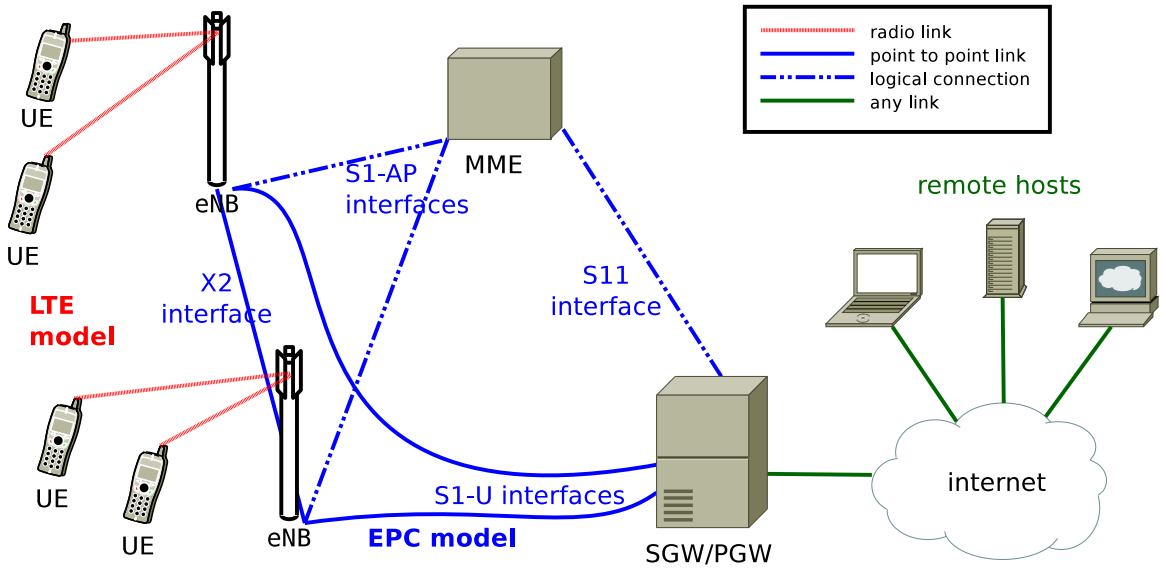

Figure 4.3: Overview of LENA simulation components

a 3GPP standard compliant simulator, in fact it is characterized by a high fidelity implementation of the complete LTE protocol stack. Figure 4.3 shows an overview on the LENA simulation components. The two main components are: LTE Radio Protocol Stack, including Radio Resource Control (RRC), Packet Data Converge Protocol (PDCP), Radio Link Control (RLC), MAC and PHY; and EPC with all the related entities, i.e. Serving Gateway (S-GW), Packet data network Gateway (P-GW) and Mobility Management Entity (MME). The interaction between the entities and the layers of LTE protocol stack are shown in figure 4.4 limited on the data plane.

In the follows, the main feature and characteristics are highlighted. This module support both the evaluation of radio-level performance and end-to-end QoE. Another important feature is the scalability, in fact this network simulator is designed to support up to few hundreds of eNB in the same simulation. This last feature is very useful when dense and ultra-dense networks are the focus of a simulation campaign. LENA has been designed to allow prototyping of algorithms for: ICIC, Self-Organized

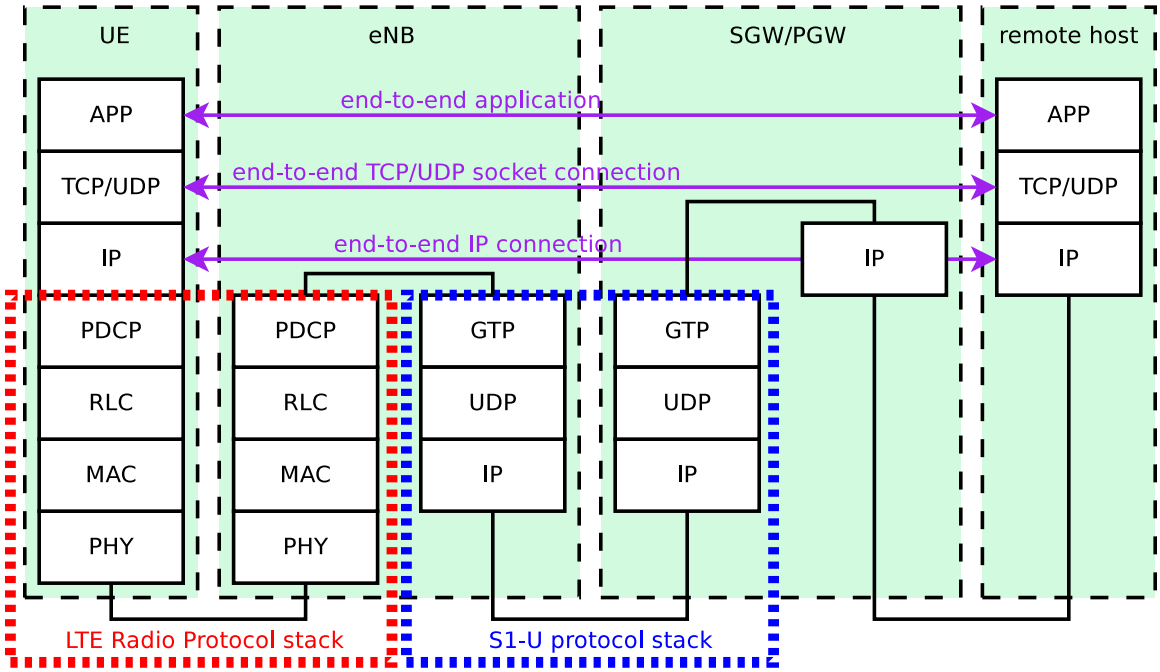

Figure 4.4: LENA: LTE-EPC protocol stack. Data Plane

Network (SON), dynamic spectrum access, QoS-aware packet scheduling and RRM. Regarding the RRM it is very important to emphasize that the resource scheduling granularity is per-RB base. To summarize, in this section a briefly description of the NS3 LTE module has been given. The aim was to justify the use of this very powerful tool in the research activity that this chapter is focusing on. In particular, the fact that LENA represents the only open-source LTE 3GPP standard compliant network simulator was the key factor in choosing this tool. In other word, implementing and analyse an algorithm in LENA has a direct relation with the performance on a real LTE network; this by itself is a very important added value.

4.6 Simulation Results

In this section the results obtained applying the proposed scheduler to the two selected M2M traffic classes are presented. These results are benchmarked to those provided by state of the art RR and MF schemes.

4.6.1 Reference System Architecture and Simulated Scenario

As anticipated the focus is on a smart city scenario where M2M traffic is served by a 3GPP LTE street light small cell network, characterized by high density. The high level scenario is depicted in Figure 4.5. The architecture that considered includes

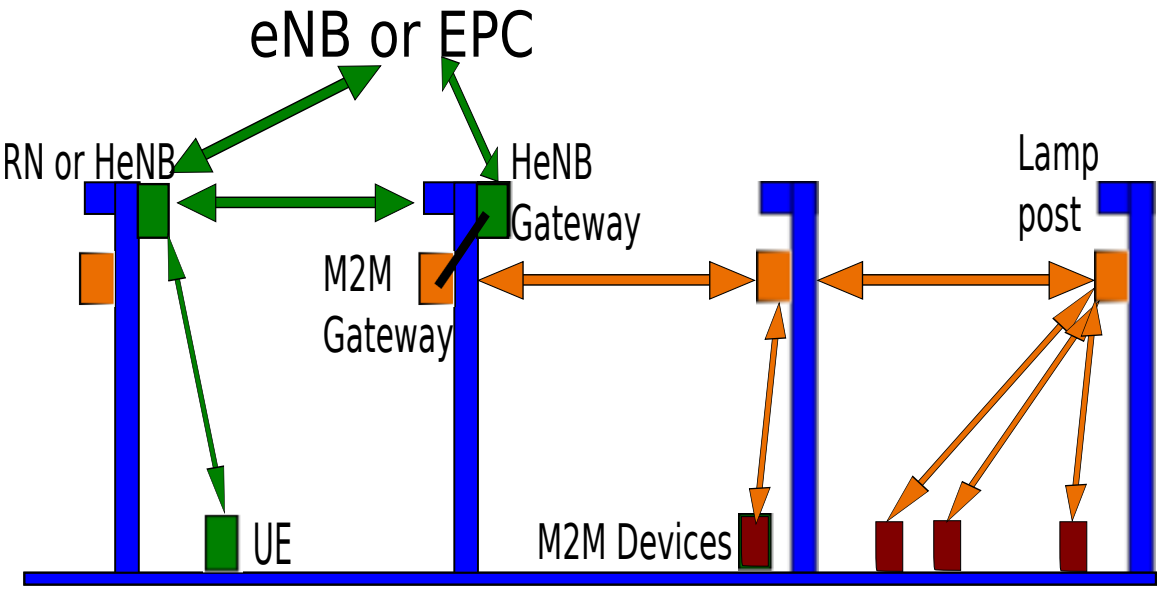

Figure 4.5: High level scenario.

M2M devices connected directly or via M2M gateways to the E-UTRAN architecture. The eNBs in E-UTRAN are connected to the EPC via S-GWs. The P-GW acts as the gateway to the core network and provides connectivity to the IP backbone. The

IP backbone provides connectivity among M2M devices, UEs, servers and users. The Evolved Packet System (EPS) including E-UTRAN and EPC form the M2M and the cellular access network. Besides getting access to E-UTRAN through an eNB, the machines can also get access through small cells, such as a Relay Node (RN) or a Home evolved Node B (HeNB). RNs are connected to the EPC via the Donor EPC, while HeNBs are directly connected to the S-GW, or through gateway. The aggregated M2M and H2H traffic collected by the small cells can be routed to a LTE gateway, then to an eNB and, finally, to the EPC. In the follows RNs or HeNBs are generically refered as SCs.

The simulation details are shown in Table 4.4. The street light SCs are located in correspondence of lamp posts or similar street furnitures. The street lights are located every 25 m and a small cell is located every 3 street lights, i.e. every 75 m, as represented in Figure 4.6. The yellow and red circles represent the street lights without and with installed SC, respectively. Each SC has to provide traffic and schedule 60 UEs over an access segment based on 50 RBs, which corresponds to a 10 MHz LTE UL implementation. Without loss of generality, it is considered a 10 MHz LTE implementation, which ensures 25 Mbps of theoretical maximum throughput to a single UE at the physical layer, so, enough for the kind of traffic on which this chapter is on, and which allows multi-user scheduling per TTI.

Each UE runs only one application, and the UEs are uniformly distributed among available applications. For the purpose of the evaluation of the proposed algorithm, a traffic based on the mix of three M2M applications is considered:

1. *Traffic monitoring*: it is considered a traffic monitoring application, in alarm

Parameter	Value
Cellular layout	Circular Cell
Inter SC distance	75m
SC radius	75m
SC height	8m
SC Ptx	10 dBm
Frequency	2.5 GHz
UL Bandwidth	10 MHz
Simulation Time	5 sec
RBs assigned per SC	50
Users distribution	Uniform in SC radius
No. of Users	60
Max Tx power of users	10 dBm
User Antenna Gain	0 dBi
Channel Model	Friss Channel Model
Control Plane	Ideal Channel

Table 4.4: Simulation System Parameters

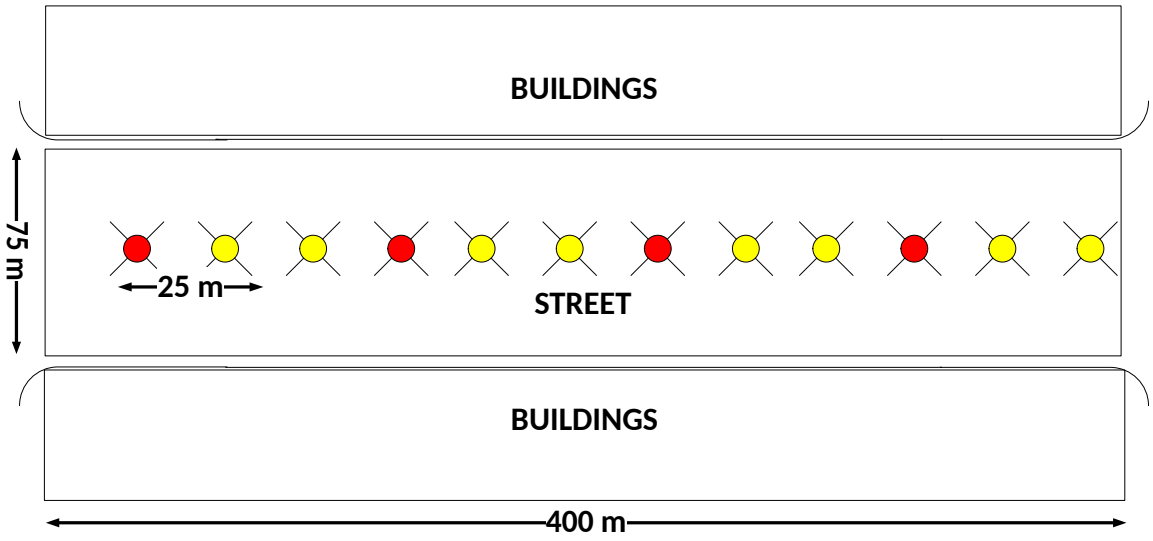

Figure 4.6: Simulated Scenario

mode, where there may be the need for exchange of several information to re-route human/vehicular traffic. The application is modelled by UDP packets with periodicity of 10 msec.

2. *Video surveillance - LQ (Low Quality)*: it is considered in this case a continuous traffic, generated for example by a LQ streaming application, or by devices that act as collectors of information from different sensors. The application is modelled by UDP packets with periodicity of 1 msec.

3. *Video surveillance - HQ (High Quality)*: it is considered in this case a continuous traffic, generated for example by a HQ streaming application, or by devices that act as collectors of information from different sensors. In both cases, there is the need to send a high amount of data. This could be modeled by a full buffer traffic generator.

4.6.2 Benchmarks

4.6.2.1 Round Robin algorithm

The details on the RR implementation can be found in the LENA open documentation [83]. This algorithm first verifies how many users sent a Buffer Status Report (BSR), i.e. the users that have something to transmit in the current TTI; then divides the total amount of RBs available by the active users. In the following with the terminology 'active user' is defined the UE that has data to transmit. The minimum amount of RBs assigned for each user is 3, this ensures a minimum of 3 bytes transmitted in a TTI, in case of worst channel quality condition, i.e., those associated to the lowest MCS index to ensure a transmission. The assignment starts

from the first user that was not scheduled in the previous TTI and proceeds in a round-robin fashion. During the assignment phase, the algorithm chooses the lowest MCS between the available in the RB set assigned to the user.

4.6.2.2 Maximum Fairness Algorithm

The MF algorithm goal is to obtain the maximum possible fairness for each user. In order to achieve this goal, the active users are sorted with respect to their average bit rate, evaluated over a temporal window of $100ms$. Each TTI the user with the lowest average bit-rate is granted the entire bandwidth, e.g. if the system has 10 MHz of uplink bandwidth, the selected user is granted 50 RBs in the current TTI.

4.6.3 Proposed Algorithms

In the follow, two different instantiations of the greedy algorithm 3, by considering two different profit functions are presented. Both have been implemented in the NS3 LENA simulator.

A first implementation is called a CDA, Channel and Demand aware version of the algorithm 3, where the profit function p_j is the user demand, i.e. d_j, the amount of bits that the user j has to transmit. The main goal of this algorithm is to maximize the overall throughput.

A second implementation in turn considers that the profit function p_j is the delay δ_j, where δ_j is defined as the delay in number of TTIs since the last time a user was scheduled. As a result, when the user j is scheduled the algorithm resets δ_j to zero, and each time an active user cannot be scheduled, δ_j is incremented by one.

During the scheduling procedure, the users are sorted by δ_j and the users with

larger value are scheduled first. This algorithm has been called CADELTA, Channel aware delta algorithm. The main goal of CADELTA is to reduce the delay in the user resource assignment.

Both solutions are channel-aware algorithms, that means that the most appropriate MCS per user and RB is selected, so that the bit error rate of the physical channel is ensured to be lower than 10%.

4.6.4 Key Performance Indicators

The following Key Performance Indicator (KPI)s to compare CDA and CADELTA algorithms, with respect to RR and MF, are considered:

- Throughput: i.e. the cumulative throughput (at RLC layer) of the RR simulation results and compare our algorithm in terms of variation of throughput. In other word, if an algorithm as an increment of throughput in the order of 30%, it means that the cumulative traffic served is 130% with respect to the RR one.

- Fairness: as fairness index it is used the well know Jain index (J-index) as it is defined in [107] and in (4.6.1)

$$J = \frac{(\sum_{j=1}^{n} z_j)^2}{\sum_{j=1}^{n} z_j^2} \tag{4.6.1}$$

  where z_j is defined as $z_j = T_j/T_j^{opt}$, T_j and T_j^{opt} are the throughput and the optimal fair throughput of user j, respectively.

- Delay: i.e. the delay at PDCP layer. This delay includes also the components associated to RLC layer, where different transmissions have to be received in order to aggregate a packet, before sending it to the PDCP layer.

4.6.5 Simulation Results

In this contribution, are shown results over 15 different realizations of scenario. In the figures the different realizations are addressed as simulation rounds. Figure 4.7 represents the throughput variation with respect to RR performances, as a function of the fairness. In this first set of results, only simulations with individual classes of traffic are considered, without mixing multiple classes. In particular, Figure 4.7 shows results in terms of fairness versus throughput, for traffic monitoring and video-surveillance (LQ), respectively. The former is characterized by a less demanding traffic, compared to the latter. With traffic monitoring, all the algorithms behave similarly, in particular, the throughput variation is in the order of 7% while the fairness is almost 1. When considering video-surveillance (LQ), simulation results show that both CDA and CADELTA outperform the RR in terms of throughput, by more than 100 % and 80 %, approximately, respectively. On the other hand, the proposed algorithms provide a reduction in fairness between 10 and 15 % with respect to the MF algorithm, which as it was to expect, provides the best fairness results. Figures 4.9 and 4.8 show the performances of the algorithms in terms of delay, defined as in 4.6.4, at PDCP layer. It is possible to observe that, when considering video-surveillance (LQ), the proposed solutions outperform RR, while MF achieves approximately the same performances. On the other hand, in case of traffic monitoring, these algorithms perform better, but in absolute terms the delay reduction is negligible.

In this part a second simulation campaign is presented. In this latter case different traffic are mixed types, with the aim of stressing the network with more demand both Low Quality (LQ) and High Quality (HQ) video surveillance applications are considered. Simulation results are shown in figures 4.10 and 4.11. The intense demand

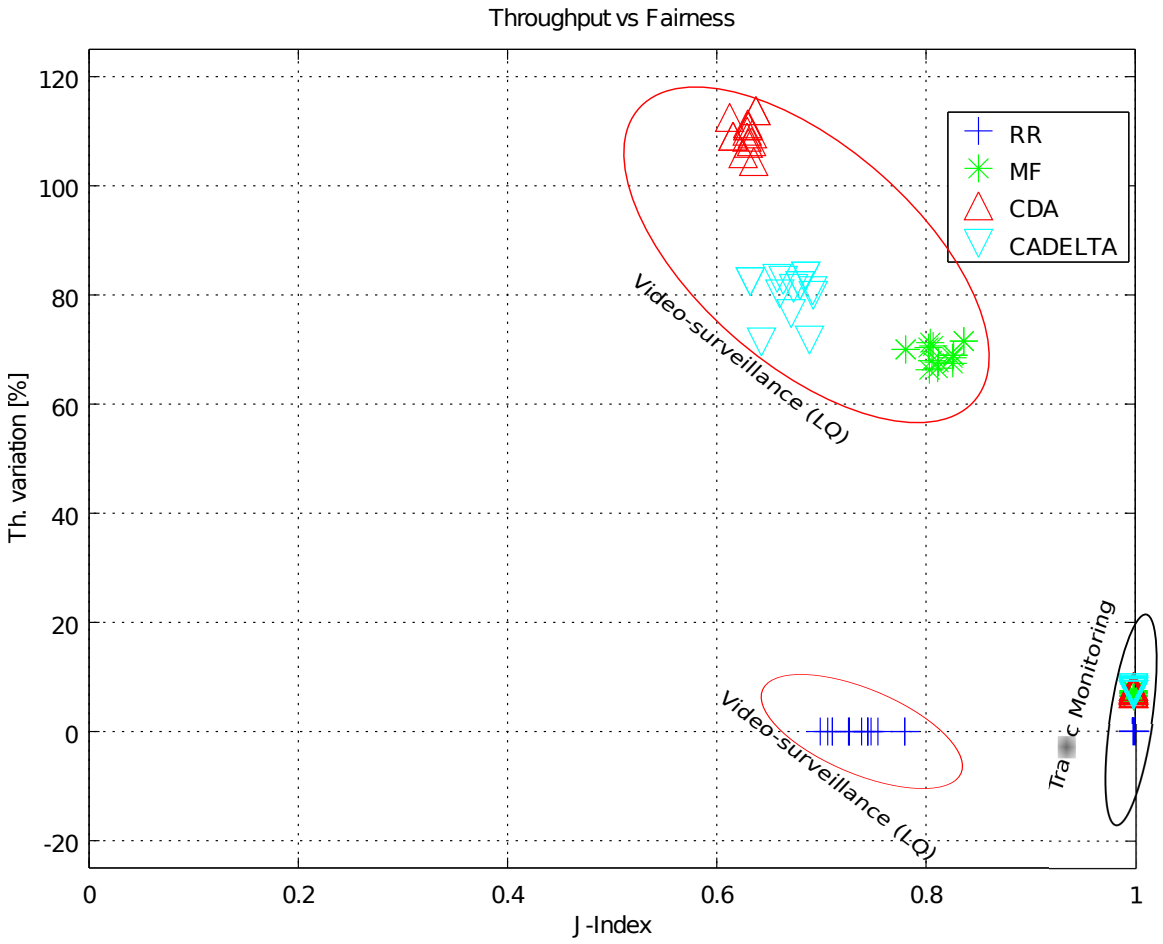

Figure 4.7: Throughput vs Fairness - Video surveillance (LQ), Traffic Monitoring

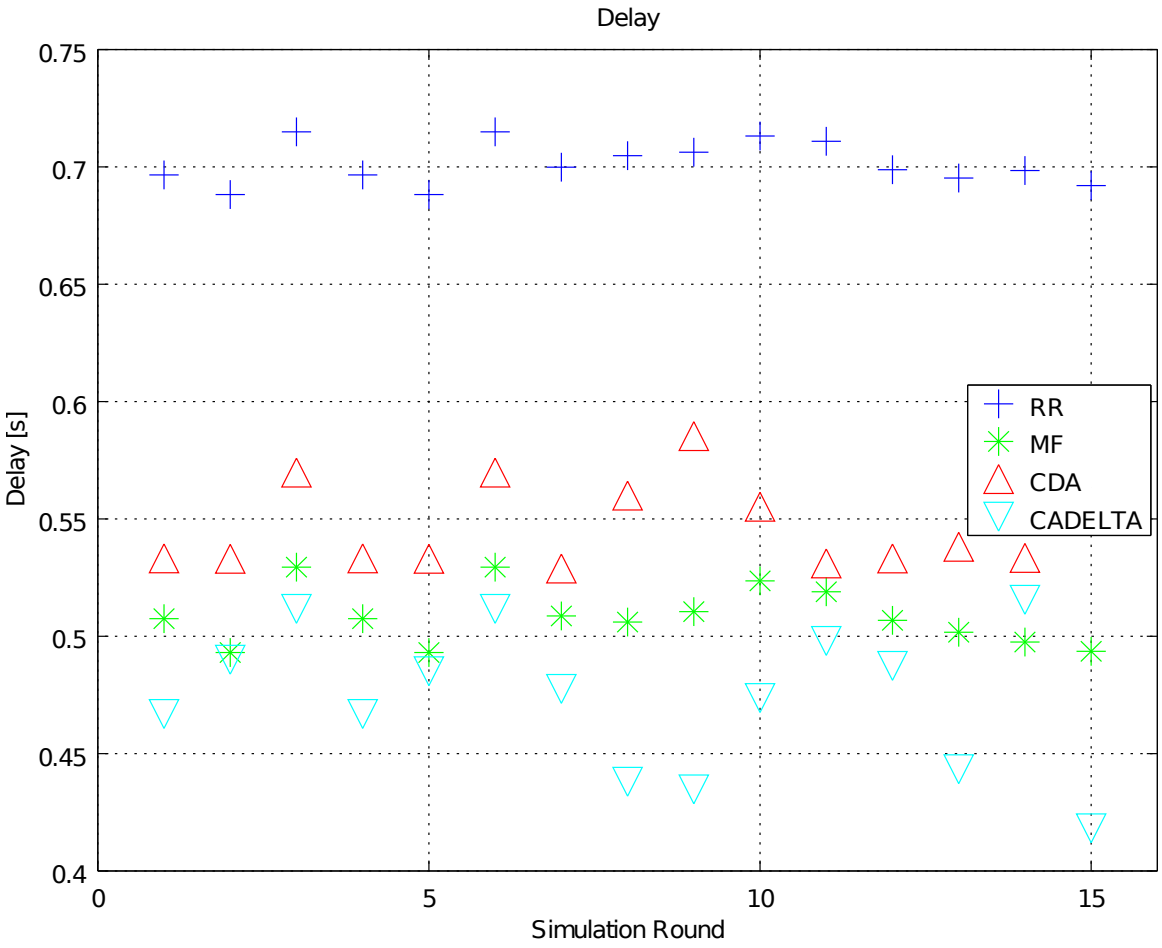

Figure 4.8: Delay - Video surveillance (LQ)

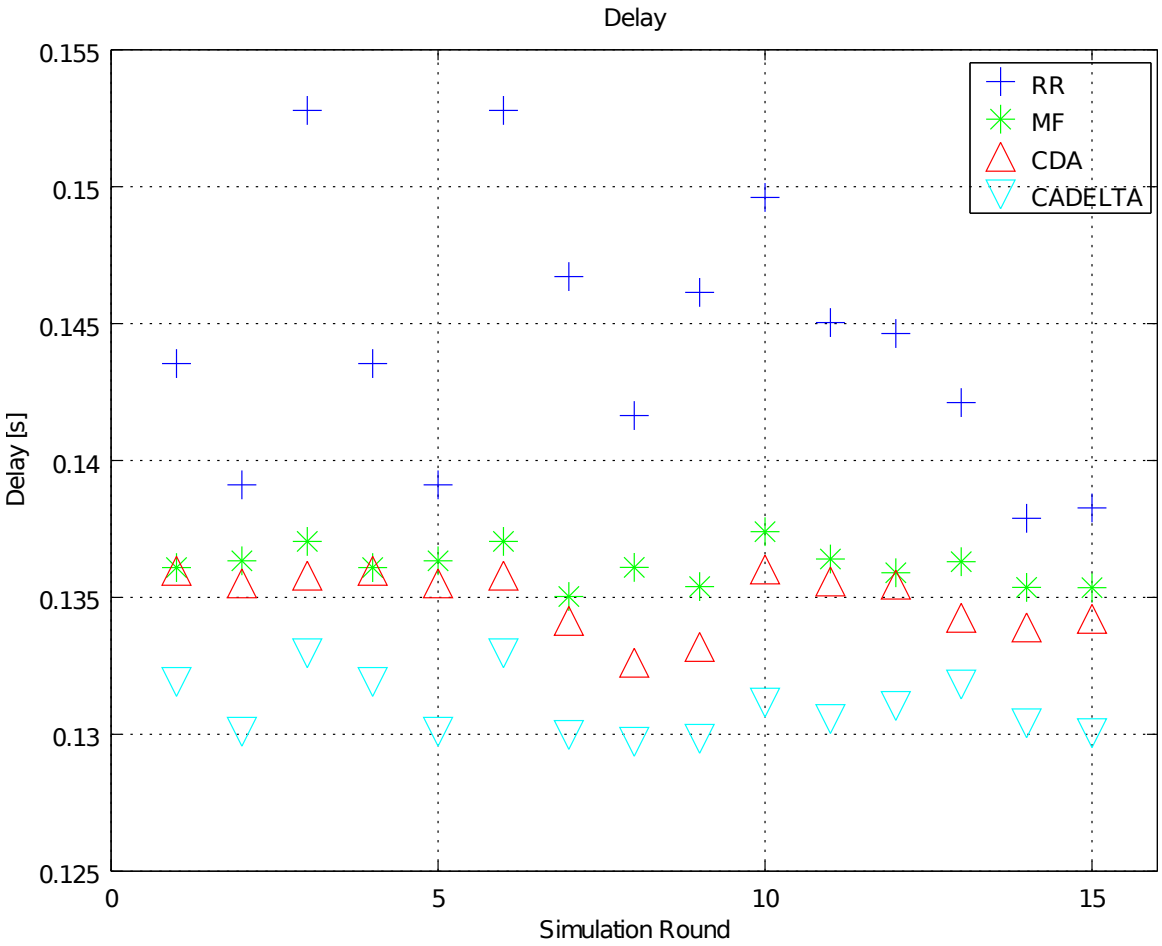

Figure 4.9: Delay - Traffic Monitoring

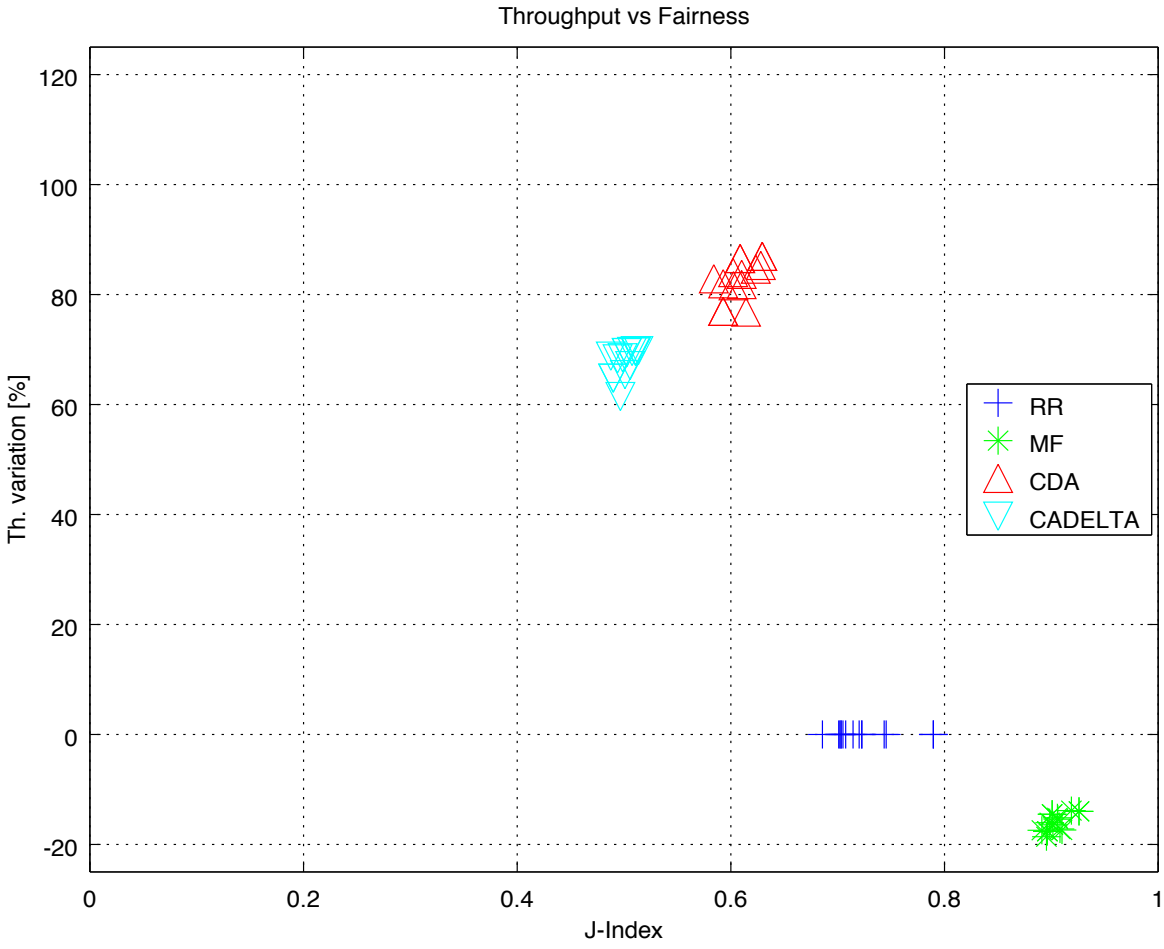

Figure 4.10: Throughput vs Fairness - Video surveillance (LQ) and Video surveillance (HQ)

has a direct impact on the MF approach, which seriously deteriorates the throughput performances, obtaining 20% less throughout than RR. On the other hand, both solutions are more robust to the traffic change and perform well, with an increment of throughput with respect to RR in the order of 70-80%. Same trends are observed in Figure 4.11, where both CDA e CADELTA have an average delay in the order of $0.4s$ against the $0.65s$ obtained on average by RR and MF algorithms, providing a performance improvement in the order of 50%.

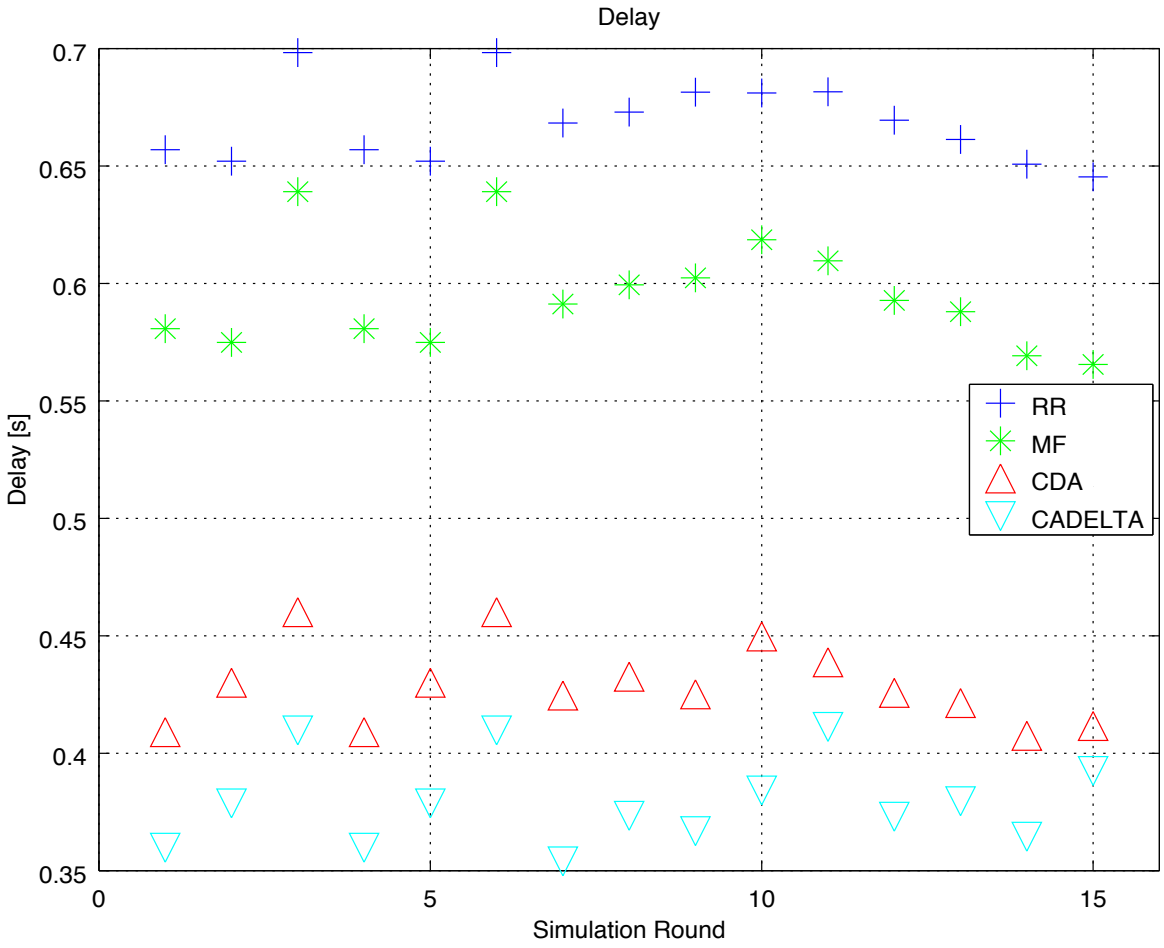

Figure 4.11: Delay - Video surveillance (LQ) and Video surveillance (HQ)

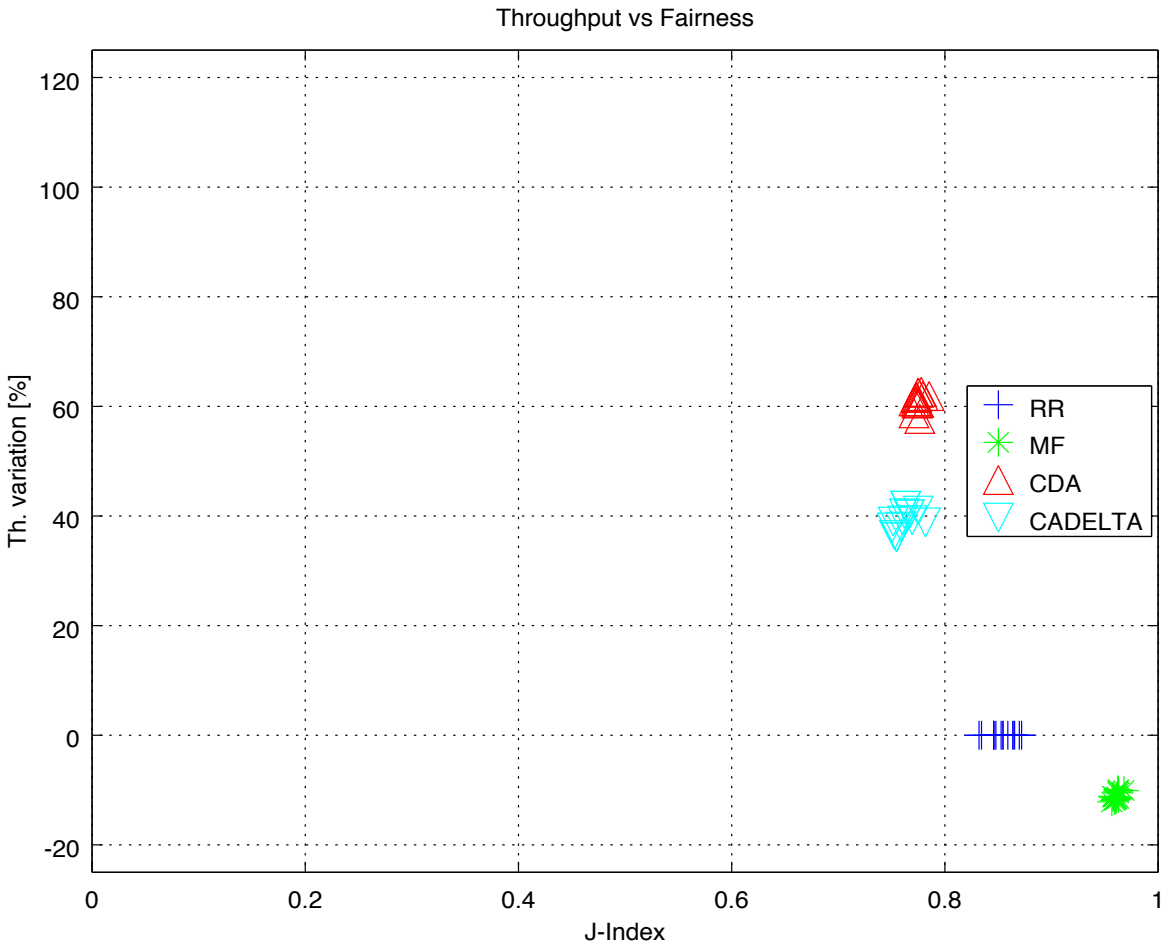

Figure 4.12: Throughput vs Fairness - Traffic Monitoring and Video surveillance (HQ)

Figures 4.12 and 4.13 depict performances of the four algorithms with a second mix of traffic based on traffic monitoring and video surveillance HQ. This simulation campaign confirms the tendency of MF to poorly perform when a high demand traffic profile is offered, obtaining performances of 60% and 80% below those provided by CDA and CADELTA, respectively. In terms of delay, the proposed solutions perform always better than RR, while the improvement with respect to MF is negligible.

Finally, figures 4.14 and 4.15 shows a simulation campaign where all the defined traffic classes are considered. In particular, the traffic mix consists of 25% of traffic

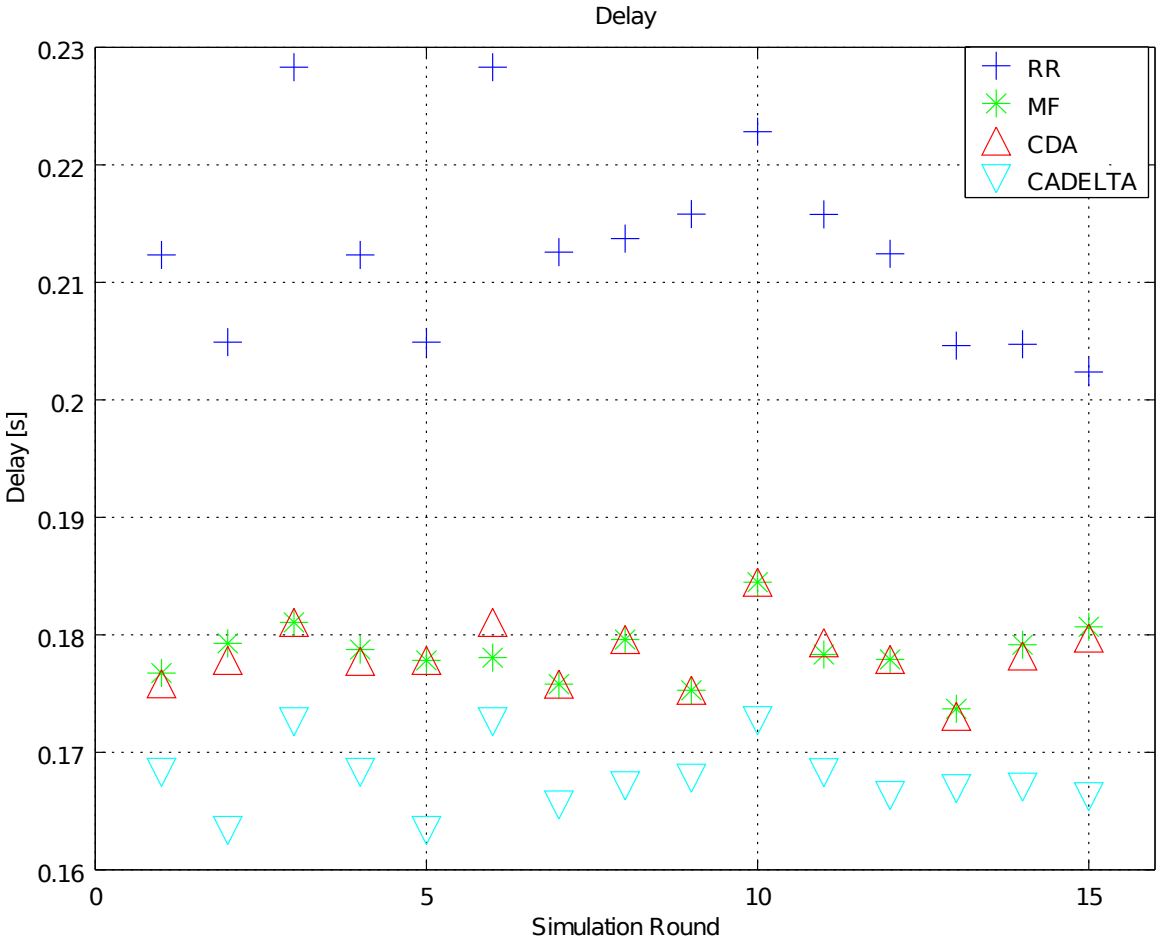

Figure 4.13: Delay - Traffic Monitoring and Video surveillance (HQ)

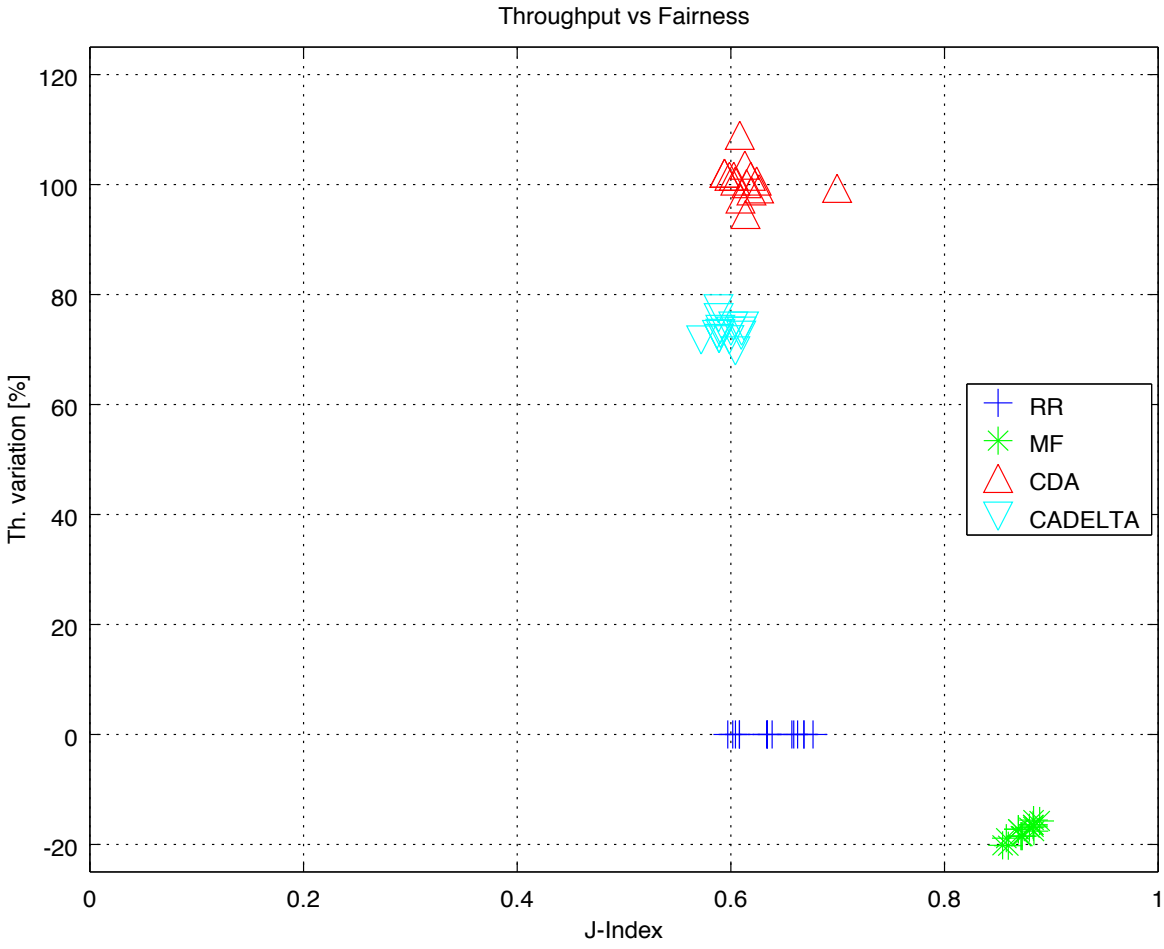

Figure 4.14: Throughput vs Fairness - Traffic Monitoring (25%), Video surveillance (LQ)(25%) and Video surveillance (HQ)(50%)

monitoring, 25% of video surveillance (LQ) and 50% of video surveillance (HQ). In this case, all the algorithms result in a reduced fairness, with respect to previous combinations. CA and CADELTA perform very similarly to RR. On the other hand, in terms of throughput, CDA and CADELTA outperform by 100% and 80%, respectively, compared to RR. With respect to MF the improvement is even larger, i.e. 120% and 100% respectively. Finally, in terms of delay, CDA and CADELTA outperform both RR and MF.

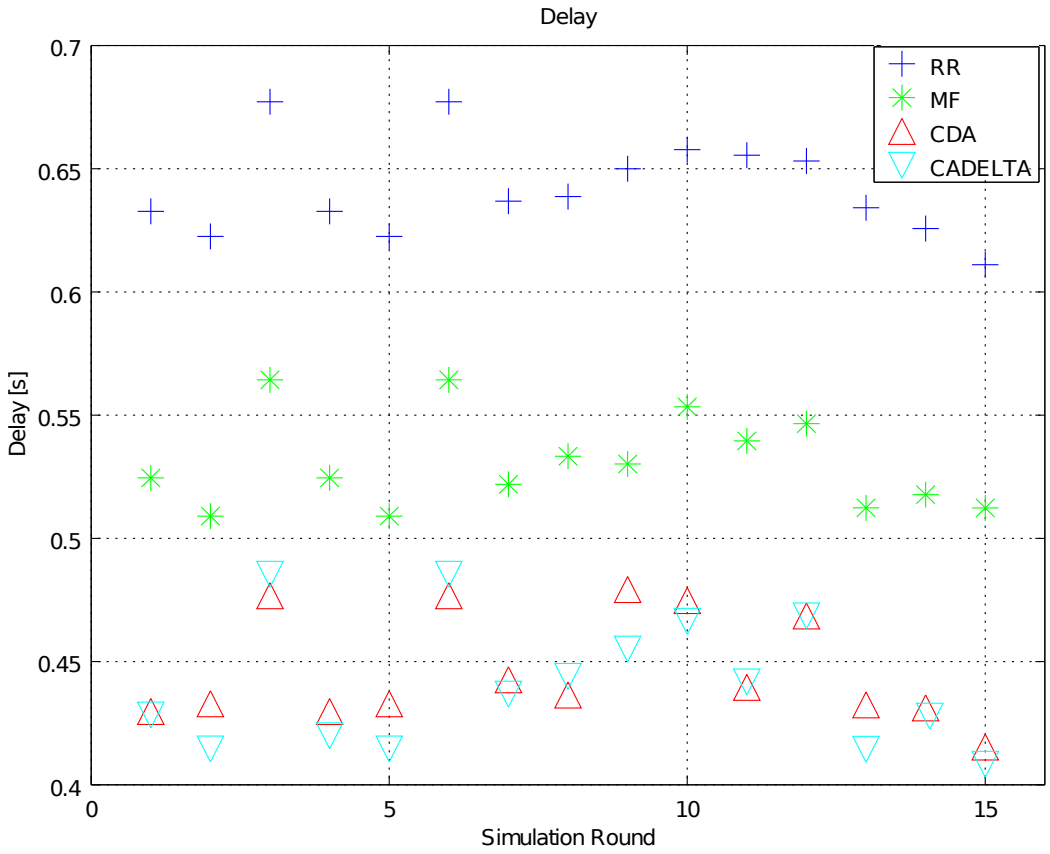

Figure 4.15: Delay - Traffic Monitoring (25%), Video surveillance (LQ)(25%) and Video surveillance (HQ)(50%)

These four simulation campaigns, based on considering multiple combinations of M2M traffic, have shown that CDA and CADELTA offer a high increment of throughput and reduction of delay, with respect to the benchmarks. This is achieved at the expense of a reduced (in the order of 10-15%) fairness. This behaviour is robust to changes in terms of traffic. In addition, the proposed scheme is parametric with the profit function, and different QoS parameters can be optimized through it. For example, comparing CDA and CADELTA, each algorithm gives higher priority to the QoS parameter that has been designed to optimize, i.e., the CDA always provides better performance in terms of throughput, while CADELTA performs better in terms of delays.

In the last simulation campaign, a new algorithm is presented. This latter is able to optimize not only one QoS parameter, but a combination of them. This implementation has been called CAA - Channel and Application Aware, which combines the principles of CADELTA and CDA. In particular, the profit function for CAA is defined as follows:

$$p_j = \alpha * d_j + \beta * \delta_j \tag{4.6.2}$$

where α and β are coefficients that depend on the particular application and traffic class. For instances, a traffic class which is more sensitive to the delay than to the throughout, will be characterized by a high α and a lower β. Figures 4.16 and 4.17 shownthe results of this approach. Simulation results are compared to RR, CDA and CADELTA, and the obtained values are averaged over all the simulations. In this case a mix of two classes of traffic is considered: video-surveillance (HQ), the most demanding class, and the traffic monitoring, the class most sensitive to delays. Simulation results show that CAA correctly works by discriminating between classes

of applications and prioritizing the QoS parameter to be optimized. In particular, in terms of throughput it can be observed an increment in the video-surveillance (HQ) traffic, and a slight reduction (about 2%) for the traffic monitoring application. In terms of delay, the CAA offers extremely low latency values for the traffic monitoring class, while it increases the delay of the video-surveillance application. On average, the behaviour is through very similar to that provided by CDA and CADELTA. To conclude, with this last implementation of the algorithm, it has been shown that the proposed framework allows to target multiple QoS parameters depending on the specific kind of traffic to be served.

4.7 Conclusions

In this chapter, a framework to address the scheduling of multiple and heterogeneous M2M applications over a dense small cell network, deployed in the street lights for smart city applications has been presented. The main focus had been on the UL scheduling problem, which, due to the constraint imposed by the standard, requires the allocation of contiguous RBs to the same user. This simple limitation makes the problem NP-hard. A multi-objective optimization, through a MILP formulation, have been presented that aims at maximizing the throughout of the network, minimizing the high ICI generated due to the intense spatial reuse in the small cell deployment, and maximizing the radio resource usage.

The first model gradually optimizes the allocation of resources in order to meet the three targeted optimization objectives. The second model allows for a more compact representation of these objectives. It have been proved that the second compact model is equivalent to the first one, based on a three step optimization. The optimal

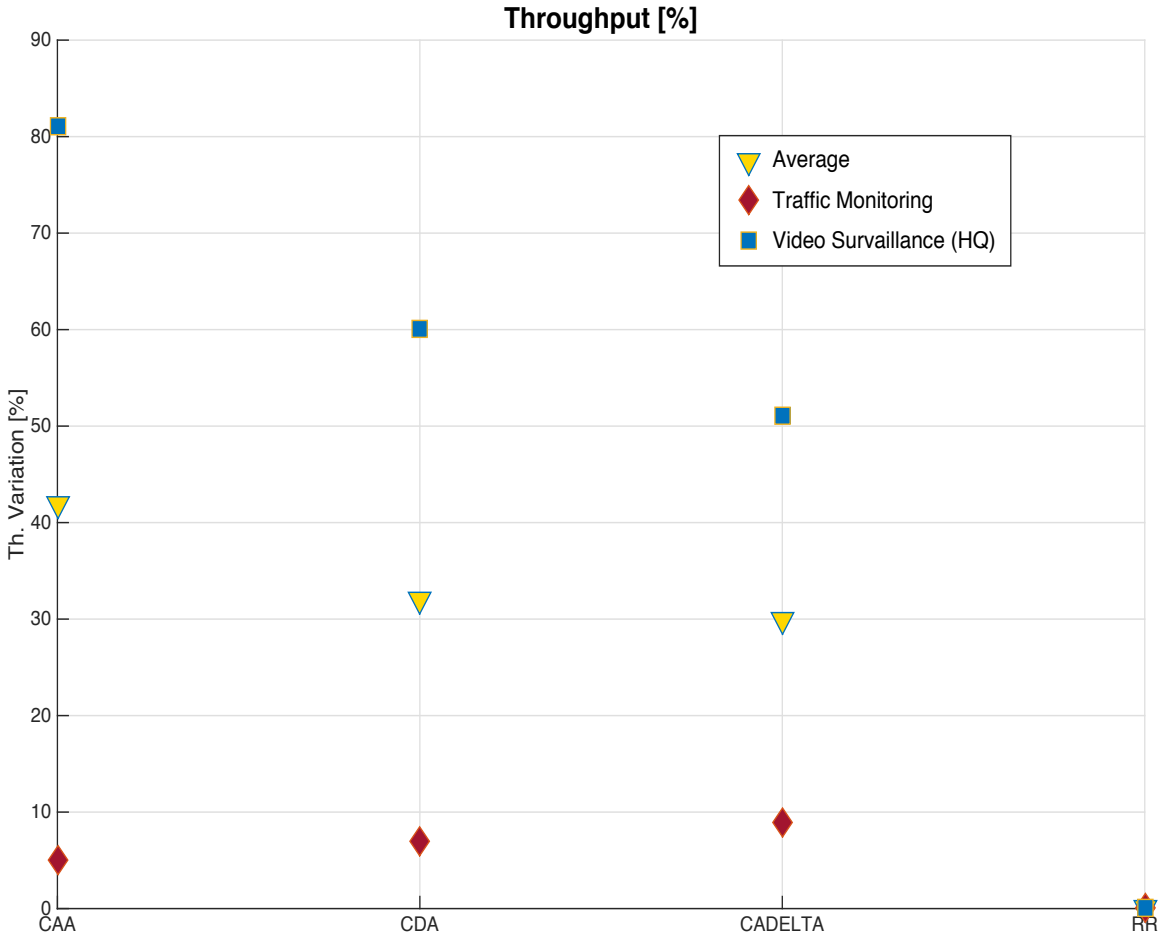

Figure 4.16: Channel and Application Aware - Throughput - Traffic Monitoring and Video surveillance (HQ)

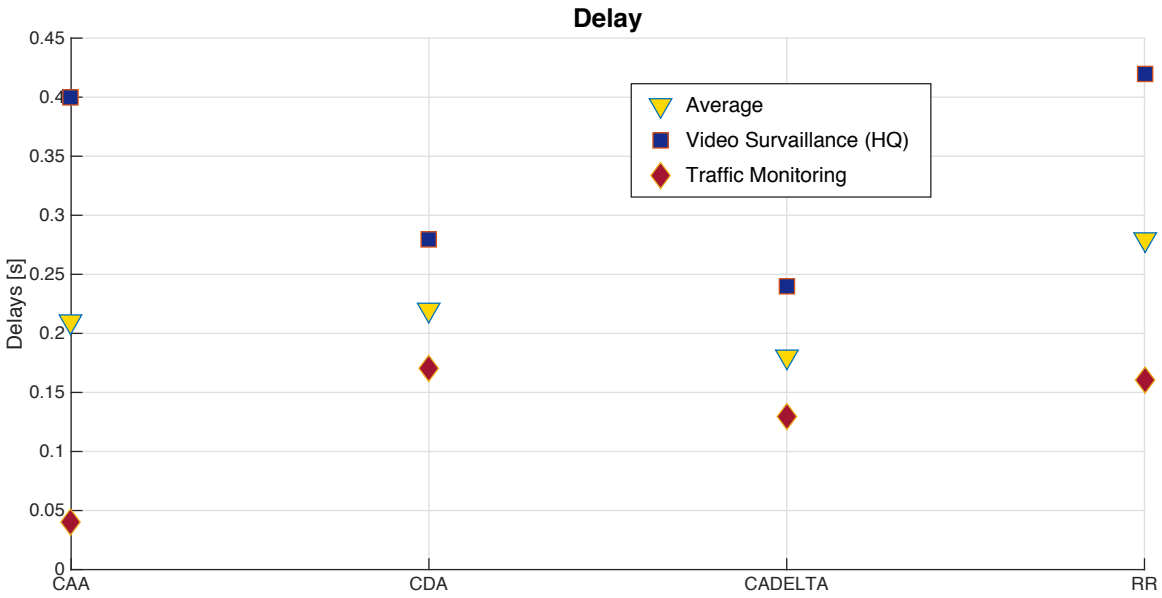

Figure 4.17: Channel and Application Aware - Delay - Traffic Monitoring and Video surveillance (HQ)

solution has been found through a CPLEX analysis, which proves that the compact model performs better and executes faster.

As a solution suitable for implementation in real world networks, it have been proposed a feasible and fast heuristic algorithm that solves the NP-hard problem. This greedy solution lowers the performance by 10% with respect to the theoretically optimal solution, in more than 90% of the cases, and its execution time runs on non-dedicated hardware in less than $1ms$, thus meeting the standard scheduling constraints.

Two different versions of the greedy algorithm have been implemented on a standard-compliant network simulator, i.e. the LTE module of NS3, implementing the complete LTE protocol stack. It have been demonstrated the superiority of our solutions, in terms of delay and throughput, with respect to benchmarks like Round Robin and Maximum Fairness approaches.

Chapter 5

RRM for M2M with uplink enhancement (Carrier Aggregation)

5.1 Carrier Aggregation

As presented in the previous chapters, several studies predict an exponential increment in data bit rate demand from cellular networks users. A much higher traffic demand is expected for mobile networks [108] in the near future, especially within urban areas. Indeed, the design requirements of the fifth generation (5G) specify $1,000$ times more capacity per unit area than 4G. It is in general well known that there is a direct relation between the available bandwidth and the increment of user data bit rate. However, the allocation of contiguous portions of spectrum is very rare. Most of the time, in fact, operators are assigned several small portions of spectrum that result in a very fragmented spectrum allocation.

All these aspects have motivated 3GPP to define a new feature for LTE technology which allows for simultaneous transmissions in more than one segment of allocated spectrum. This new feature, added in LTE-A, is referred to as CA, and it consists of

aggregated transmissions across multiple Component Carrier (CC)s. CA will play a crucial role in the evolution of LTE in general and in the so-called "Licensed-Assisted Access (LAA)" extensions, which allow the use of licensed bands to be augmented by carriers located in unlicensed bands, as it has been under discussion and evaluation in Release 13. The standardization process is now going on also in Release 14. CA will enable Secondary Cells (SCells) to carry data transmissions in unlicensed spectrum, while anchored to a primary cell (PCell) in the licensed spectrum, which maintains the essential control messages and also provides always-available robust spectrum for real-time or high-value traffic.

The rest of this chapter is structured as follow: sec. 5.2 gives an overview CA technology and the possible configuration scenarios; in sec. 5.3 a brief review on the state of the art it is presented with a particular attention on the UL related literature; sec. 5.4 shows an extension of the MILP model already presented in chap. 4 when CA is enabled; in sec. 5.5 the contribution to NS3 community is presented, in particular it shows a first implementation of CA in NS3 and its impact on the simulator structure; conclusion are summarized in sec 5.6.

5.2 CA technology overview

The feature of CA has been introduced in 3GPP releases for the first time in release R10. This new feature offers to the UE the opportunity to aggregate radio resources belonging to different carriers, in order to have more bandwidth available, and a higher potential throughput. The main references in the standard are [109], [110], [111] and [112].

The general concept is that users can be scheduled simultaneously on more than

one CC. Each CC can use a particular bandwidth from those originally defined in LTE 3GPP R8: 1.4, 3, 5, 10, 15 or 20 MHz. This choice was made in order to maintain backward compatibility with previous releases. The CCs can be adjacent or non-adjacent, either in the same or in different frequency bands. Different scenarios can then be foreseen:

- intra-band contiguous CA: this is the simplest case, but the most unlikely to happen, where two contiguous CC are within the same band. In order to maintain backward compatibility with the 100 KHz raster of LTE R8, and in order to preserve the orthogonality of the subcarriers, i.e. 15 kHz spacing, the CCs central frequency should be a multiple of 300 kHz.

- intra-band non-contiguous CA: similarly to the previous scenario, in this case CCs are within the same band, but they are not adjacent.

- inter-band non-contiguous CA: this is probably the most interesting scenario. In this case, multiple CCs belonging to separate bands are aggregated. This is also of interest in case of heterogeneous networks where the diversity in the frequency domain can improve the mobility robustness.

CA allows new flexibility also from the system deployment point of view, i.e. CCs can be:

- Co-located and overlaid in the same frequency band. Using this system settings, all UEs within the cell coverage area can access to all CCs, so that they can exploit all the CA functionalities to increase their own throughput

- Co-located and overlaid with different frequency band. This system design setting is of interest in case the objective is to boost the cell edge performance.

In fact, it is possible to take advantage from the different propagation condition of the different carriers and consequently optimize the cell coverage.

- Not co-located. This latter case is, maybe, the most important in terms of heterogeneous networks. In that case, a macro-cell can provide coverage while RRHs and SCs provide improved throughput at the traffic hot-spots.

In Frequency Division Duplex (FDD) mode, in R10, only DL CA is allowed, and the CCs should be on the same band. In the other release, i.e. R11, R12 and R13, several additional aggregation schemes are introduced both in UL and DL. In general, 3GPP requires that aggregated CCs in UL and DL can be different, but the number of CCs aggregated in DL should always be equal or higher than those aggregated in UL.

Regarding UEs, 3GPP defines three different CA bandwidth classes for R10 and R11:

- Class A: Aggregated Transmission Bandwidth Configuration (ATBC) ≤ 100, maximum number of CC $= 1$
- Class B: ATBC ≤ 100, maximum number of CC $= 2$
- Class C: ATBC $\leq$ ATBC ≤ 200, maximum number of CC $= 2$

In order to maintain backward compatibility and then having a smooth migration from LTE to LTE-A, some configuration parameters have been added. In particular each CC is treated as a separate cell, with its own unique cell identifier. Moreover, each CC broadcasts its own System Information (SI).

Currently, devices that are not CA ready, can move from one CC to the other through the handover procedure. On the other hand, a UE device that has CA capability tries to associate to the network by executing the random access procedure on a specific CC called Primary Carrier Component (PCC). After the association, additional resources can be configured; in this case the CCs are generically called Secondary Carrier Component (SCC). 3GPP allows the eNB to use load balancing techniques, so that a different PCC can be set for each UE.

5.3 Review the state of the art

In this section the current state of the art regarding LTE CA is presented. Since the focus of this dissertation is on MTC, the analysis of scientific literature is mainly oriented to UL case. Moreover, UL seems to be the most challenge, in fact in literature many works dealing with DL solutions where the gain of applying CA is more directly viewed. On the other hand, due to the many constraints regarding UEs capability results in a less straightforward gains when CA is applied. In [113]the main challenges from the PHY layer prospective are presented. Authors are focused on an UL scenario and in particular in case of high mobility, they propose analysis and solutions when the fast fading and frequency offset become of relevant interest due to the possible degradation of the system performance.

CC selection is a topic of interest when CA is implemented. The main concept is that the eNB must decide on which frequency bands assign a UE. This procedure has a large impact on energy consumption, in particular with maximization of power reduction (MPR), power control techniques and consequently it can have an impact on cell-edge users. This topic is discussed in [114] where only load balance and cell

selection are studied and extended in [115] where UL power control and performance analysis on cell-edge are presented. In the same way, authors in [116] present simulation result on cross-layer CC selection with power control; meanwhile a similar scenario is studied in [117] where MPR for cell-edge UEs is the focus.

In [118] and [119] the focus is on user scheduling algorithm. In the former a channel-aware CA scheduling algorithm is presented. In this case, the algorithm aims to maximize the utility function of the cell-edge user by prioritizing them over the rest of UEs. The latter, propose a QoE measurement framework and applied that on a joint resource allocation algorithm.

All the works presented above are related to a single macro cell scenario, while [120] and [121] are related to a femto cell indoor scenario and to a inter-site macro - small cell scenario respectively. In [120] the focus is on reducing the signaling traffic required to apply CA in this particular scenario. While [121] is more oriented on 3GPP R11 - R13 where is possible to have UL CA where the CCs are not co-located, in specific some are assigned by a macro cell while other CCs could be assigned by a SC.

5.4 Extended Milp Model

In this section an extension of the MILP model for FDPS in UL LTE already described in chapter 4 is presented. This extension allows the model to be used in case the CA is available in the scenario of interest. In the follows, the model already presented in chapter 4 is called LTE MILP model, while its extension is called LTE-A MILP model. For sake of readability, in the follows, the LTE MILP is restated:

$$max \sum_{j=1}^{n} \sum_{i=1}^{m} (\alpha d_j - \beta f_{i,j} - \gamma r_{i,j}) x_{i,j} \tag{5.4.1}$$

subject to:

$$f_{i,j} x_{i,j} \geq 0; \quad j = 1, \ldots, n; \quad i = 1, \ldots, m; \tag{5.4.2}$$

$$\sum_{i}^{m} x_{i,j} \leq 1, \ j = 1, \ldots, n \tag{5.4.3}$$

$$\sum_{j=1}^{n} \sum_{k=1}^{i} b_{i,k}^{j} x_{k,j} \leq 1, \ i = 1, \ldots, m; \tag{5.4.4}$$

The LTE-A MILP model in order to taking into account the possibility to use CA technique need as assumption that a priori it is possible to decide the amount of data that have to be sent on each CC. For instance, given a system with a maximum of 2 CCs and a user j with a demand d_j, the model is still valid if "virtual" users j_1 and j_2 are defined. These "virtual" users have demand $d_{j1} + d_{j_2} = d_j$ and are served in the same TTI. The new model is described by the following equations:

$$\max \sum_{j=1}^{3n} \sum_{i=1}^{m} (\alpha d_j - \beta f_{i,j} - \gamma r_{i,j}) x_{i,j} \tag{5.4.5}$$

subject to:

$$\sum_{i}^{m} x_{i,j+n} = \sum_{i}^{m} x_{i,j+2n}, \ j = 1, \ldots, n \tag{5.4.6}$$

$$f_{i,j} x_{i,j} \geq 0; \quad j = 1, \ldots, 3n; \quad i = 1, \ldots, m; \tag{5.4.7}$$

$$\sum_{i}^{m} x_{i,j} \leq 1, \ j = 1, \ldots, 3n \tag{5.4.8}$$

$$\sum_{i}^{m} x_{i,j+n} \leq (1 - \sum_{i}^{m} x_{i,j}),\ j = 1, \ldots, n \tag{5.4.9}$$

$$\sum_{j=1}^{n} \sum_{k=1}^{i} (b_{i,k}^{j} + b_{i,k}^{j+n} + b_{i,k}^{j+2n}) x_{k,j} \leq 1,\ i = 1, \ldots, m; \tag{5.4.10}$$

The first difference is in the objective function. In fact, comparing eq. 5.4.1 and eq. 5.4.5, the latter model has a larger set of users, i.e. $j = 1..3n$ instead of $j = 1..n$. In the LTE-A MILP model the "virtual" users j_1 and j_2 have index $j_1 = j + n$ and $j_2 = j + 2n$, where n is the total number of users. In order to include the "virtual" users eqs. 5.4.6, 5.4.3 and 5.4.4 are modify accordingly. The equivalent equations in LTE-A MILP model are eqs. 5.4.7, 5.4.8 and 5.4.10 respectively.

Each new CC added increase the dimension of the problem by $2n$. The LTE-A MILP model is practical the same problem as the previous where two more constraints are added. Eq 5.4.6 forces to assign both the "virtual user" or neither; while eq 5.4.9 forces the solver to either assign the resource to j or to both virtual user j_1 and j_2. The extended model is still valid and it solve the new instance. As it was expected, it is a relaxed version of the model already defined. The fact that is a relaxation of the LTE MILP has two main implication: i) the dimension of the new problem is larger, that means potentially an increasing in the execution time; ii) on the other hand, it is very well known that a relaxation of the problem gives a better upper bound. As in previous case, the model was tested using CPLEX over a large set of instances (around 6000). The test shows that in most of the case CPLEX solver found an optimal solution which is larger or equal to the optimal solution achieved with the LTE MILP model. Generally the LTE-A MILP model execution time is larger with respect to the LTE MILP model, however in some case the execution

time needed to find the optimal solution increases from few seconds o several hours. This issue is due to the particular symmetry of the instance. Practically, the solver finds several solution with a very small gap (in the other of 0.36%) and, so many assignment scheme can be used to achieve the optimal feasible solution.

5.5 NS3 contribution to the community

In this section the contribution to NS3 community is presented. The section is structured as follows: first of all a brief state of the art on LTE-A simulators is given, then the impact on LTE protocol stack, both on user and control plane is presented, finally the implementation is described.

5.5.1 State of the art

Among the available LTE-A open source simulators, only LTE-Sim [122] provides this functionality. LTE-Sim is a C++ object oriented open source simulator designed for supporting LTE and LTE-A technologies. The main drawback of this simulator is that it does not allow to simulate scenarios typical of CA, where LTE-A has to coexist with other technologies like WiFi. Moreover, it does not model TCP, which limits the range of experiment that can be performed. Regarding LAA and CA in general, several studies have been carried out in 3GPP with proprietary simulators [123, 124]. However, the usage of proprietary simulators does not allow to reproduce the results and validate the models. The evaluations have been performed by means of system level simulators, which implies that they do not consider upper layer protocols (i.e., UDP and TCP) and realistic applications.

For all those reasons, in this section it is presented an extension the ns-3 LTE module to include CA. This work has been carried out in the framework of the Google Summer of Code 2015 program [1]. The main contributions are represented by the creation of new APIs for managing several CCs, a simple CA algorithm and an example simulation script for providing a guide on its usage.

5.5.2 Impact on LTE Stack

Hereafter, it is described the impact of CA implementation over the LTE stack in both control and user planes. In addition, it is briefly discussed the software architecture proposed to introduce CA. Figure 5.1 shows the impact of CA on the different layers of the LTE protocol stack.

5.5.3 Control Plane

Mainly to maintain the backward compatibility, in LTE-A, each UE establish the cell connection following the R8 procedure. In other words, it starts a cell search and selections, than SI acquisition phase; finally it initializes the random access procedure. As anticipated above, All the CCs broadcast their own SI and synchronization signals. RRC is in charged of the connection procedure, it selects the PCC. Ones the UE is in CONNECTED state, eNB RRC query the UE in order to understand on which class it belongs and its capabilities. The RRC layer at the eNB is responsible to perform reconfiguration, addition and remove of SCCs. The standard define PCC as UE related and not eNB related, in other word PCC is the CC that is perceived with the most robust connection for each UE. After UE move to CONNECTED state,

[1] The souce code is available at: `http://code.nsnam.org/daniloa/ns-3-dev-lte-ca/`

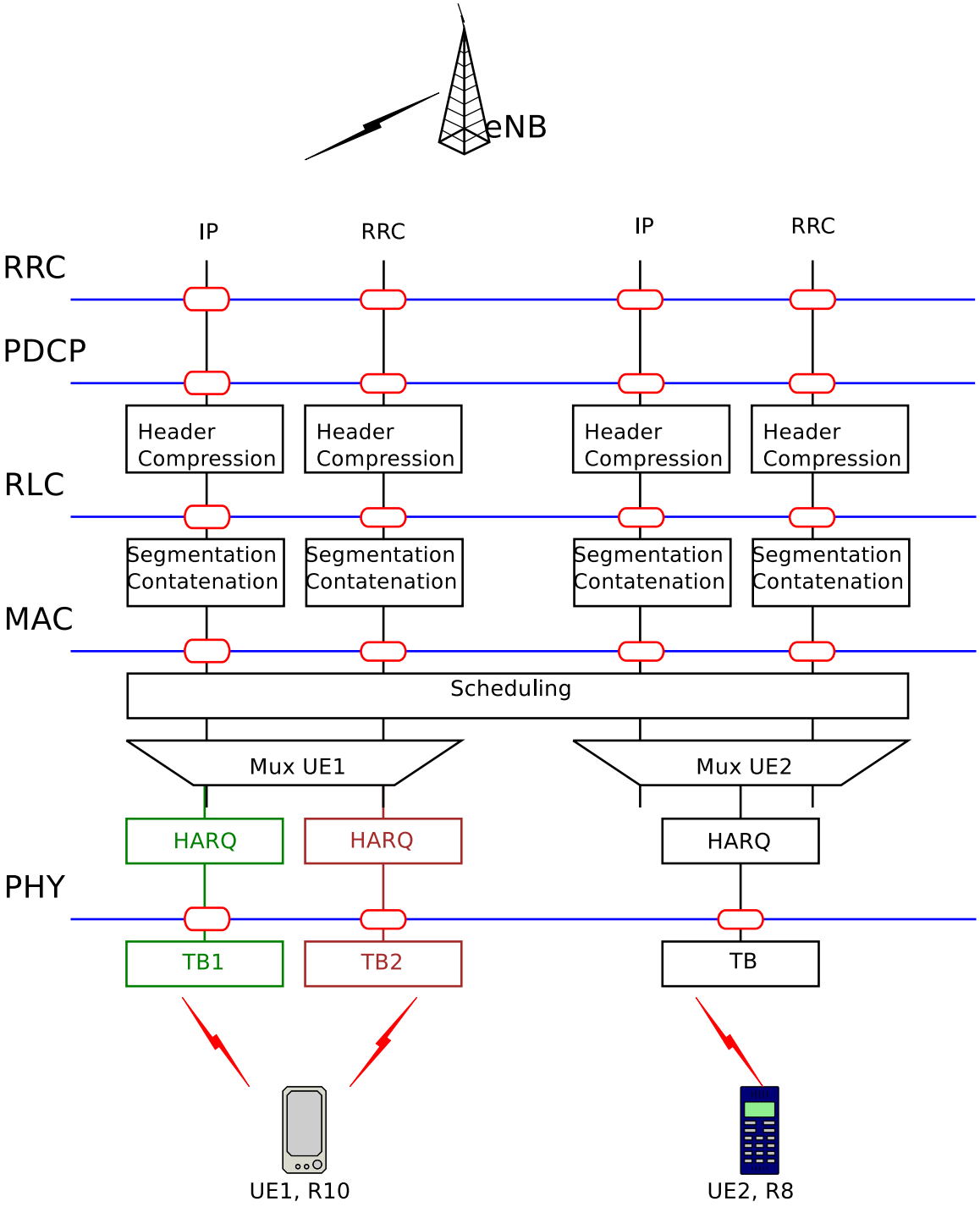

Figure 5.1: Carrier Aggregation.

load balance policies can be applied, e.g. force the UE to perform handover toward a less congested CC. As it is possible to image, this modification in the connection procedure is the main impact on RRC layer.

5.5.4 User Plane

CA was designed to be completely transparent to both PDCP layer and RLC layer. In fact no modification are needed in this two layer due to CA implementation. The only possible impact could be from the hardware/software view point, i.e. due to potentially throughput increasing larger buffer should be set at those layer to receive the data-stream coming from lower layers. On the other hand, CA has a large impact on MAC layer. MAC layer is responsible to schedule the resource and handle the priority, multiplexing the data-stream coming from the different transport channels and of Hybrid Automatic Repeat reQuest (HARQ). Due to its role MAC layer should be aware of the number of CC enabled. Two different scheduling scheme are allowed:

- Independent Carrier Scheduling (ICS), where each CC transmit its grant using its own Physical Downlink Control Channel (PDCCH) and scheduler allocates traffic per CC-bases

- Joint Carrier Scheduling (JCS), where all grants are transmitted in one CC despite they belong to the same CC or not, this is called cross-scheduling. In order to allow this latter schema, a modification in PDCCH was made. In any case, each CC has its own HARQ process.

5.5.5 Implementation on the NS3

The rest of this section is related to the specific implementation of CA in LENA, the LTE module of NS3. This work was supported by the program Google Summer of Code and all these results are available online. Due to its technical details, some knowledge about NS3, the rules adopted in the developers community and about the LTE module are required. Suggested documents are [104], [83], [125], [126] and [127].

5.5.5.1 Change on LteNetDevice

Both LteEnbNetDevice and LteUeNetDevice are create by the LteHelper using the method InstallSingleEnbDevice and InstallSingleUeDevice. In 5.2 it is shown all the parameters defined within these objects. Basically with this implementation all the attributes formerly part of the Lte[Enb/Ue]NetDevice are migrated within the ComponentCarrier[Enb/Ue] object. The ComponentCarrier object contains all the parameters necessary to characterize each CC plus the pointer to the related physical layer. The attributes currently are maintained in the Lte[Enb/Ue]NetDevice mainly for backward compatibility purpose. By default the Lte[Enb/Ue]NetDevice attributes are the same as the primary carrier attributes. In order to help in configuring the map a specific helper was introduced, i.e. CcHelper.

5.5.5.2 eNB Class Structure: Data Plane

In 5.3 it is shown the relation between the different classes related to the eNB data plane. Thanks to the LTeEnbComponentCarrierManager, the Carrier Aggregation is basically transparent to the upper layers. The main different with respect to the former architecture is that each MAC layer object sees only one LteMacSapUser. In

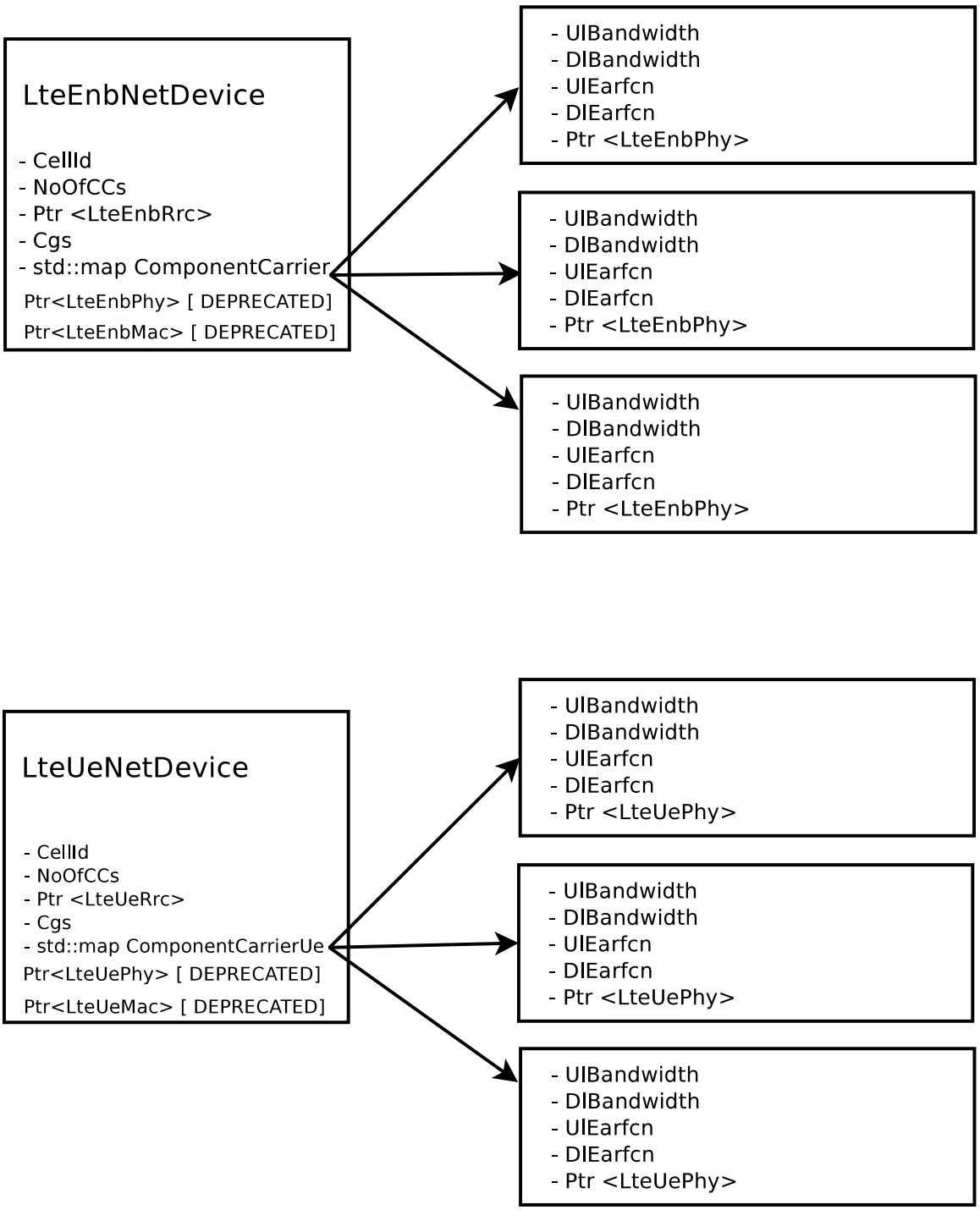

Figure 5.2: Class relations.

the same way, each RLC instance sees only one LteMacSapProvider. The LteEnbComponentCarrierManager it is responsible of the (re)mapping. In the current implementation, a PDCP and a RLC instances are activated each time a new Data Radio Bearer (DRB) is configured. The correspondence between a new Data Radio Bearer and a RLC Logical Channel is one to one. Logical channel configurations are propagated "as it is" to the Mac layer. In order to maintain the same behaviour LteEnbComponentCarrierManager, when a new logical channel is activated, propagate the logical channel configurations to each Mac layer object. The logical channel configuration sent to each MAC layer object changing accordingly to the algorithm implemented.

In 5.4 it is show an example on how the downlink buffer status report is propagated. Each time an RLC instance sends a BSR, the LteEnbComponentCarrierManager propagates and splits the BSR between all the CCs accordingly to policies.

5.5.5.3 eNB Class Structure: Control Plane

In 5.5 it is shown the relation between the different classes for the eNB control plane. During the design phase was chosen to maintain the same link as in the former architecture. To do so, each CC (either PHY layer and MAC layer objects) is connected in a one-to-one fashion to the RRC instance. However, the RRC instance is connected to the LteEnbComponentCarrierManager since this one it is responsible to enable/disable the carrier components. To clarify, when the simulation start, the number of CC is fixed, but only the primary carrier component is enabled. Depending on the LteEnbComponentCarrierManager algorithm the other carrier components could be activated or not.

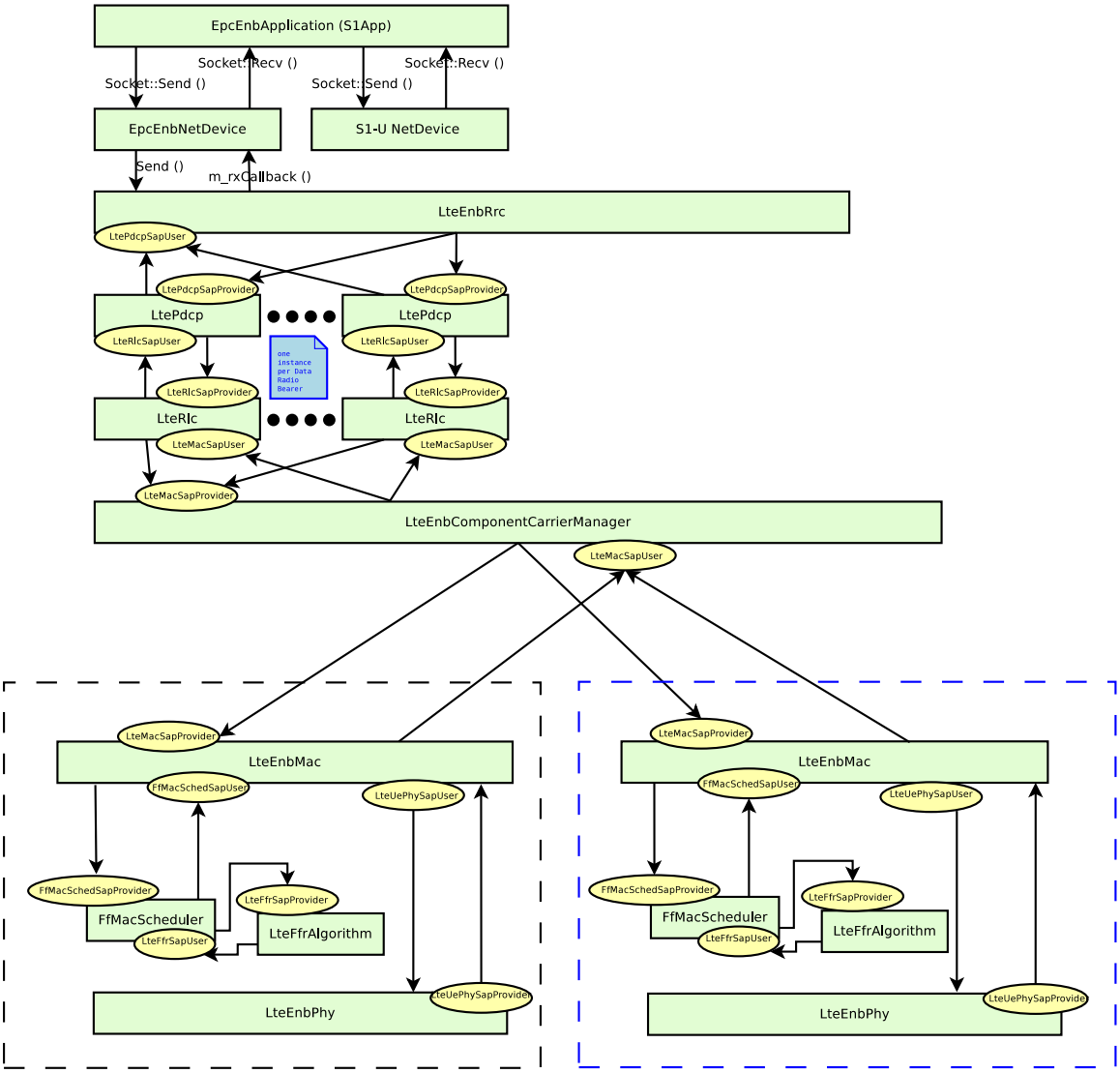

Figure 5.3: Lte Enb Data Plane Architecture

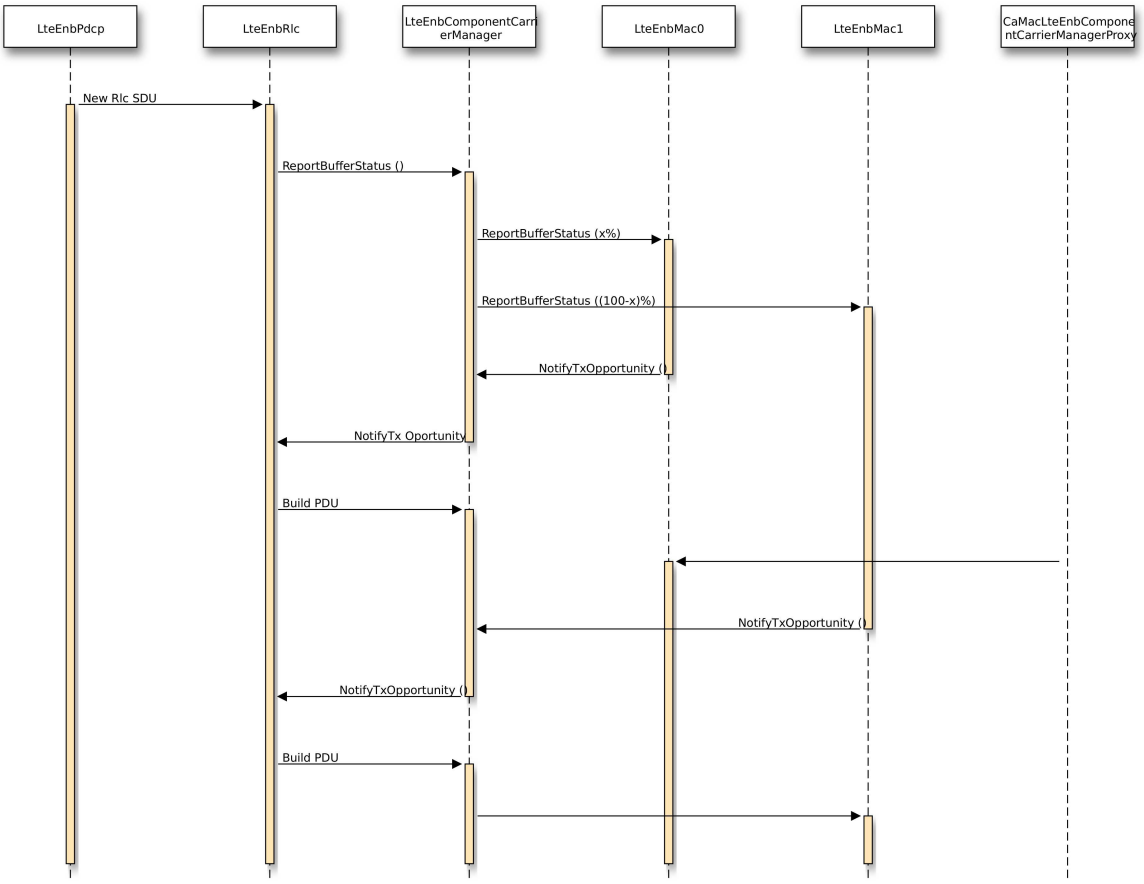

Figure 5.4: Sequence Diagram of downlink BSR

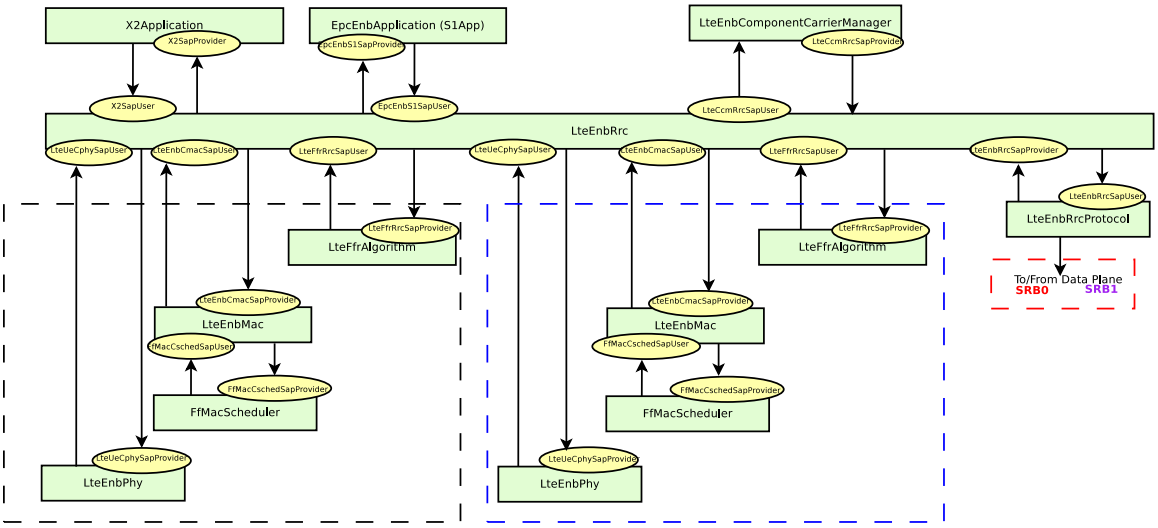

Figure 5.5: Lte Enb Control Plane Architecture

In 5.6 it is shown how the Radio Bearer are configured.

5.5.5.4 UE Class Structure: Data Plane

In 5.7 it is shown the relation between the different classes related to the UE data plane. The UE data plane architecture is similar to the eNB data plane implementation. The LteUeComponentCarrierManager is responsible to (re)map each MacSap[User/Provider] to the correspondence RLC instance or to proper Mac instance. The channel remapping depend on algorithm used as LteUeComponentCarrierManager. A particular case is represented by the UE buffer status report (BSR) to eNB. Since, i) the standard do not specify how the buffer status have to be reported on each CC and ii) it was decided to map one-to-one the logical channel to each MAC layer. The only way to send BSR to the eNB was through the primary carrier. 5.8 show the sequence diagram. Each time a BSR is generated, the LteUeComponentCarrierManager sends it through the primary carrier component. When the primary carrier

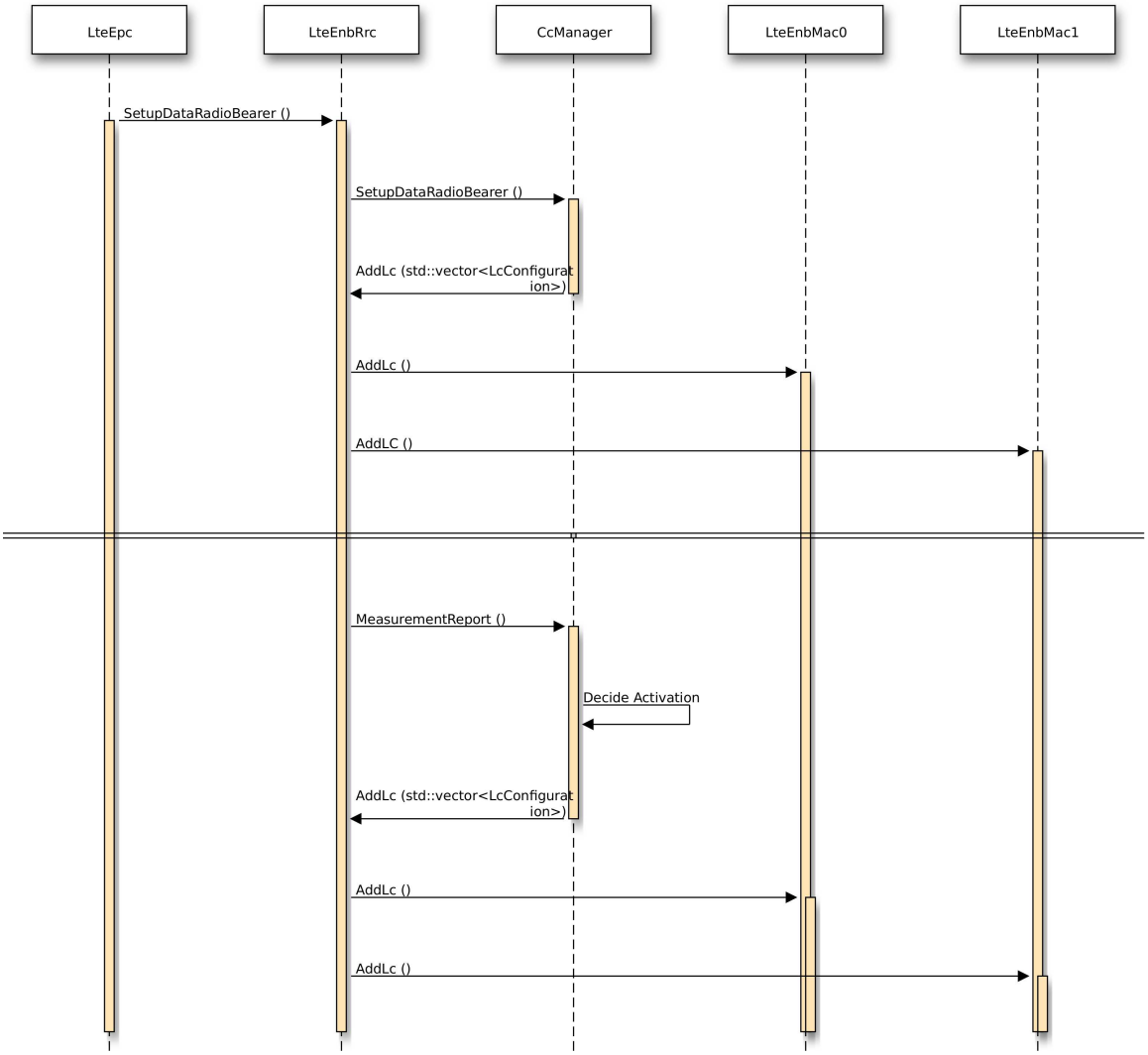

Figure 5.6: Sequence Diagram of Data Radio Bearer Setup

component, at the eNB, receive the BSR send it to LteEnbComponentCarrierManager. The latter, accordingly to algorithm dependent policies, send a BSR packet to each CC. The communication LteEnbMac <–> LteEnbComponentCarrierManager is done through a specific set of Sap: LteUlCcmRrcSap[User/Provider].

5.5.5.5 UE Class Structure: Control Plane

In 5.9 it is shown the relation between the different classes related to the UE control plane. The control plane implementation at the UE is basically the same as the eNB control plane implementation. Each CC control sap (both for PHY and MAC layer objects) is linked in a one-to-one fashion directly to RRC instance. The UE RRC instance is then connected to LteUeComponentCarrierManager in the same way as in the eNB.

5.6 Conclusions

In this chapter, the Carrier Aggregation concept has been introduced, and it has been expanding through subsequent Releases. This feature responds to the urgent need of operators to take advantage of multiple and sparse pieces of spectrum, in addition, it is a basic feature for the implementation of novel evolutions of LTE in unlicensed spectrum, which are under discussion currently in both Release 13 and 14.

A brief overview on the state of the art for CA in UL was presented. The main concept and research directions were shown. Moreover, an extension of MILP model for LTE UL problem was presented. This last model allows to use that one presented in chapter 4 when CA is available.

Finally a contribution to the ns-3 LTE module to support the very important

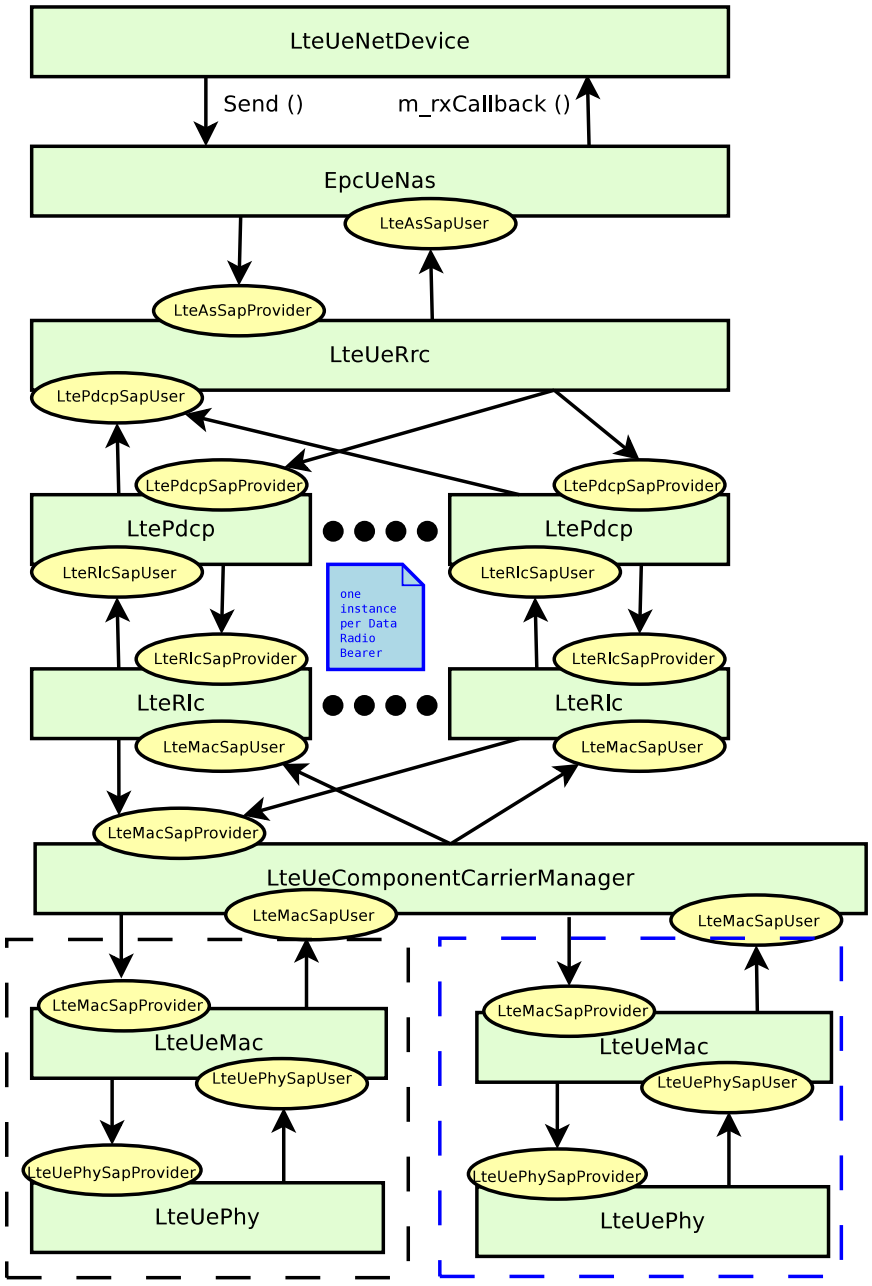

Figure 5.7: Lte Ue Data Plane Architecture

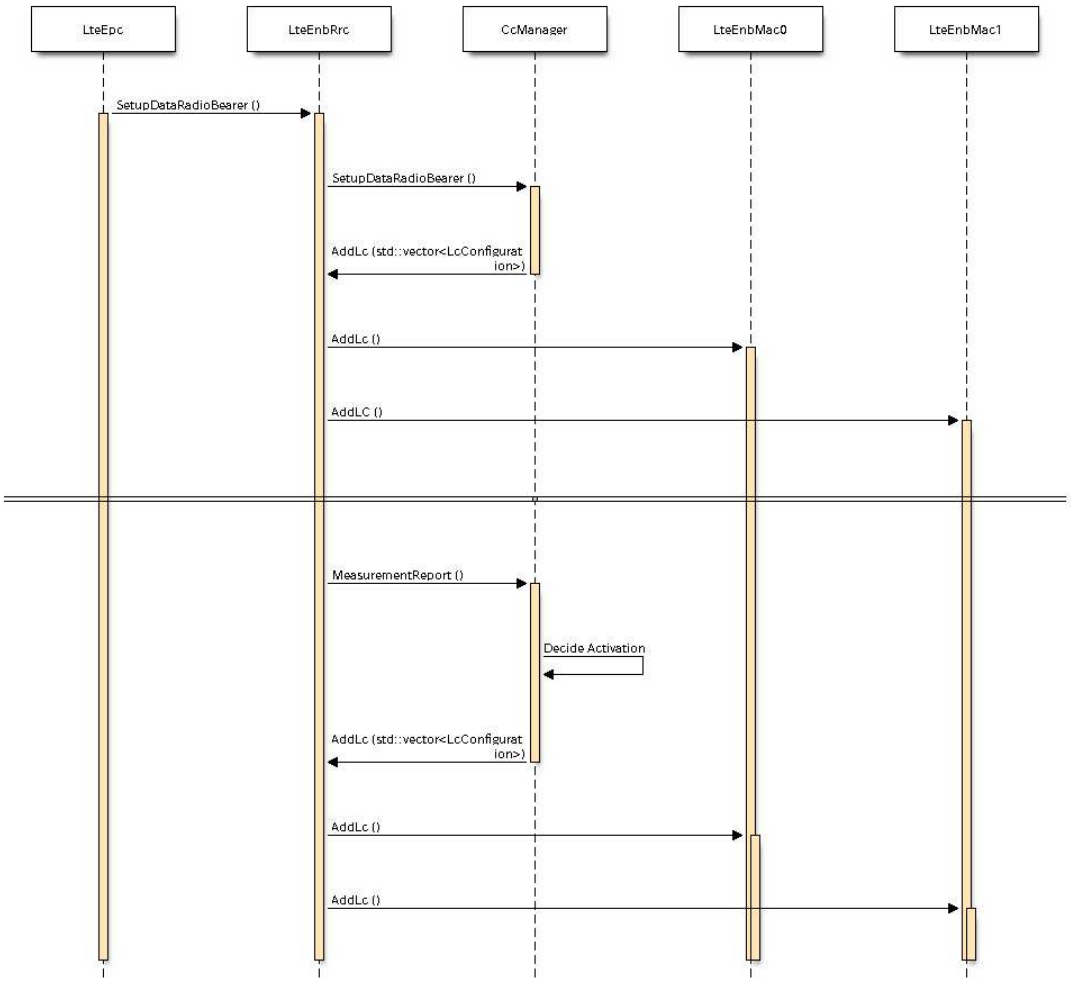

Figure 5.8: Carrier Aggregation Ul Tx Opportunity

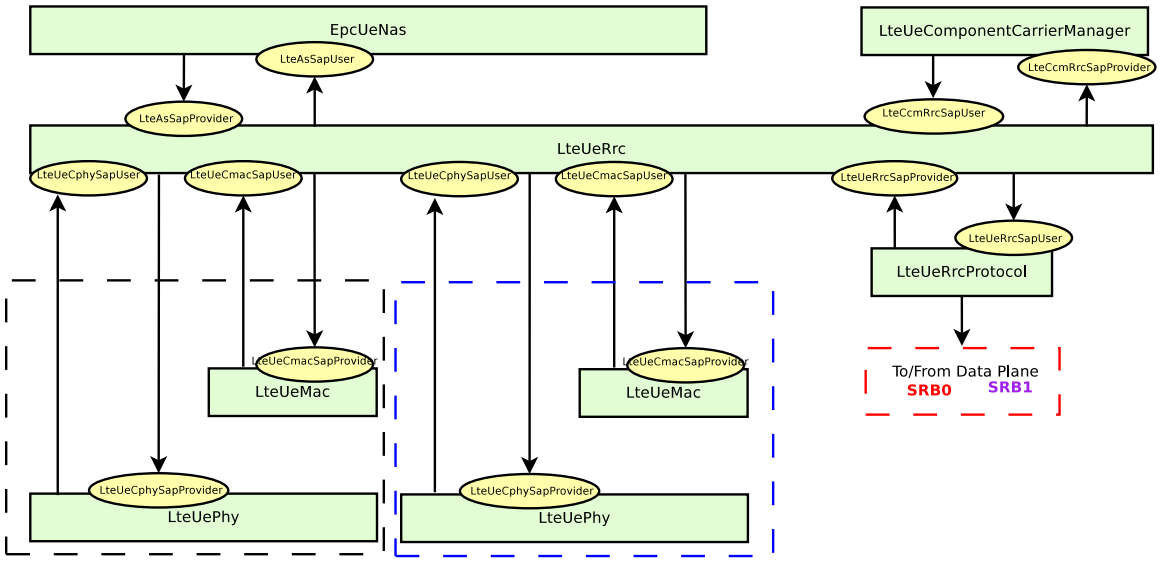

Figure 5.9: Lte Ue Control Plane Architecture

feature of Carrier Aggregation has been presented. This work has been carried out also thanks to the support of the Google Summer of Code program and it is planned to be merged to the ns-3 release as soon as the tests are finalized, which is an on-going activity close to finalization. As a result, this contribution is key and strategic for the evolution of the LTE module of ns-3.

Conclusions

In this thesis the Internet of Things (IoT) context have been presented and studied. Due to its novelty and huge impact on nowadays life and potential market the Machine to Machine (M2M) application and Machine Type Communications (MTC) protocols have been presented. Through both theoretical/simulation and experimental approaches different protocols have been studied and presented. In Chapter 1 the IoT concept has been presented. Main issues and research challenges have been addressed. Moreover, a vision on the standardization context have been given. Finally, the M2M paradigm have been presented and a focus on M2M traffic models have been shown. Chapter 2 was devoted to present short range solution for IoT mainly an experimental approach was used. Results provided in this chapter are outcomes of works developed within European Lab on Wireless Communications for the Future Internet (EuWIn) lab in Bologna. In Chapter 2 outcomes of both industrial and scientific research collaboration have been given. Moreover a focus on deployment tools for fast prototyping and test have been presented.

Chapter 3 is a propaedeutic introduction to the interaction of MTC on cellular network. As in Chapter 1, the main research challenges have been presented.

Furthermore, a focus on Long Term Evolution (LTE) and LTE-Advanced (LTE-A) architecture for MTC have been given.

Chapter 4 is mainly devoted to LTE network. A mathematical framework for M2M application on cellular network has been presented. The outcome of this chapter have been obtained in a research collaboration with CTTC (ES). After having defined the mathematical framework the model has been implemented on a standard compliant network simulator. The implementation and the main features of the network have been presented together with the achieved results.

Finally, Chapter 5 presents results obtained within the Google Summer of Code program, i.e. the implementation of Carrier Aggregation (CA) feature on NS3. Moreover, an extension of the mathematical framework already presented in Chapter 4 have been discussed. This new mathematical model enables a new degree of freedom in Radio Resource Management (RRM) for MTC since it can take advantages of the use of CA.

Bibliography

[1] ITU-T. Series y: Global information infrastructure, internet protocol aspects and next-generation networks. Recommendation Y.2060, International Telecommunication Union, Geneva, June 2012.

[2] D. Dicks, J. Blau, and T.Kridle. *M2M on the rise: the technology perspective.* Heavy Reading Mobile Networks Insider, July 2010.

[3] Mobile Broadband Connected Future: From Billions of People to Billions of Things. Yankee Group, commissioned by 4G Americas, White paper, 2011.

[4] Juniper Networks. Machine to machine - The rise of machines - Juniper Networks, White paper, 2011, 2011.

[5] 3GPP. RACH intensity of time controlled devices. 3GPP R2-102296, Technical report, TSG-RAN meeting, WG2, Beijing, China, April 2012.

[6] Xin Jian, Xiaoping Zeng, Yunjian Jia, Li Zhang, and Yuan He. Beta/M/1 Model for Machine Type Communication. *IEEE Communications Letter*, 17(3):584–587, 2013.

[7] 3GPP. Service requirements for Machine Type Communications. 3GPP TS 22.368 v13.0.0, July 2014.

[8] Navid Nikaein, Markus Laner, Kaijie Zhou, Philipp Svoboda, Dejan Drajic, Milica Popovic, and Srdjan Krco. Simple traffic modeling framework for machine type communication. In *Wireless Communication Systems (ISWCS 2013), Proceedings of the Tenth International Symposium on*, pages 1–5, 2013.

[9] Muhammad Zubair Shafiq, Lusheng Ji, Alex X. Liu, Jeffrey Pang, and Jia Wang. A first look at cellular machine-to-machine traffic: Large scale measurement and characterization. *SIGMETRICS Perform. Eval. Rev.*, 40(1):65–76, June 2012.

[10] Zigbee Alliance. Website: http://www.zigbee.org.

[11] IPv6 over Low power WPAN Working Group. Website: http://www.ietf.org/html.charters/6lowpan-charter.html.

[12] IEEE Standard for Information Technology - Telecommunications and Information Exchange Between Systems - Local and Metropolitan Area Networks - Specific Requirements Part 15.4: Wireless Medium Access Control (MAC) and Physical Layer (PHY) Specifications for Low-Rate Wireless Personal Area Networks (WPANs). *IEEE Std 802.15.4-2006 (Revision of IEEE Std 802.15.4-2003)*, pages 1–305, 2006.

[13] Zigbee specification. ZigBee Alliance, 2008.

[14] C. E. Perkins and E. M. Royer. Ad-hoc on-demand distance vector routing. In *Proc. of IEEE Workshop on Mobile Computing Systems and Applications, 1999*, pages 90–100, February 1999.

[15] Texas Instruments CC2530 datasheet. Texas Instruments.

[16] IETF RFC 4919. IPv6 over Low-Power Wireless Personal Area Networks (6LoWPANs): Overview, assumptions, problem statement, and goals.

[17] T. Winter et al. RPL: IPv6 Routing Protocol for Low-Power and Lossy Networks. In *RFC 6550 (Proposed Standard), Internet Engineering Task Force*, March 2012.

[18] S. Costanzo, L. Galluccio, G. Morabito, and S. Palazzo. Software defined wireless networks: Unbridling SDNs. In *Software Defined Networking (EWSDN), 2012 European Workshop on*, Oct 2012.

[19] EuWIn website. Website: http://www.euwin.org/.

[20] A. Mahmud and R. Rahmani. Exploitation of OpenFlow in wireless sensor networks. In *Computer Science and Network Technology (ICCSNT), 2011 International Conference on*, volume 1, Dec 2011.

[21] P. Dely, A. Kassler, and N. Bayer. OpenFlow for wireless mesh networks. In *Computer Communications and Networks (ICCCN), 2011 Proceedings of 20th International Conference on*, July 2011.

[22] C. Chaudet and Y. Haddad. Wireless software defined networks: Challenges and opportunities. In *Microwaves, Communications, Antennas and Electronics Systems (COMCAS), 2013 IEEE International Conference on*, Oct 2013.

[23] T. Miyazaki, S. Yamaguchi, K. Kobayashi, J. Kitamichi, Song Guo, T. Tsukahara, and T. Hayashi. A software defined wireless sensor network. In *Computing, Networking and Communications (ICNC), 2014 International Conference on*, Feb 2014.

[24] Lili Liang, Lianfen Huang, Xueyuan Jiang, and Yan Yao. Design and implementation of wireless smart-home sensor network based on Zigbee protocol. In *Communications, Circuits and Systems, 2008. ICCCAS 2008. International Conference on*, May 2008.

[25] S.D.T. Kelly, N.K. Suryadevara, and S.C. Mukhopadhyay. Towards the implementation of IoT for environmental condition monitoring in homes. *Sensors Journal, IEEE*, 13(10):3846–3853, Oct 2013.

[26] C. Gezer and C. Buratti. A Zigbee smart energy implementation for energy efficient buildings. In *Vehicular Technology Conference (VTC Spring), 2011 IEEE 73rd*, pages 1–5, May 2011.

[27] D. M. Abrignani, C. Buratti, and R. Verdone. Testing the impact of Wi-Fi interference on ZigBee networks. In *Proc. of IEEE Euro Med, 2014*, Nov 2014.

[28] M. Armholt, S. Junnila, and I Defee. A non-beaconing Zigbee network implementation and performance study. In *Communications, 2007. ICC '07. IEEE International Conference on*, June 2007.

[29] E.D. Pinedo-Frausto and J.A Garcia-Macias. An experimental analysis of Zigbee networks. In *Local Computer Networks, 2008. LCN 2008. 33rd IEEE Conference on*, Oct 2008.

[30] M. Franceschinis, C. Pastrone, M.A Spirito, and C. Borean. On the performance of Zigbee Pro and Zigbee IP in IEEE 802.15.4 networks. In *Wireless and Mobile Computing, Networking and Communications (WiMob), 2013 IEEE 9th International Conference on*, Oct 2013.

[31] B. Pediredla, Kevin I-Kai Wang, Z. Salcic, and A. Ivoghlian. A 6LoWPAN implementation for memory constrained and power efficient wireless sensor nodes. In *Industrial Electronics Society, IECON 2013 - 39th Annual Conference of the IEEE*, Nov 2013.

[32] G. Pellerano, M. Falcitelli, M. Petracca, M. Pagano, and P. Pagano. 6LoWPAN conform ITS-station for non safety-critical services and applications. In *ITS Telecommunications (ITST), 2013 13th International Conference on*, Nov 2013.

[33] S. Dawans, S. Duquennoy, and O. Bonaventure. On link estimation in dense RPL deployments. In *Local Computer Networks Workshops (LCN Workshops), 2012 IEEE 37th Conference on*, Oct 2012.

[34] K. Heurtefeux and H. Menouar. Experimental evaluation of a routing protocol for wireless sensor networks: RPL under study. In *Wireless and Mobile Networking Conference (WMNC), 2013 6th Joint IFIP*, April 2013.

[35] M. Kovatsch, M. Weiss, and D. Guinard. Embedding Internet technology for home automation. In *Emerging Technologies and Factory Automation (ETFA), 2010 IEEE Conference on*, Sept 2010.

[36] E. Toscano and L. Lo Bello. Comparative assessments of IEEE 802.15.4/Zigbee and 6LoWPAN for low-power industrial WSNs in realistic scenarios. In *Wireless and Mobile Networking Conference (WMNC), 2013 6th Joint IFIP*, May 2012.

[37] Ieee standard for information technology - telecommunications and information exchange between systems - local and metropolitan area networks - specific requirements - part 11: Wireless lan medium access control (mac) and physical layer (phy) specifications. *IEEE Std 802.11-2007*, pages 1–1076, June 2007.

[38] IEEE 802.15.4 Standard. *Part 15.4: Wireless Medium Access Control (MAC) and Physical Layer (PHY) Specifications for Low-Rate Wireless Personal Area Networks (LR-WPANs).*

[39] R. Musaloiu-Elefteri and A. Terzis. Minimising the effect of wifi interference in 802.15.4 wireless sensor networks. *ACM International Journal of Sensor Networks*, 3(1):43–54, December 2008.

[40] A. Sikora and V. Groza. Coexistence of ieee 802.15.4 with other systems in the 2.4 ghz-ISM-band. In *IEEE Instrumentation and Measurement Technology Conference. IMTC 2005.*, volume 3, page 1786171791, May 2005.

[41] R.G. Garroppo, L. Gazzarrini, S. Giordano, and L. Tavanti. Experimental assessment of the coexistence of Wi-Fi, ZigBee, and Bluetooth devices, year=2011, month=June,. In *IEEE International Symposium on a World of Wireless, Mobile and Multimedia Networks (WoWMoM), 2011.*

[42] S. Y. Shin, H. S. Park, S. Choi, and W. H. Kwon. Packet error rate analysis of zigbee under wlan and bluetooth interferences. *IEEE Transactions on Wireless Communications*, 6(8):2825172830, 2007.

[43] I. Howitt and J.A. Gutierrez. IEEE 802.15.4 low rate - wireless personal area network coexistence issues. In *IEEE Wireless Communications and Networking, 2003. WCNC 2003*, volume 3, March 2003.

[44] M. Petrova, J. Riihijarvi, P. Mahonen, and S. Labella. Performance study of IEEE 802.15.4 using measurements and simulations. In *IEEE Wireless Communications and Networking Conference, 2006. WCNC 2013*, volume 1, April 2006.

[45] S. Fomel and J.F. Claerbout. Guest editors' introduction: Reproducible research. *Computing in Science Engineering*, 11(1):5–7, Jan 2009.

[46] P. De, A. Raniwala, S. Sharma, and Tzi cker Chiueh. MiNT: a miniaturized network testbed for mobile wireless research. In *INFOCOM 2005. 24th Annual Joint Conference of the IEEE Computer and Communications Societies. Proceedings IEEE*, volume 4, pages 2731–2742 vol. 4, 2005.

[47] D. Raychaudhuri, I. Seskar, M. Ott, S. Ganu, K. Ramachandran, H. Kremo, R. Siracusa, H. Liu, and M. Singh. Overview of the ORBIT radio grid testbed for evaluation of next-generation wireless network protocols. In *Wireless Communications and Networking Conference, 2005 IEEE*, volume 3, pages 1664–1669 Vol. 3, 2005.

[48] V. Naik, E. Ertin, Hongwei Zhang, and A. Arora. Wireless testbed bonsai. In *Modeling and Optimization in Mobile, Ad Hoc and Wireless Networks, 2006 4th International Symposium on*, pages 1–9, 2006.

[49] Jing Lei, R. Yates, L. Greenstein, and Hang Liu. Mapping link snrs of real-world wireless networks onto an indoor testbed. *Wireless Communications, IEEE Transactions on*, 8(1):157–165, Jan 2009.

[50] L. Sanchez, V. Gutierrez, J.A. Galache, P. Sotres, J.R. Santana, J. Casanueva, and L. Munoz. Smartsantander: Experimentation and service provision in the smart city. In *Wireless Personal Multimedia Communications (WPMC), 2013 16th International Symposium on*, pages 1–6, June 2013.

[51] Angelo Cenedese, Andrea Zanella, Lorenzo Vangelista, and Michele Zorzi. Padova smart city: An urban internet of things experimentation. In *A World of Wireless, Mobile and Multimedia Networks (WoWMoM), 2014 IEEE 15th International Symposium on*, pages 1–6, June 2014.

[52] Mihael Mohorcic, Miha Smolnikar, and Tomaz Javornik. Wireless sensor network based infrastructure for experimentally driven research. In *Wireless Communication Systems (ISWCS 2013), Proceedings of the Tenth International Symposium on*, pages 1–5, Aug 2013.

[53] A.G. Dludla, A.M. Abu-Mahfouz, C.P. Kruger, and J.S. Isaac. Wireless sensor networks testbed: ASNTbed. In *IST-Africa Conference and Exhibition (IST-Africa), 2013*, pages 1–10, May 2013.

[54] Paolo Casari, Angelo P. Castellani, Angelo Cenedese, Claudio Lora, Michele Rossi, Luca Schenato, and Michele Zorzi. The wireless sensor networks for city-wide ambient intelligence (WISE-WAI)17 project. *Sensors*, 9(6):4056–4082, 2009.

[55] Vlado Handziski, Andreas Köpke, Andreas Willig, and Adam Wolisz. TWIST: A scalable and reconfigurable testbed for wireless indoor experiments with sensor network. In *Proc. of the 2nd Intl. Workshop on Multi-hop Ad Hoc Networks: from Theory to Reality, (RealMAN 2006)*, May 2006.

[56] Very large scale open wireless sensor network testbed, sensLAB. https://www.iot-lab.info/.

[57] Rainer E Burkard, Mauro Dell'Amico, and Silvano Martello. Assignment problems, revised reprint, 2009.

[58] Sartaj Sahni and Teofilo Gonzalez. P-complete approximation problems. *J. ACM*, 23(3):555–565, July 1976.

[59] A. Stajkic, M.D. Abrignani, C. Buratti, A. Bettinelli, Daniele Vigo, and R. Verdone. From real deployment to a downscaled testbed: A methodological approach. *to appear Internet of Things Journal, IEEE*, PP(99):1–1, 2015.

[60] Z at al. Youping. Network support-the radio environment map. *Cognitive Radio Technology, BA FETTE, Ed. Elsevier*, 2006.

[61] Ryosuke at al. Murata. Experimental evaluation of coexistence method for zigbee under wlan interference. *Journal of Communications*, 10(3), 2015.

[62] D. at al. Denkovski. Small-cells radio resource management based on radio environmental maps. In *Computer Communications Workshops (INFOCOM WKSHPS), 2014 IEEE Conference on*, pages 155–156, April 2014.

[63] Zhiqing Wei, Qixun Zhang, Zhiyong Feng, Wei Li, and T.A. Gulliver. On the construction of radio environment maps for cognitive radio networks. In *Wireless Communications and Networking Conference (WCNC), 2013 IEEE*, pages 4504–4509, April 2013.

[64] Sangwook Bak, Seokseong Jeon, Young-Joo Suh, Chansu Yu, and Dongsoo Han. Characteristics of a large-scale wifi radiomap and their implications in indoor localization. In *Network of the Future (NOF), 2013 Fourth International Conference on the*, pages 1–5, Oct 2013.

[65] Bluetooth specification version 2.1+edr, bluetooth sig, inc. std., july 2007.

[66] 3GPP. Study on RAN improvements for Machine Type Comunications. 3GPP TR 37.868, July 2010.

[67] M. Beale. Future Challenges in Efficiently Supporting M2M in the LTE standards. In *International Workshop on Internet of Things Enabling Technologies, Embracing M2M Communications and Beyond*, Paris, France, April 2012.

[68] M. E. Rivero-Angeles, D. Lara-Rodriguez, and F. A. Cruz-Prez.

[69] S. Lien and K. Chen. Massive Access Management for QoS Guarantees in 3GPP Machine-to Machine Communications. *IEEE Communications Letters*, 15(3), 2011.

[70] N. Nikaein and S. Krco. Latency for Real Time Machine to Machine Communication in LTE Based System Architecture. In *Proc. of European Wireless 2011*.

[71] G. Wang, X. Zhong, S. Mei, and J. Wang. An adaptive medium access control mechanism for cellular based machine to machine (M2M) communication. In *Proc. IEEE International Conference on Wireless Information Technology and Systems (IEEE ICWITS)*, Hawaii, USA.

[72] K. Zheng, F. Hu, W. Wang, W. Xiang, and M. Dohler. Radio Resource Allocation in LTE-Advanced Cellular Networks with M2M Communications. *IEEE Communications Magazine*, 18(7):184–192, 2012.

[73] C. Ide, B. Dusza, M. Putzke, C. Mller, and C. Wietfeld. Influence of M2M Communication on the Physical Resource Utilization of LTE. In *Proc. of Wireless Telecommunications Symposium*, London, UK, April 2012.

[74] R. Ratasuk, J. Tan, and A. Ghosh. Coverage and Capacity Analysis for Machine Type Communications in LTE. In *Proc. of IEEE Vehicular Technology Conference (IEEE VTC 2012)*, St. Petersburg, Russia, August 2011.

[75] S. T. Sheu, C. H. Chiu, S. Lu, and H. H. Lai. Efficient Data Transmission Scheme for MTC Communications in LTE System. In *Proc. of 11th International Conference on ITS Telecommunications (ITST 2011)*, Yokohama, Japan, May 2012.

[76] K. D. Lee, S. Kim, and B. Yi. Throughput Comparison of Random Access Methods for M2M Service over LTE Networks. In *Proc. of International Workshop on Machine to Machine Communications in GLOBECOM 2011*, Houston, Texas, December 2011.

[77] S. Sheu, C. H. Chiu, Y. C. Cheng, and K. H. Kuo. Self-adaptive Persistent Contention Scheme for Scheduling based Machine Type Communications in LYE System. In *Proc. of International Conference on Selected Topics in Mobile and Wireless Networking*, Avignone, France, July 2012.

[78] Small Cell Forum. Small Cell Market Status. White paper, December 2012.

[79] A.S. Hamza, S.S. Khalifa, H.S. Hamza, and K. Elsayed. A survey on inter-cell interference coordination techniques in OFDMA-based cellular networks. *Communications Surveys Tutorials, IEEE*, 15(4):1642–1670, Fourth 2013.

[80] N. Abu-Ali, A.-E.M. Taha, M. Salah, and H. Hassanein. Uplink Scheduling in LTE and LTE-Advanced: Tutorial, Survey and Evaluation Framework. *Communications Surveys Tutorials, IEEE*, 16(3):1239–1265, Third 2014.

[81] IBM Corp. *IBM ILOG CPLEX v12.1 - User's Manual For CPLEX*, 2009.

[82] J.G. Andrews. Seven ways that hetnets are a cellular paradigm shift. *Communications Magazine, IEEE*, 51(3):136–144, March 2013.

[83] CTTC. *LTE Simulator Documentation*. CTTC, release M6 edition, April 2013.

[84] Optimizing stadium and special venue networks with 3D modeling. Nokia - Nokia Networks, White paper.

[85] 4G Femtocell Solutions for Stadium Environments. Fujitsu, White paper.

[86] F.D. Calabrese, P.H. Michaelsen, C. Rosa, M. Anas, C.U. Castellanos, D.L. Villa, K.I. Pedersen, and P.E. Mogensen. Search-Tree Based Uplink Channel Aware Packet Scheduling for UTRAN LTE. In *Vehicular Technology Conference, 2008. VTC Spring 2008. IEEE*, pages 1949–1953, May 2008.

[87] Shao-Yu Lien, Kwang-Cheng Chen, and Yonghua Lin. Toward ubiquitous massive accesses in 3gpp machine-to-machine communications. *Communications Magazine, IEEE*, 49(4):66–74, April 2011.

[88] A.M. Maia, D. Vieira, M.F. de Castro, and Y. Ghamri-Doudane. A mechanism for uplink packet scheduler in lte network in the context of machine-to-machine communication. In *Global Communications Conference (GLOBECOM), 2014 IEEE*, pages 2776–2782, Dec 2014.

[89] Sun Zhenqi, Yu Haifeng, Chi Xuefen, and Li Hongxia. Research on uplink scheduling algorithm of massive m2m and h2h services in lte. In *Information and Communications Technologies (IETICT 2013), IET International Conference on*, pages 365–369, April 2013.

[90] I. Abdalla and S. Venkatesan. A qoe preserving m2m-aware hybrid scheduler for lte uplink. In *Mobile and Wireless Networking (MoWNeT), 2013 International Conference on Selected Topics in*, pages 127–132, Aug 2013.

[91] Yen-Kai Liao, Chih-Han Wang, De-Nian Yang, and Wen-Tsuen Chen. Uplink scheduling for LTE 4g video surveillance system. *CoRR*, abs/1410.1009, 2014.

[92] Kai Yang, Steven Martin, and Tara Ali Yahiya. Interference aware resource allocation for LTE uplink transmission. In *Computers and Communication (ISCC), 2014 IEEE Symposium on*, pages 1–6, June 2014.

[93] A. Afifi, K.M.F. Elsayed, and A. Khattab. Interference-aware radio resource management framework for the 3GPP LTE uplink with QoS constraints. In *Computers and Communications (ISCC), 2013 IEEE Symposium on*, pages 000693–000698, July 2013.

[94] X. Xiang, C. Lin, X. Chen, and X.S. Shen. Toward Optimal Admission Control and Resource Allocation for LTE-A Femtocell Uplink. *Vehicular Technology, IEEE Transactions on*, PP(99):1–1, 2014.

[95] P. Frank, A. Muller, H. Droste, and J. Speidel. Cooperative interference-aware joint scheduling for the 3GPP LTE uplink. In *Personal Indoor and Mobile Radio Communications (PIMRC), 2010 IEEE 21st International Symposium on*, pages 2216–2221, Sept 2010.

[96] L. Ruiz de Temino, Gilberto Berardinelli, S. Frattasi, and P. Mogensen. Channel-aware scheduling algorithms for SC-FDMA in LTE uplink. In *Personal, Indoor and Mobile Radio Communications, 2008. PIMRC 2008. IEEE 19th International Symposium on*, pages 1–6, Sept 2008.

[97] Fengyuan Ren, Yinsheng Xu, Hongkun Yang, Jiao Zhang, and Chuang Lin. Frequency Domain Packet Scheduling with Stability Analysis for 3GPP LTE Uplink. *Mobile Computing, IEEE Transactions on*, 12(12):2412–2426, Dec 2013.

[98] R. Ruby and V. Leung. Towards QoS Assurance with Revenue Maximization of LTE Uplink Scheduling. In *Communication Networks and Services Research Conference (CNSR), 2011 Ninth Annual*, pages 202–209, May 2011.

[99] Elias Yaacoub and Zaher Dawy. Achieving the nash bargaining solution in OFDMA uplink using distributed scheduling with limited feedback. *AEU - International Journal of Electronics and Communications*, 65(4):320 – 330, 2011.

[100] Suk-Bok Lee, I. Pefkianakis, A. Meyerson, Shugong Xu, and Songwu Lu. Proportional Fair Frequency-Domain Packet Scheduling for 3GPP LTE Uplink. In *INFOCOM 2009, IEEE*, pages 2611–2615, April 2009.

[101] A.S. Lioumpas and A. Alexiou. Uplink scheduling for machine-to-machine communications in lte-based cellular systems. In *GLOBECOM Workshops (GC Wkshps), 2011 IEEE*, pages 353–357, Dec 2011.

[102] 3GPP. X2 General Aspects and Principles (Release 8). 3GPP TS 36.420 V8.0.0 (2007-12), December 2007.

[103] 3GPP. X2 Application Protocol (X2AP) (Release 8). 3GPP TS 36.423 V8.2.0 (2008-06), June 2008.

[104] CTTC. *The LTE-EPC Network Simulator (LENA) project*. http::/iptechwiki.cttc.es/.

[105] 3GPP. Conveying MCS and TB size via PDCCH. 3GPP R1-081483, April 2008.

[106] 3GPP. LTE - Evolved Universal Terrestrial Radio Access (E-UTRA) Physical layer procedures. 3GPP TS 36.213,ETSI TS 136 213 v8.8.0, October 2009.

[107] R. Jain, D.-M. Chiu, and W. Hawe. A quantitative measure of fairness and discrimination for resource allocation in shared computer system. *Digital Equipment Corp.*, Tech. Rep., 1984.

[108] Cisco. The Internet of Things. *[Online]*, Jan 2014.

[109] 3GPP. E-UTRA Physical layer procedures. 3GPP TS 36.213 V10.0.0 (2010-12), December 2010.

[110] 3GPP. E-UTRA Physical Channels and Modulation. 3GPP TS 36.211 V10.0.0 (2011-01), January 2011.

[111] 3GPP. E-UTRA Radio Link Control (RLC) protocol specification. 3GPP TS 36.322 V10.0.0 (2011-01), January 2011.

[112] 3GPP. E-UTRA Radio Resource Control (RRC) protocol specification. 3GPP TS 36.331 V10.0.0 (2011-01), January 2011.

[113] Yun Rui, Peng Cheng, Mingqi Li, Q.T. Zhang, and M. Guizani. Carrier aggregation for lte-advanced: uplink multiple access and transmission enhancement features. *Wireless Communications, IEEE*, 20(4):101–108, August 2013.

[114] Hua Wang, C. Rosa, and K. Pedersen. Uplink component carrier selection for lte-advanced systems with carrier aggregation. In *Communications (ICC), 2011 IEEE International Conference on*, pages 1–5, June 2011.

[115] Hua Wang, C. Rosa, and K. Pedersen. Performance of uplink carrier aggregation in lte-advanced systems. In *Vehicular Technology Conference Fall (VTC 2010-Fall), 2010 IEEE 72nd*, pages 1–5, Sept 2010.

[116] Ran Zhang, Miao Wang, Zhongming Zheng, X.S. Shen, and Liang-Liang Xie. Cross-layer carrier selection and power control for lte-a uplink with carrier aggregation. In *Global Communications Conference (GLOBECOM), 2013 IEEE*, pages 4668–4673, Dec 2013.

[117] M.A. Lema, M. Garcia-Lozano, S. Ruiz, and D.G. Gonzalez. Improved component carrier selection considering mpr information for lte-a uplink systems.

In *Personal Indoor and Mobile Radio Communications (PIMRC), 2013 IEEE 24th International Symposium on*, pages 2191–2196, Sept 2013.

[118] R. Sivaraj, A. Pande, Kai Zeng, K. Govindan, and P. Mohapatra. Edge-prioritized channel- and traffic-aware uplink carrier aggregation in lte-advanced systems. In *World of Wireless, Mobile and Multimedia Networks (WoWMoM), 2012 IEEE International Symposium on a*, pages 1–9, June 2012.

[119] Yujae Song, Youngnam Han, and Yonghoon Choi. A qoe-aware joint resource allocation algorithm for uplink carrier aggregation in lte-advanced systems. In *Communications (ICC), 2014 IEEE International Conference on*, pages 1–5, June 2014.

[120] L.G.U. Garcia, F. Sanchez-Moya, J. Villalba-Espinosa, K.I. Pedersen, and P.E. Mogensen. Enhanced uplink carrier aggregation for lte-advanced femtocells. In *Vehicular Technology Conference (VTC Fall), 2011 IEEE*, pages 1–5, Sept 2011.

[121] Hua Wang, C. Rosa, and K.I. Pedersen. Uplink inter-site carrier aggregation between macro and small cells in heterogeneous networks. In *Vehicular Technology Conference (VTC Fall), 2014 IEEE 80th*, pages 1–5, Sept 2014.

[122] D. Robalo, F.J. Velez, R.R. Paulo, and G. Piro. Extending the lte-sim simulator with multi-band scheduling algorithms for carrier aggregation in lte-advanced scenarios. In *Vehicular Technology Conference (VTC Spring), 2015 IEEE 81st*, May 2015.

[123] 3GPP TSG-RAN WG1 R1-081483. *Technical Specification Group Radio Access Network; Study on Licensed-Assisted Access to Unlicensed Spectrum; (Release 13)*, June 2015.

[124] Qualcomm Whitepaper. Lte in unlicensed spectrum: Harmonious coexistence with wi-fi. available at `https://www.qualcomm.com/documents/lte-unlicensed-coexistence-whitepaper`, 2014.

[125] NS3 Consortium. *NS3 Manual*. https://www.nsnam.org/docs/release/3.24/manual/singlehtml/index

[126] NS3 Consortium. *NS3 Tutorial*. https://www.nsnam.org/docs/release/3.24/tutorial/singlehtml/inde

[127] M. Danilo Abrignani. *NS3 Gsoc 2015*. https://www.nsnam.org/wiki/GSOC2015LTECA.

Publications

Besides Newcom#, this Ph.D. activity was performed in the framework of the COST Actions IC1004 (Cooperative Radio Communications for Green Smart Environments). The work described in this thesis has led to the following publications to Journals:

- Buratti, Chiara; Stajkic, Andrea; Gardasevic, Gordana; Milardo, Sebastiano; Abrignani, Melchiorre; Mijovic, Stefan; Morabito, Giacomo; Verdone, Roberto; "Testing Protocols for The Internet of Things on The EuWIn Platform"; *"IEEE Internet of Things Journal"*; July 2015.

- Stajkic, Andrea; Abrignani, Melchiorre; Buratti, Chiara; Bettinelli, Andrea; Vigo, Daniele; Verdone, Roberto; "From a Real Deployment to a Downscaled Testbed: A Methodological Approach"; to appear in *"IEEE Internet of Things Journal"*; November 2015.

- Abrignani, Melchiorre Danilo; Giupponi, Lorenza; Lodi, Andrea; Verdone, Roberto; "Scheduling MTC over 3GPP LTE Uplink of a Dense Small Cell Network"; *" submitted to IEEE Transactions on Vehicular Technologies "*; November 2015.

and to the following papers presented to International Conferences:

- Abrignani, Melchiorre Danilo; Gezer, Cengiz; Verdone, Roberto; "Poster: A Multi-Service Wireless Lamp Post Backbone for Smart Cities - Centralized vs Distributed Control"; *European Conference of Wireless Sensor Networks (EWSN), February 2013, Ghent, Belgium*;

- Abrignani, Melchiorre Danilo; Buratti, Chiara; Dardari, Davide; El Rachkidy, Nancy; Guitton, Alex; Martelli, Flavia; Stajkic, Andrea; Verdone, Roberto; "The EuWIn Testbed for 802.15.4/Zigbee Networks: From the Simulation to the Real World"; *IEEE International Symposium on Wireless Communication Systems (ISWCS), August 2013, Ilmenau, Germany*;

- Abrignani, Melchiorre Danilo; Buratti, Chiara; Frost, Linsday; Verdone, Roberto;"Testing the impact of Wi-Fi interference on Zigbee networks"; *Euro Med Telco Conference (EMTC), November 2014, Naples, Italy*;

- Abrignani, Melchiorre Danilo; Giupponi, Lorenza; Lodi, Andrea; Verdone, Roberto; "Scheduling M2M Traffic over LTE Uplink of a dense Small Cells Network"; *IEEE International Symposium on Wireless Communication Systems (ISWCS), September 2015, Bruxelles, Belgium*;

- Abrignani, Melchiorre Danilo; Buratti, Chiara; Contino, Giulio; Verdone,

Roberto;"Fast-Deployment and Continuous Monitoring through REM: A Low-Cost Device Prototype"; *Telfor 2015, November 2015, Belgrade, Serbia*;

- Kattila, Charles J.; Abrignani, Melchiorre Danilo; Verdone, Roberto;"Neighbours-Aware Proportional Fair Schedulerfor Future Wireless Networks."; submitted to: *11th EAI International Conference on Cognitive Radio Oriented Wireless Networks (CrownCOM), May 2016, Grenoble, France*;

Other Temporary Documents (TD) presented at COST Action IC1004 Meetings follow:

- Abrignani, Melchiorre Danilo; Giupponi, Lorenza; Verdone, Roberto; "Evaluation of M2M Scheduling Opportunities in a LTE Small Cell Network for Smart City Applications"; TD(14)09040 presented at the IX Management Committee Meeting of Cost IC1004, Ferrara (IT), February 2014.

- Abrignani, Melchiorre Danilo; Giupponi, Lorenza; Lodi, Andrea; Verdone, Roberto; "Scheduling the 3GPP LTE Uplink over a Dense Heterogeneous Network"; TD(15)12014 presented at the XII Management Committee Meeting of Cost IC1004, Dublin (EI), January 2015.

- Abrignani, Melchiorre Danilo; Giupponi, Lorenza; Lodi, Andrea; Verdone, Roberto; "Packet-scheduling for Machine-Type communication over the 3GPP LTE Uplink of a Dense Network"; TD(15)13042 presented at the XIII Management Committee Meeting of Cost IC1004, Valencia (ES), May 2015.

As for the Newcom# project, contributions to the following deliverables were given:

- D13.1 – "Fundamental issues on energy- and bandwidth-efficient communications and networking", edited by Andreas Zalonis and Andreas Polydoros, November 2013.

- D13.2 – "Fundamental issues on energy- and bandwidth-efficient communications and networking", edited by Andreas Zalonis and Andreas Polydoros, November 2014.

- D13.3 – "Overall assessment of selected techniques on energy- and bandwidth-efficient communications and networking", edited by Andreas Zalonis and Andreas Polydoros, November 2015.

- D22.1 – "Definition of EuWIn@CNIT/Bologna testbed interfaces and preliminary plan of activities", edited by Davide Dardari, April 2013.

- D22.2 – "Preliminary tests over the lab infrastructures ", edited by Davide Dardari, November 2013.

- D22.3 – "Experimental results over the lab infrastructure", edited by Davide Dardari, November 2014.

- D22.4 – "Final results obtained in the lab infrastructures", edited by Davide Dardari, November 2014.

- D35.3 – "Report on third-year mobility and awards", edited by Melchiorre Danilo Abrignani, November 2015.

Acknowledgements

"Call it a clan, call it a network, call it a tribe, call it a family. Whatever you call it, whoever you are, you need one. " [J. Howard]

This thesis has been possible only thanks to the support of many people.
First of all, I would like to express my sincere gratitude to my supervisor, Prof. Roberto Verdone, and to Dr. Chiara Buratti for them constant guidance.
Special thanks to Prof. Andrea Lodi and to Dr. Lorenza Giupponi for them help and fruitful collaboration during this years. To the latter, double thanks are owned, because of her really welcoming reception and priceless supervision during my semester at CTTC. Furthermore, I would also like to extend my thanks Dr. Nicola Baldo and Marco Miozzo for them support and guidance during the Google Summer of Code.
I am very thankful to RadioNetworks group both 'old' and 'new' members, for sure without them these years would had been much less funnier and much more harder.
I cannot forget to thanks all those people I met in Barcelona, everyone contributed to make my semester there an unforgettable experience.
Moreover, I wish to thanks my closest friends for all the chats and time spent together, for the support and the presence in the worst moments. Finally, I would like to thank my family and Marianna, for them support and presence. This thesis in dedicated to them.